NTNU – Trondheim
Norwegian University of
Science and Technology

Petrography, diagenesis and reservoir quality of the Triassic Fruholmen, Snadd and Kobbe formations, southern Barents Sea.

Hege Walderhaug Porten

Earth Sciences and Petroleum Engineering
Submission date: June 2012
Supervisor: Mai Britt E. Mørk, IGB

Norwegian University of Science and Technology
Department of Geology and Mineral Resources Engineering

Objectives of study

This study has focused on sandstone petrography, diagenesis and reservoir quality in the Triassic Fruholmen, Snadd and Kobbe formations in wells 7131/4-1 and 7222/11-1 in the southern Barents Sea. The main objectives of the work have been to describe and compare the composition of the sandstones of the three formations, document and explain their diagenetic evolution, and to determine the controls on reservoir quality. Sandstone provenance is also briefly discussed, and an attempt has been made to estimate the magnitude of uplift in the two wells.

Background

This thesis is based on a thin-section study of cores and side wall cores from the wells 7131/4-1 and 7222/11-1. Well 7131/4-1 is located in the Finnmark East area, whereas well 7222/11-1 is situated on the Bjarmeland Platform, both in the Barents Sea. Both wells are exploration wells that were drilled as wildcats by Statoil ASA. Well 7131/4-1 was drilled in 2005, but it proved to be a dry well and was abandoned in May the same year. Well 7222/11-1 was drilled in 2008 and both oil and gas shows were discovered. However, the well was permanently abandoned late in 2008 as an oil and gas discovery.

All thin-sections, core descriptions and porosity and permeability data were provided by Statoil ASA.

The thesis has been carried out in the period: *January-June 2012*
MSc programme in Earth Sciences and Petroleum Engineering, *Petroleum Geoscience*

Main supervisor: Professor Mai Britt Engeness Mørk

Signature student | Signature main supervisor

Abstract

Petrographic composition, diagenesis and reservoir quality of the Upper Triassic fluvial to marginal marine Fruholmen Formation, the Middle and Upper Triassic estuarine and coastal plain Snadd Formation, and the Middle Triassic estuarine Kobbe Formation have been examined in wells 7131/4-1 and 7222/11-1 located on the eastern Finnmark Platform and on the western Bjarmeland Platform in the southern Barents Sea. Twenty-nine thin-sections from the Fruholmen Formation, sixty-eight from the Snadd Formation and eleven from the Kobbe Formation were studied with a petrographic microscope, forty were point-counted, and four were studied with a cathodoluminescence microscope. The petrographic observations were compared with plug measurements of porosity and permeability.

The Fruholmen Formation sandstones are moderately well and well sorted fine-, medium- and coarse-grained quartz arenites. The Snadd Formation sandstones are moderately well and well sorted and fine- and medium-grained, and the Kobbe Formation sandstones are mostly well sorted and fine-grained. Both the Snadd and Kobbe Formations comprise sublitharenites and lithic arenites with common to abundant metasedimentary rock fragments, but the Snadd Formation contains both K-feldspar and plagioclase, whilst the Kobbe Formation contains plagioclase only. The compositional differences between the three formations may largely be a result of the Snadd and Kobbe formations having had an eastern source area (Uralides), and the Fruholmen Formation a more southerly source area (Scandinavia), although a shift to a more humid climate in the Late Triassic may also have influenced sand composition.

The Fruholmen Formation sandstones contain very little diagenetic cement, typically 1-2% quartz overgrowths, traces of pyrite cement, and occasionally 1-2% authigenic kaolin. The main diagenetic cement in the Snadd Formation is early diagenetic chlorite that occurs as grain coatings and more rarely as pervasive microporous pore-filling cement. Siderite is present in most Snadd Formation samples in amounts of 1-6%, and a few thin zones are strongly calcite-cemented. Up to 3% authigenic kaolin is commonly present, and traces of pyrite cement and quartz overgrowths occur. The Kobbe Formation sandstones contain the same diagenetic minerals as the Snadd Formation, plus a few albitic overgrowths on plagioclase. However, the total volumes of diagenetic minerals in the Kobbe Formation are typically very low, 1-5% in the point-counted samples.

Diagenetic chlorite or poorly crystalline chlorite precursors may have formed from iron-rich colloidal material brought in by rivers and flocculated where fluvial waters mixed with marine waters. These colloids may also have been the main source for iron in early diagenetic siderite. Partly dissolved biogenic carbonate is still present in the Snadd and Kobbe formations, and carbonate fossils are probably the source of the calcite cement. The calcite cement engulfs and therefore postdates chlorite grain coats, siderite cement and authigenic kaolin. Quartz overgrowths were sourced from dissolution of quartz grains at stylolites evolved from clay laminae when temperatures reached 70-80°C.

Reservoir quality is largely excellent in the Fruholmen Formation sandstones (25-32% helium porosity, 1 000-38 000mD permeability) because contents of detrital clay and diagenetic minerals are almost zero. Snadd Formation porosities are also in most cases high to very high, 26-36%, partly due to the chlorite coatings inhibiting quartz cementation. Permeabilities are mostly 100 to 5 000mD, but where microporous diagenetic chlorite fills the pore system permeabilities are very low to low, 0.1-15mD. The Kobbe Formation sandstones have been more deeply buried than the overlying formations, approximately 3.5km, content of soft components (detrital and authigenic clay, mica-rich rock fragments) is high, and compaction has therefore been severe. Porosities are consequently quite low, 15-21%, even in the best of the cored Kobbe Formation sandstones, and together with the fine grain size this results in low permeabillities, 1-20mD.

Burial depth for the shallowest examined cores is only 0.4 and 0.56km, and present temperatures are around 30°C. The consolidated nature of these cores and the presence of quartz overgrowths that normally start forming at 70-80°C therefore suggest that the sandstones have been more deeply buried than at present. Lack of illitization of kaolin in the deepest samples indicates that they have not been subjected to temperatures above 130°C. Together with the degree of quartz cementation in the various examined samples this suggests uplift of around 1.5km in well 7131/4-1 and 1.7km in well 7222/11-1. Comparison of the present porosities in the quartz arenites of the Fruholmen Formation with the porosity depth trend for the Garn Formation also suggests 1.5km of uplift in well 7131/4-1.

Sammendrag

Petrografisk sammensetning, diagenese og reservoarkvalitet i fluviale til marginalmarine overtriassiske sandsteiner fra Fruholmenformasjonen, estuarine og kystslette midttriassiske og overtriassiske sandsteiner fra Snaddformasjonen, og estuarine midttriassiske sandsteiner fra Kobbeformasjonen er undersøkt i brønnene 7131/4-1 og 7222/11-1 som er lokalisert på den østlige delen av Finnmarkplattformen og den vestlige delen av Bjarmelandsplattformen i det sørlige Barentshavet. Tjueni tynnslip fra Fruholmenformasjonen, sekstiåtte fra Snaddformasjonen og elleve fra Kobbeformasjonen ble studert med et petrografisk mikroskop, førti ble punkttelt og fire ble studert med et katodeluminescensmikroskop. De petrografiske observasjonene ble sammenlignet med pluggmålinger av porøsitet og permeabilitet.

Sandsteinene fra Fruholmenformasjonen er middels godt og godt sorterte fin-, middels- og grovkornete kvartsarenitter. Sandsteinene fra Snaddformasjonen er middels godt og godt sorterte og fin- og middelskornete, og sandsteinene fra Kobbeformasjonen er hovedsakelig godt sorterte og finkornete. Sandsteinene fra både Snadd- og Kobbeformasjonen er sublitarenitter og litiske arenitter med tallrike metasedimentære bergartsfragmenter, men Snaddformasjonen inneholder både kalifeltspat og plagioklas, mens Kobbeformasjonen kun inneholder plagioklas. Forskjellene i sammensetning mellom de tre formasjonene kan i stor grad være et resultat av at Snadd- og Kobbeformasjonen hadde en østlig sedimentkilde (Uralidene), mens Fruholmenformasjonen hadde et mer sørlig kildeområde (Skandinavia), selv om en endring til et mer fuktig klima i seintrias også kan ha påvirket sandsammensetningen.

Sandsteinene i Fruholmenformasjonen inneholder svært lite diagenetisk sement, typisk 1-2% kvartsovervekster, spormengder av pyrittsement, og i noen tilfeller 1-2% autigen kaolin. Det dominerende diagenetiske mineralet i Snaddformasjonen er tidligdiagenetisk kloritt som forekommer som kornbelegg og sjeldnere som porefyllende mikroporøs sement. Sideritt forekommer i de fleste prøvene fra Snaddformasjonen i mengder av 1-6%, og noen få tynne soner er sterkt kalsittsementerte. Inntil 3% autigen kaolin er ofte til stede, og spormengder av pyrittsement og kvartsovervekster forekommer. Sandsteinene i Kobbeformasjonen inneholder de samme diagenetiske mineralene som Snaddformasjonen, i tillegg til noen få albittiske overvekster på plagioklas. Totalvolumet av diagenetiske mineraler i Kobbeformasjonen er imidlertid meget lavt, 1-5% i de punkttelte prøvene.

Diagenetisk kloritt eller svakt krystalliserte klorittforløpere kan ha blitt dannet fra jernrike kolloider brakt inn av elver og flokkulert i blandingssonen mellom fluvialt og marint vann. Disse kolloidene kan også ha vært hovedkilden til jernet i tidligdiagenetisk sideritt. Delvis oppløst biogent karbonat er fremdeles til stede i Snadd- og Kobbeformasjonen, og oppløsning av karbonatfossiler er sannsynligvis kilden til kalsittsementen. Kalsittsementen omslutter og er derfor utfelt etter klorittbelegg, siderittsement og autigen kaolin. Kilden for kvartsovervekster er oppløsning av kvartskorn ved stylolitter utviklet fra leirlamina da temperaturen nådde 70-80°C.

Reservoarkvaliteten er for det meste utmerket i sandsteinene i Fruholmenformasjonen (25-32% heliumporøsitet, 1 000-38 000mD permeabilitet) fordi innholdet av detrital leire og diagenetiske mineraler er nær null. Porøsiteten i Snaddformasjonen er også i de fleste tilfeller høy til svært høy, 26-36%, delvis på grunn av klorittbelegg som forhindrer kvartssementering. Permeabiliteten er for det meste 100 til 5 000mD, men i områder der mikroporøs diagenetisk kloritt fyller poresystemet er permeabiliteten lav til svært lav, 0.1-15mD. Sandsteinene i Kobbeformasjonen har vært dypere begravd enn de overliggende formasjonene, omtrent 3.5km, innholdet av mekanisk svake komponenter (detrital og autigen leire, glimmerrike bergartsfragmenter) er høyt, og kompaksjon har derfor vært omfattende. Porøsiteten er følgelig relativt lav, 15-21%, selv i de beste av de kjernetatte sandsteinene i Kobbeformasjonen, og sammen med liten kornstørrelse resulterer dette i lav permeabilitet, 1-20mD.

Dagens begravningsdyp for de grunneste studerte kjernene er bare 0.4 og 0.56km, og nåværende temperaturer er rundt 30°C. Den konsoliderte tilstanden av disse kjernene og tilstedeværelsen av kvartsovervekster som normalt dannes ved temperaturer over 70-80°C indikerer derfor at sandsteinene har vært begravd mye dypere enn dagens dyp. Mangelen på illittisering av kaolin i de dypeste prøvene indikerer at de ikke har vært utsatt for temperaturer over 130°C. Sammen med graden av kvartssementering i de ulike undersøkte prøvene indikerer dette hevning på rundt 1.5km i brønn 7131/4-1 og 1.7km i brønn 7222/11-1. Sammenligning av dagens porøsitet i kvartsarenittene i Fruholmenformasjonen med porøsitet mot dyp-trenden i Garnformasjonen indikerer også hevning på 1.5km i brønn 7131/4-1.

Acknowledgements

I would like to thank my supervisor, Professor Mai Britt Engeness Mørk, for helpful guidance throughout this process and for always answering my questions. I would also like to thank Statoil ASA, and especially Nils Einar Aase and Linda Sæbø, for providing me with thin-sections and the core data necessary to make this work possible, giving me access to equipment in their Stavanger offices, and for helping me with taking micrographs with petrographic and cathodoluminescence microscopes. Finally, I would like to thank my family and friends for their continuous support.

Table of Contents

1 Introduction

This master's thesis has been carried out for the Department of Geology and Mineral Resources Engineering at the Norwegian University of Science and Technology (NTNU), as the final thesis of my master's degree in petroleum geology.

1.1 Background

This thesis is based on a thin-section study of cores and side wall cores from the wells 7131/4-1 and 7222/11-1. Well 7131/4-1 is located in the Finnmark East area, whereas well 7222/11-1 is situated on the Bjarmeland Platform, both in the Barents Sea (Figure 1.1.1). Both wells are exploration wells that were drilled as wildcats by Statoil ASA. Well 7131/4-1 was drilled in 2005, but it proved to be a dry well and was abandoned in May the same year. Well 7222/11-1 was drilled in 2008 and both oil and gas shows were discovered. However, the well was permanently abandoned late in 2008 as an oil and gas discovery.

All thin-sections, core descriptions and porosity and permeability data were provided by Statoil ASA.

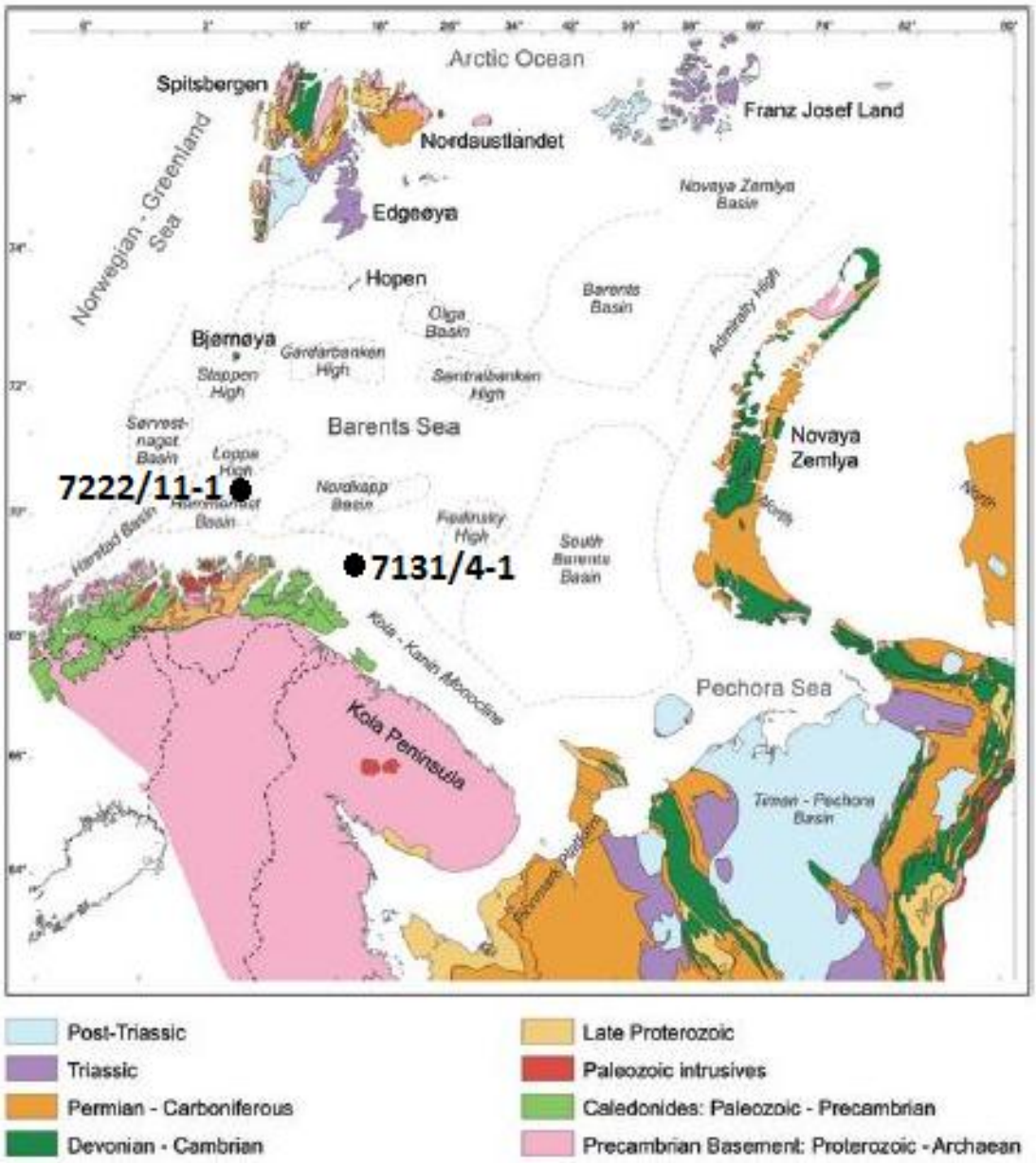

Figure 1.1.1: Study area. Modified from Mørk (1999) and Worsley (2008).

1.1.1 Objectives of study

This study has focused on sandstone petrography, diagenesis and reservoir quality in the Triassic Fruholmen, Snadd and Kobbe formations in wells 7131/4-1 and 7222/11-1 in the southern Barents Sea. The main objectives of the work have been to describe and compare the composition of the sandstones of the three formations, document and explain their diagenetic evolution, and to determine the controls on reservoir quality. Sandstone provenance is also briefly discussed, and an attempt has been made to estimate the magnitude of uplift in the two wells.

1.1.2 Previous work

The geological evolution of the Barents Sea area has been discussed in numerous publications (e.g., Doré, 1995; Ryseth et al., 2003; Ramberg et al., 2007; Gabrielsen et al., 2011), and detailed studies of the sedimentology of certain parts of the Mesozoic succession are also available. For instance, the depositional settings of Jurassic sandstones in the Hammerfest Basin have been reviewed by Olaussen et al. (1984), Folkestad (2007) and Johannessen and Nødtvedt (2007), and the sedimentology of Cretaceous sandstones is discussed by Brekke and Olaussen (2007). The geological evolution of the Barents Sea area in the Triassic has been discussed by Bugge et al. (2007), Nystuen et al. (2007) and Riis et al. (2008). However, studies focusing specifically on diagenesis and reservoir quality have concentrated on the Jurassic part of the Mesozoic succession (Olaussen et al., 1984; Berglund et al., 1986; Walderhaug and Bjørkum 2003), the Triassic succession has received less attention. However, the regional study of Triassic sandstone provenance carried out by Mørk (1999) and the work of Bergan and Knarud (1992) where a marked upward shift from lithic subarkoses to quartz arenites is shown to take place in the uppermost Triassic has implications for both diagenesis and reservoir quality because marked changes in sand composition may strongly influence both subsequent burial diagenesis and reservoir quality (Bjørlykke, 2010).

1.2 Methods and sample material

1.2.1 Thin-section analysis

Well 7131/4-1

From well 7131/4-1 seventy-four thin-sections were produced by Statoil from the cored intervals, including twenty-nine thin-sections from the Norian Fruholmen Formation interval 915-943mRKB (metres below the rotary table), and forty-five from cores from the Carnian Snadd Formation (1070-1118mRKB). Water depth at the well location is 331m and the distance from the rotary table to the sea surface is 25m (NPD factpages). Burial depth of the cored intervals in well 7131/4-1 is therefore 559-587mRSF (metres relative to the sea floor) and 714-762mRSF. All thin-sections were made from plugs used for measurements of helium porosity and air permeability. All thin-sections were polished, and porosity was filled with blue epoxy.

The thin-sections were studied with a petrographic microscope, and micrographs were taken of selected samples with a Nikon DS-Fi1 digital camera. Ten thin-sections from the

Fruholmen Formation (Table 1.2.2a) and thirteen thin-sections from the Snadd Formation were point-counted with three hundred points per thin-section (Table 1.2.2b). Grain size was determined by measuring the longest axis of thirty grains per sample and calculating the mean value. Sorting was defined as the sample standard deviation for the thirty grains used for long axis measurements divided by the grain size, i.e., the sorting values reported in Table 1.2.1 are relative standard deviations for the grain size measurements (= coefficients of variation). The numeric sorting values can be converted to a verbal scale according to the table below. The corresponding ϕ standard deviations (Folk, 1974) are given at the right hand side of the table.

Very well sorted

0.25----------0.35 ϕ

Well sorted

0.36----------0.50 ϕ

Moderately well sorted

0.52----------0.71 ϕ

Moderately sorted

0.79----------1.00 ϕ

Poorly sorted

2.42----------2.00 ϕ

Very poorly sorted

Table 1.2.1: Sorting. The numbers to the left are the relative standard deviations for the grain size measurements.

Two thin-sections from the Fruholmen Formation (Table 1.2.2a) and two from the Snadd Formation (Table 1.2.2b) were also examined in the cathodoluminescence mode with a Technosyn Cathodoluminescence Unit Mk II mounted on a Nikon Optiphot microscope. Cathodoluminescence micrographs were taken using a Nikon DS-Ri1 digital camera and exposure times of 30-100 seconds. Accelerating voltages were 6-10kV and gun currents 0.1-0.15mA. Nikon 4x CG Achromat and 10x CF Plan Achromat objectives were used. Cathodoluminescence was used to distinguish between different types of feldspar, between feldspar and quartz grains in unstained thin-sections, and between quartz grains and quartz cement (Amieux, 1982; Marshall, 1988).

Thin section no.	Well no.	Sample type	Formation	Depth (mRKB)	Depth (mRSF)	Lithology description	Type of thin section	Point count	Other analyses	Hor.Porosity(%)	Hor.Perm.(mD)
1	7131/4-1	COPL 1	Fruholmen	915,00	559,00	Sandstone	Polished	Yes		22,9	1032
2	7131/4-1	COPL 5	Fruholmen	916,00	560,00	Sandstone	Polished	Yes		19,4	125
3	7131/4-1	COPL 9	Fruholmen	917,00	561,00	Sandstone	Polished	No		29,4	3832
4	7131/4-1	COPL 13	Fruholmen	918,00	562,00	Sandstone	Polished	Yes		28,9	4225
5	7131/4-1	COPL 17	Fruholmen	919,00	563,00	Sandstone	Polished	Yes		30,5	NMP
6	7131/4-1	COPL 21	Fruholmen	920,00	564,00	Sandstone	Polished	No		31,4	19292
7	7131/4-1	COPL 25	Fruholmen	921,00	565,00	Sandstone	Polished	Yes	CL	29,7	20246
8	7131/4-1	COPL 29	Fruholmen	922,00	566,00	Sandstone	Polished	No		31,1	14947
9	7131/4-1	COPL 33	Fruholmen	923,00	567,00	Sandstone	Polished	Yes		28,6	3579
10	7131/4-1	COPL 37	Fruholmen	924,00	568,00	Sandstone	Polished	Yes	CL	28,6	7165
11	7131/4-1	COPL 41	Fruholmen	925,75	569,75	Siltstone	Polished	No		14,5	28,5
12	7131/4-1	COPL 42	Fruholmen	926,20	570,20	Siltstone	Polished	No		19,8	0,704
13	7131/4-1	COPL 46	Fruholmen	927,00	571,00	Siltstone	Polished	No		20,4	0,609
14	7131/4-1	COPL 50	Fruholmen	928,00	572,00	Siltstone	Polished	No		15,4	0,159
15	7131/4-1	COPL 54	Fruholmen	929,00	573,00	Siltstone	Polished	No		NMP	NMP
16	7131/4-1	COPL 58	Fruholmen	930,00	574,00	Siltstone	Polished	No		25,0	NMP
17	7131/4-1	COPL 62	Fruholmen	931,00	575,00	Siltstone	Polished	No		21,8	4,75
18	7131/4-1	COPL 66	Fruholmen	932,05	576,05	Siltstone	Polished	No		21,1	NMP
19	7131/4-1	COPL 70	Fruholmen	933,00	577,00	Siltstone	Polished	No		14,9	NMP
20	7131/4-1	COPL 74	Fruholmen	934,40	578,40	Siltstone	Polished	No		13,5	0,290
21	7131/4-1	COPL 77	Fruholmen	935,00	579,00	Siltstone	Polished	No		9,3	0,066
22	7131/4-1	COPL 81	Fruholmen	936,09	580,09	Siltstone	Polished	No		19,0	NMP
23	7131/4-1	COPL 85	Fruholmen	937,00	581,00	Sandstone	Polished	Yes		29,4	3436
24	7131/4-1	COPL 89	Fruholmen	938,00	582,00	Sandstone	Polished	No		17,6	NMP
25	7131/4-1	COPL 93	Fruholmen	939,00	583,00	Sandstone	Polished	Yes		27,8	1456
26	7131/4-1	COPL 97	Fruholmen	940,00	584,00	Sandstone	Polished	No		16,2	NMP
27	7131/4-1	COPL 101	Fruholmen	941,00	585,00	Sandstone	Polished	Yes		29,0	2276
28	7131/4-1	COPL 105	Fruholmen	942,00	586,00	Sandstone	Polished	No		22,3	1486
29	7131/4-1	COPL 108	Fruholmen	943,00	587,00	Sandstone	Polished	No		25,5	NMP

Table 1.2.2a: Fruholmen Formation thin-sections in well 7131/4-1. NMP: No measurement possible, CL: Cathodoluminescence, COPL: Core plug.

Thin section no.	Well no.	Sample type	Formation	Depth (mRKB)	Depth (mRSF)	Lithology description	Type of thin section	Point count	Other analyses	Hor.Porosity(%)	Hor.Perm.(mD)
30	7131/4-1	COPL 112	Snadd	1070,00	714,00	Sandstone	Polished	No		32,5	NMP
31	7131/4-1	COPL 116	Snadd	1071,00	715,00	Sandstone	Polished	No		32,5	2,26
32	7131/4-1	COPL 120	Snadd	1072,00	716,00	Sandstone	Polished	No		30,6	0,283
33	7131/4-1	COPL 124	Snadd	1073,00	717,00	Sandstone	Polished	Yes		29,0	NMP
34	7131/4-1	COPL 128	Snadd	1074,00	718,00	Sandstone	Polished	No		32,6	0,33
35	7131/4-1	COPL 132	Snadd	1075,00	719,00	Sandstone	Polished	Yes		32,7	0,36
36	7131/4-1	COPL 136	Snadd	1076,00	720,00	Sandstone	Polished	Yes		34,5	0,657
37	7131/4-1	COPL 140	Snadd	1077,00	721,00	Sandstone	Polished	No		29,0	0,187
38	7131/4-1	COPL 144	Snadd	1078,00	722,00	Sandstone	Polished	No		22,2	0,070
39	7131/4-1	COPL 148	Snadd	1079,00	723,00	Sandstone	Polished	No		34,0	1,71
40	7131/4-1	COPL 152	Snadd	1080,00	724,00	Sandstone	Polished	No		30,0	332
41	7131/4-1	COPL 156	Snadd	1081,00	725,00	Sandstone	Polished	Yes		32,1	1480
42	7131/4-1	COPL 160	Snadd	1082,00	726,00	Sandstone	Polished	No		32,6	2286
43	7131/4-1	COPL 164	Snadd	1083,00	727,00	Sandstone	Polished	Yes		34,5	3902
44	7131/4-1	COPL 168	Snadd	1084,00	728,00	Sandstone	Polished	No		30,8	906
45	7131/4-1	COPL 172	Snadd	1085,00	729,00	Sandstone	Polished	No		32,5	838
46	7131/4-1	COPL 176	Snadd	1086,00	730,00	Sandstone	Polished	No		33,4	101
47	7131/4-1	COPL 180	Snadd	1087,00	731,00	Sandstone	Polished	Yes		35,4	3812
48	7131/4-1	COPL 184	Snadd	1088,00	732,00	Sandstone	Polished	Yes	CL	36,0	3468
49	7131/4-1	COPL 188	Snadd	1089,05	733,05	Sandstone	Polished	No		23,7	151
50	7131/4-1	COPL 192	Snadd	1090,00	734,00	Sandstone	Polished	No		18,2	2,71
51	7131/4-1	COPL 195	Snadd	1091,00	735,00	Sandstone	Polished	No		28,4	275
52	7131/4-1	COPL 199	Snadd	1092,00	736,00	Sandstone	Polished	No		27,1	191
53	7131/4-1	COPL 203	Snadd	1093,00	737,00	Sandstone	Polished	No		17,0	1,78
54	7131/4-1	COPL 207	Snadd	1094,00	738,00	Sandstone	Polished	Yes		29,6	1283
55	7131/4-1	COPL 211	Snadd	1095,00	739,00	Sandstone	Polished	No		28,8	482
56	7131/4-1	COPL 215	Snadd	1096,00	740,00	Sandstone	Polished	No		26,9	427
57	7131/4-1	COPL 219	Snadd	1097,00	741,00	Sandstone	Polished	Yes		28,7	1067
58	7131/4-1	COPL 223	Snadd	1098,00	742,00	Sandstone	Polished	No		28,3	267
59	7131/4-1	COPL 227	Snadd	1099,13	743,13	Sandstone	Polished	No		29,0	442
60	7131/4-1	COPL 231	Snadd	1100,00	744,00	Sandstone	Polished	Yes		30,4	517
61	7131/4-1	COPL 235	Snadd	1101,00	745,00	Sandstone	Polished	No		31,1	723
62	7131/4-1	COPL 239	Snadd	1102,00	746,00	Sandstone	Polished	Yes		8,0	0,028
63	7131/4-1	COPL 243	Snadd	1103,00	747,00	Sandstone	Polished	Yes	CL	33,4	2325
64	7131/4-1	COPL 247	Snadd	1104,00	748,00	Sandstone	Polished	No		29,5	735
65	7131/4-1	COPL 251	Snadd	1105,00	749,00	Sandstone	Polished	No		32,4	695
66	7131/4-1	COPL 255	Snadd	1106,00	750,00	Sandstone	Polished	No		32,3	559
67	7131/4-1	COPL 259	Snadd	1107,00	751,00	Sandstone	Polished	Yes		30,9	215
68	7131/4-1	COPL 263	Snadd	1108,00	752,00	Sandstone	Polished	No		31,9	476
69	7131/4-1	COPL 267	Snadd	1109,00	753,00	Sandstone	Polished	No		33,3	1145
70	7131/4-1	COPL 271	Snadd	1110,00	754,00	Sandstone	Polished	No		32,5	1576
71	7131/4-1	COPL 275	Snadd	1111,05	755,05	Sandstone	Polished	Yes		34,2	1925
72	7131/4-1	COPL 279	Snadd	1112,15	756,15	Sandstone	Polished	No		18,0	0,093
73	7131/4-1	COPL 280	Snadd	1113,00	757,00	Sandstone	Polished	No		18,9	0,585
74	7131/4-1	COPL 284	Snadd	1117,75	761,75	Sandstone	Polished	No		13,9	NMP

Table 1.2.2b: Thin-sections from the Snadd Formation in well 7131/4-1. NMP: No measurement possible, CL: Cathodoluminescence, COPL: Core plug.

Well 7222/11-1

From well 7222/11-1 thirty-four thin-sections made by Statoil from cores and side wall cores were examined. Ten were made from the upper cored Carnian to Early Norian Snadd Formation interval 778-807.2mRKB and five from the deepest Carnian Snadd Formation core at 1287-1299.4mRKB. The eight remaining thin-sections from the Snadd Formation are from side wall cores (Table 1.2.3). All eleven thin-sections from the Anisian Kobbe Formation were made from the cored interval 2209.5-2243.4mRKB. Water depth is 356m and the distance between the sea surface and the rotary table is 23m (NPD factpages). Burial depth is therefore 399-428.2mRKB and 908-920.4mRKB for the Snadd Formation cores in well 7222/11-1 and 1830.5-1864.4mRKB for the Kobbe Formation cores. Thin-sections from cores were made from the plugs used for routine measurements of helium porosity and air permeability. The thin-sections were stained for carbonates with Alizarin Red solution and potassium ferricyanide, and for K-feldspar with sodium cobaltinitrite. This gives non-ferroan calcite a reddish pink colour while ferroan calcite appears blue. Ferroan dolomite and ankerite are stained paler blue whereas dolomite and siderite are not stained by these solutions (Dickson, 1966). K-feldspar is stained yellow by the sodium cobaltinitrite solution (Scholle, 1979). Porosity was impregnated with blue epoxy. From the sampled depths 2236.50 and 2238.50mRKB polished thin-sections were also made in addition to the stained thin-sections from these depths.

All thin-sections were studied with a petrographic microscope, and micrographs were taken of representative samples with a Nikon DS-Fi1 digital camera. Twelve thin-sections from the Snadd Formation and five thin-sections from the Kobbe Formation were point-counted with three hundred points per thin-section (Table 1.2.3). Grain size was determined by measuring the long axis of thirty grains on each point-counted thin-section and calculating the mean value. Sorting was determined as described above for well 7131/4-1.

Two thin-sections from the Kobbe Formation were also examined in the cathodoluminescence mode (Table 1.2.3). Instrumentation and instrument settings were the same as described above for well 7131/4-1.

Thin section no.	Well no.	Sample type	Formation	Depth (mRKB)	Depth (mRSF)	Lithology	Type of thin section	Point count	Other analyses	Hor.Porosity (%)	Hor.Perm. (mD)
1	7222/11-1	SWC 1	Snadd	641,70	262,70	Sandstone	Stained	No		34,3	213,0
2	7222/11-1	SWC 6	Snadd	680,70	301,70	Sandstone	Stained	No		32,2	93,2
3	7222/11-1	COPC 1	Snadd	778,03	399,03	Sandstone	Stained	Yes		32,8	1732
4	7222/11-1	COPL 9	Snadd	780,02	401,02	Sandstone	Stained	No		31,4	1149
5	7222/11-1	COPL 17	Snadd	782,02	403,02	Sandstone	Stained	Yes		31,8	1358
6	7222/11-1	COPL 26	Snadd	784,25	405,25	Sandstone	Stained	Yes		31,7	1290
7	7222/11-1	COPL 33	Snadd	786,02	407,02	Sandstone	Stained	No		31,4	995
8	7222/11-1	COPL 41	Snadd	788,05	409,05	Sandstone	Stained	Yes		33,9	1737
9	7222/11-1	COPL 57	Snadd	792,02	413,02	Sandstone	Stained	No		32,9	1268
10	7222/11-1	COPL 65	Snadd	794,02	415,02	Sandstone	Stained	Yes		33,6	1802
11	7222/11-1	COPL 73	Snadd	796,02	417,02	Sandstone	Stained	No		32,7	1298
12	7222/11-1	COPL 87	Snadd	799,02	420,02	Sandstone	Stained	Yes		31,0	369
13	7222/11-1	SWC 23	Snadd	1102,00	723,00	Sandstone	Stained	Yes		27,8	214,0
14	7222/11-1	COPL 117	Snadd	1287,00	908,00	Sandstone	Stained	Yes		33,7	91,3
15	7222/11-1	COPL 125	Snadd	1289,00	910,00	Sandstone	Stained	No		31,8	91,1
16	7222/11-1	COPL 133	Snadd	1291,00	912,00	Sandstone	Stained	Yes		32,4	157
17	7222/11-1	COPL 142	Snadd	1293,25	914,25	Sandstone	Stained	No		15,8	0,386
18	7222/11-1	COPL 157	Snadd	1297,00	918,00	Sandstone	Stained	No		21,7	0,191
19	7222/11-1 T2	SWC 49	Snadd	1495,40	1116,40	Sandstone	Stained	Yes		21,6	31,7
20	7222/11-1 T2	SWC 48	Snadd	1617,30	1238,30	Sandstone	Stained	Yes		6,8	0,078
21	7222/11-1 T2	SWC 46	Snadd	1647,70	1268,70	Sandstone	Stained	No		23,8	31,4
22	7222/11-1 T2	SWC 43	Snadd	1792,10	1413,10	Sandstone	Stained	No		14,4	0,564
23	7222/11-1 T2	SWC 42	Snadd	1800,60	1421,60	Sandstone	Stained	Yes		17,7	5,62
24	7222/11-1 T3	COPL 177	Kobbe	2215,25	1836,25	Sandstone	Stained	Yes		12,5	0,037
25	7222/11-1 T3	COPL 202	Kobbe	2221,50	1842,50	Sandstone	Stained	No		14,4	0,289
26	7222/11-1 T3	COPL 239	Kobbe	2235,00	1856,00	Sandstone	Stained	Yes		19,1	2,76
27	7222/11-1 T3	COPL 241	Kobbe	2235,52	1856,52	Sandstone	Stained	Yes		19,8	13,2
28	7222/11-1 T3	COPL 245	Kobbe	2236,50	1857,50	Sandstone	Stained	No		19,5	5,06
29	7222/11-1 T3	COPL 245	Kobbe	2236,50	1857,50	Sandstone	Polished	No	CL	19,5	5,06
30	7222/11-1 T3	COPL 246	Kobbe	2237,00	1858,00	Sandstone	Stained	No		18,7	3,55
31	7222/11-1 T3	COPL 251	Kobbe	2238,50	1859,50	Sandstone	Stained	Yes		20,7	19,9
32	7222/11-1 T3	COPL 251	Kobbe	2238,50	1859,50	Sandstone	Polished	Yes	CL	20,7	19,9
33	7222/11-1 T3	COPL 253	Kobbe	2239,00	1860,00	Sandstone	Stained	No		17,0	0,456
34	7222/11-1 T3	COPL 261	Kobbe	2241,10	1862,10	Sandstone with large mudclasts	Stained	No		14,1	0,331

Table 1.2.3: Thin-sections from the Snadd and Kobbe formations, well 7222/11-1. CL: Cathodoluminescence, COPL: Core plug, SWC: Side wall core.

1.3 Sources of errors

In the thin-section study only 300 points were counted per thin-section, which means that the whole thin-section is not accounted for, only a selection of points that are assumed to be representative for the sample. Due to this statistical element of the analysis, the results from the point-counting are only estimates of sample composition. In addition it is difficult to register microporosity, and point-counted porosity values may therefore be somewhat lower than measured helium porosities. Also, some thin-sections are somewhat damaged and therefore contain some false pores. In some thin-sections in well 7222/11-1 the staining of K-feldspar with sodium cobaltinitrite solution was quite poor and difficult to register. It is therefore possible that some K-feldspar grains in this well were point-counted as quartz since some feldspar grains lack clear twinning. There will also be a possibility for misinterpretation of highly dissolved grains, especially feldspars (K-feldspar versus plagioclase), and of dirty and damaged grains. Sometimes it was difficult to distinguish between chert and polycrystalline quartz, and between quartz clasts and quartz overgrowths due to a lack of well-defined dust rims on some quartz grains.

The calculated values of grain size will also have some errors since the measurements were performed on a selection of grains. Also, because the thin-sections will often not show the maximum diameter of a grain, the measured grain sizes are probably slightly smaller than the true grain sizes. This effect has been considered to make grain size measured in thin-section 10-15% smaller than true grain size (Johnson, 1994).

In a few samples where drilling mud is found in the pore system, measured helium porosities and air permeabilities will be too low.

2 Geological setting

2.1 The Barents Sea area

The Barents Sea area is located between Novaya Semlja and an imaginary line from the South Cape of Spitsbergen via Bjørnøya to the North Cape of Norway (Figure 1.1.1). It extends to Franz Josef Land in the North. The Barents Sea area is made up of several different basins, platforms and structures (Doré, 1995; Gabrielsen et al., 2011), and the basins are separated by deep-seated faults, structural highs and subplatforms. The structure of the Barents Sea has been formed by different geological events, most notably two major orogenies succeeded by separation of the continents. Approximately 400 million years ago (Late Silurian-Early Devonian) the continental plates of Laurentia (Greenland, North America) and the Baltic plate (Scandinavia, western Russia) collided and formed a new large area of land called the Laurasian continent. This continent collision culminated with the Caledonian orogeny and closing of the Iapetus ocean (Doré, 1995). Further collision between the Laurasian continent and Western Siberia, which occurred approximately 240 million years ago in the latest Permian-earliest Triassic, is known as the Uralian orogeny and is considered to have created the eastern margin of the Barents Sea. The Uralian orogeny marks the final event in the formation of the Pangaean supercontinent in Permian-Triassic times (Scotese, 1987).

In the Early Carboniferous the area that today is considered the Barents Sea was situated close to the Equator in the tropics, and the climate was warm and humid. The period is characterized by rift basins, such as the Nordkapp Basin, with continental sandstones, mudstones and coal, and the main depositional environments were rivers and swamps (see Figure 2.1.1). The area drifted northwards throughout the Carboniferous and in the Mid Carboniferous it moved from a tropical zone into an arid and warm desert climate. Main deposits were red sand- and mudstones, limestones and evaporites in narrow rift basins. A separation of Norway and Greenland was initiated in the Mid Carboniferous, but this movement ended in the Late Carboniferous-Early Permian (Nøttvedt and Worsley, 2007). In the Late Carboniferous and the Early Permian, a thick succession of shallow- and warm-water carbonates formed (Ehrenberg, 2004).

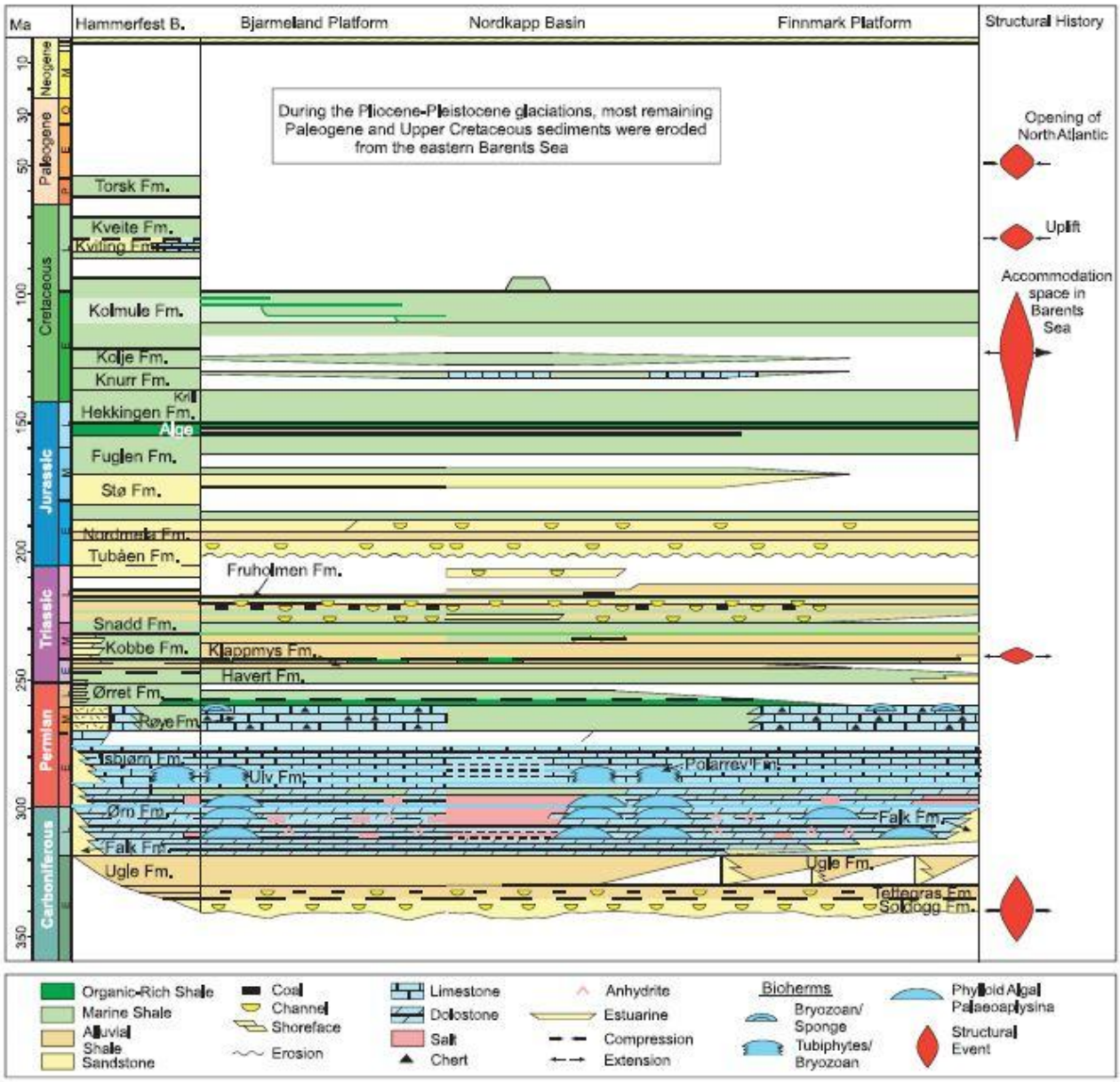

Figure 2.1.1: Stratigraphic column showing the main lithologies in the Hammerfest Basin, Bjarmeland Platform, Nordkapp Basin and Finnmark Platform. From Ohm et al. (2008).

Fossils of Late Permian age suggest a change in depositional environment in the whole Barents Sea area. The area drifted northwards to cooler waters from the arid zone to a more temperate climate. Mudstones, sandstones and limestones were the most notable deposits, and in the latest Permian spiculites were also deposited (Nøttvedt and Worsley, 2007). In the end of the Permian, deglaciation led to sea level rise and major deposition of mud in a large portion of the Barents Sea area. This mud hardened into limestone and flint-like mudstone in the transition period from the Permian to the Triassic. Throughout the Triassic the south western part of the Barents Sea area, including the areas that in the Jurassic evolved into the

Hammerfest-, Tromsø-, Bjørnøya- and Nordkapp basins, subsided rapidly, but a large sediment supply led to these areas being filled up with sediments (Nystuen et al., 2007). In the Early Triassic a transition to deposition of mud and sand layers in shallow marine depositional settings is seen, while the deposition of carbonates ended. Sediment supplied from the Urals in the east spread westward (Mørk, 1999; Riis et al., 2008), and in the Early Triassic there also occurred movement of Permian salt in the Nordkapp basin, and the salt in the form of pillows and pillars rose through the Triassic layers (Bugge et al., 2002). In the Mid Triassic dark grey and black phosphatic mudstones with large contents of organic material were deposited, and these have proven to be source rocks for oil. The evolution of the Barents Sea area in the Triassic ended with a fall in sea level. This led to deposition of sand with a high content of quartz (Bergan and Knarud, 1992), which implies that the areas were exposed to major chemical weathering in a warm and humid climate. In the Goliat Field in the Hammerfest Basin the oil is found in reservoir units from the entire Triassic period. Estimates from the Norwegian Petroleum Directorate for recoverable resources in the Goliat Field are 30.6Sm^3 oil, 7.3 billion Sm^3 gas and 0.3 billion tonnes of natural gas liquids. According to the NPD the main reservoir is the Kobbe Formation and the Realgrunnen Group (NPD factpages).

Throughout the Early and Middle Jurassic the most important deposits were shallow marine sands. The Middle Jurassic Stø Formation is considered to be the most important reservoir rock in the southern part of the Barents Sea. It contains massive sands with good porosity and permeability and low content of mud (Johannessen and Nøttvedt, 2007). In the Late Jurassic the conditions in the Barents Sea area were relatively calm, but the rifting that was occurring further south reached the southern parts of the Barents Sea area and continued into the Early Cretaceous. The rifting resulted in rotated fault blocks, which have been shown to work as oil traps, and the creation of for instance the Loppa-, Stappen- and Sentralbanken highs. Since these highs were uplifted and eroded in the Late Jurassic and Early Cretaceous, no Upper Jurassic deposits are seen on these highs today. The Upper Jurassic Hekkingen Formation contains organic-rich mud deposits. The mudstones have a high content of marine algae and plankton and are therefore good source rocks. The Hekkingen Formation is considered to be the source of a lot of the oil and gas in the Hammerfest Basin (Nøttvedt and Johannessen, 2007).

The Middle Jurassic Stø and Normela formations are reservoir rocks in the Snøhvit Field (Folkestad, 2007). The field consists of the Askeladd, Albatross and Snøhvit discoveries and is located in the central Hammerfest Basin. Recoverable resources have been estimated as 191 million Sm^3 oil equivalents, which consist of 160.6 million Sm^3 gas, 18.1 million Sm^3 condensate, and 6.4 million tonnes natural gas liquids (NPD factpages). On the first of April 2011 it was announced that hydrocarbons had been found in the Skrugard well in the Bjørnøyrenna fault complex. The well had a gas column of 33m and an oil column of 90m, and the oil is considered to be of good quality (Statoil ASA homepages). Gas and oil is present in the Stø Formation and oil is found in the Nordmela Formation.

Throughout the Cretaceous the Barents shelf is considered to have been a large platform area. Mud and calcareous mud was deposited over most of the area plus some sand around highs like the Loppa High (Brekke and Olaussen, 2007). The rifting between Norway and Greenland continued throughout the Cretaceous, and severe uplift and erosion has resulted in Cretaceous deposits having been removed from large areas of the Barents Sea. Paleocene to Eocene deposits are shale-dominated from open to deep marine environments. It is difficult to say much about the Oligocene and Miocene because hardly any sediment is preserved, but further west in the Sørvestnaget Basin sediments of Paleocene to Miocene age are found (Ryseth et al., 2003). Throughout the Early Paleocene to Late Eocene a deep marine environment is suggested, with sandy fans deposited within the shale dominated package. At the boundary between the Eocene and the Oligocene the depositional environment becomes more shallow, and throughout the Oligocene and the Miocene it was shallow marine. The area continued to move further north, and from the Pliocene until today a succession of ice ages led to glaciers eroding large parts of the area to the east, with sediment deposition in the form of fans to the west (Gabrielsen et al., 1990; Vorren and Mangerud, 2007).

2.2 The Finnmark Platform

Well 7131/4-1 is situated in the Finnmark East area, which is located on the eastern part of the Finnmark Platform. The Finnmark platform is located between the outcrop of the Caledonides on the Norwegian mainland, and the Hammerfest and Nordkapp basins (Figure 1.1.1). In the Norwegian sector the eastern part of the Finnmark Platform is seen as an underlying rift topography with fault blocks. These fault blocks consist mainly of Early Carboniferous siliciclastic rocks, and above these blocks a carbonate-dominated sequence of Late

Carboniferous to Permian age is present (Ehrenberg, 2004). Throughout the Permian a transgression of the western part of the Finnmark Platform resulted in deposition of siliciclastic and carbonate sequences. During the Triassic parts of the Finnmark Platform were covered by siliciclastic sediment derived from Norway and from the Urals to the east. The platform was modified in the Late Jurassic due to movement along pre-existing faults, and some Cretaceous marine sandstones and mudstones were deposited on parts of the platform (400m present in well 7131/4-1). Uplift in the Late Tertiary led to the present day northward tilt of the platform and erosion of Tertiary and Cretaceous strata (Gabrielsen et al., 1990; Larssen et al., 2002).

2.3 The Bjarmeland Platform

Well 7222/11-1 was drilled on the the Bjarmeland Platform which is situated between the Hammerfest and Nordkapp basins to the south and southeast, and the Sentralbanken and Gardarbanken highs to the North (Figure 1.1.1). The southern and western areas of the platform are divided into smaller highs and sub-basins, one of these being the Svalis Dome characterized by evaporites and diapirism. The platform is of Permian age but due to Tertiary uplift the platform sediments have a slight dip to the south and older sediments subcrop to the north at the unconformity at the base of the Quaternary. A transition from siliciclastics in the Early Carboniferous to carbonates in the Late Carboniferous and Permian is registered, and this boundary is thought to represent the transition from a pre-platform to a platform development. During the Triassic thick siliciclastic deposits (more than 2km in well 7222/11-1) sourced from the south and east covered the platform. Due to erosion in the Tertiary, the preserved post-Triassic succession is thin, and often comprises less than a few hundred metres of Jurassic to Cretaceous sediments overlain by thin Pleistocene to recent sediments (Gabrielsen et al., 1990; Larssen et al., 2002).

2.4 The Kobbe Formation

The Kobbe Formation is a part of the Ingøydjupet Group and is of Anisian age. The reference well for the Kobbe Formation is well 7120/12-2, with the Kobbe Formation section extending from 2927 to 3095mRKB. This Kobbe Formation section is 168m thick and consists of a basal approximately 20m thick shale sequence that passes upward into interbedded shale, siltstone and carbonate-cemented sandstone. The depositional environment is characterized by

a transgressive pulse, with subsequent buildout of siliciclastic marginal marine regimes from southern coastal areas (Worsley et al., 1988).

2.5 The Snadd Formation

The Snadd Formation is also a part of the Ingøydjupet Group and of Ladinian to Early Norian age. The reference well for this formation is the same as for the Kobbe Formation, well 7120/12-2, with the Snadd Formation represented from 2354 to 2927mRKB. The section contains basal grey shales that coarsen upwards into shales with interbeds of grey siltstones and sandstones. In the lower and middle part of the section limestones and calcareous beds are common, whereas further up thin lenses of coal have developed locally. Towards the top of the section there is an occurrence of red-brown shales.

Deposits from the Ladinian are distal marine, following a major transgressive pulse which submerged all structural highs and platforms in the region. Some southern silts and sands are suggested to be storm-derived. The Carnian sequence is considered to represent large-scale progradation of deltaic systems in the whole area (Worsley et al., 1988).

2.6 The Fruholmen Formation

The Fruholmen Formation is a part of the Realgrunnen Group and of Norian to Rhaetian age. This formation was originally defined by the Norwegian Petroleum Directorate based on the succession encountered in well 7121/5-1 where the Fruholmen Formation is present from 2572 to 2793mRKB and on the interval 2337-2535mRKB in well 7120/12-1. The section in well 7120/12-1 consists of basal grey to dark shales that gradually pass into sandstones, shales and coals upward in the section. The middle part of the section is dominated by sand, while the upper part is more shaly.

The basal shales are thought to be open marine, and the sandstone dominated sequence further up is considered to be coastal and fluvial. This indicates northward fluviodeltaic progradation with the depocentre situated in the south. A lateral shift in the deltaic input has led to a large portion of the central and southern parts of the basin becoming a site of flood-plain deposition, with more marine environments to the north (Worsley et al., 1988).

3 Well 7131/4-1

3.1 The Fruholmen Formation

3.1.1 Depositional environment

The core description from well 7131/4-1 (Figures 3.1.1a and b) shows that the lowermost 10m of the cored section from the Fruholmen Formation comprise medium- to coarse-grained and dominantly clay-poor sandstone. Individual beds are typically a few tens of centimeters thick and often cross-bedded or contain current ripples. Some bioturbation and fragments of coal or plants are seen. The interval comprises several fining upward units, and the depositional setting is probably fluvial or tidal channels. Above the channel sandstones an approximately 10m thick (934.5-925m) more muddy interval is found where up to 1m thick fine- and more rarely medium-grained sandstones are interbedded with siltstones and very fine-grained muddy sandstones. Some of the sandstones show wave ripples, and bioturbation is quite common. This more muddy interval is interpreted as lagoon or bay deposits with the sandstones representing minor mouth bars and crevasse splays. The lagoonal or bay deposits are overlain by 6m of upward fining, clay-free coarse and medium-grained sandstone with large foresets and some coal fragments. The base of this unit is erosive, and the interval 925-919m was probably deposited in a fluvial channel. The fluvial channel sandstone is capped by 4m of thin (0.1-0.5m) and partly muddy very fine- and fine-grained sandstone beds with current ripples and a few bioturbation structures. This uppermost interval is thought to represent infilling of a more or less abandoned fluvial channel.

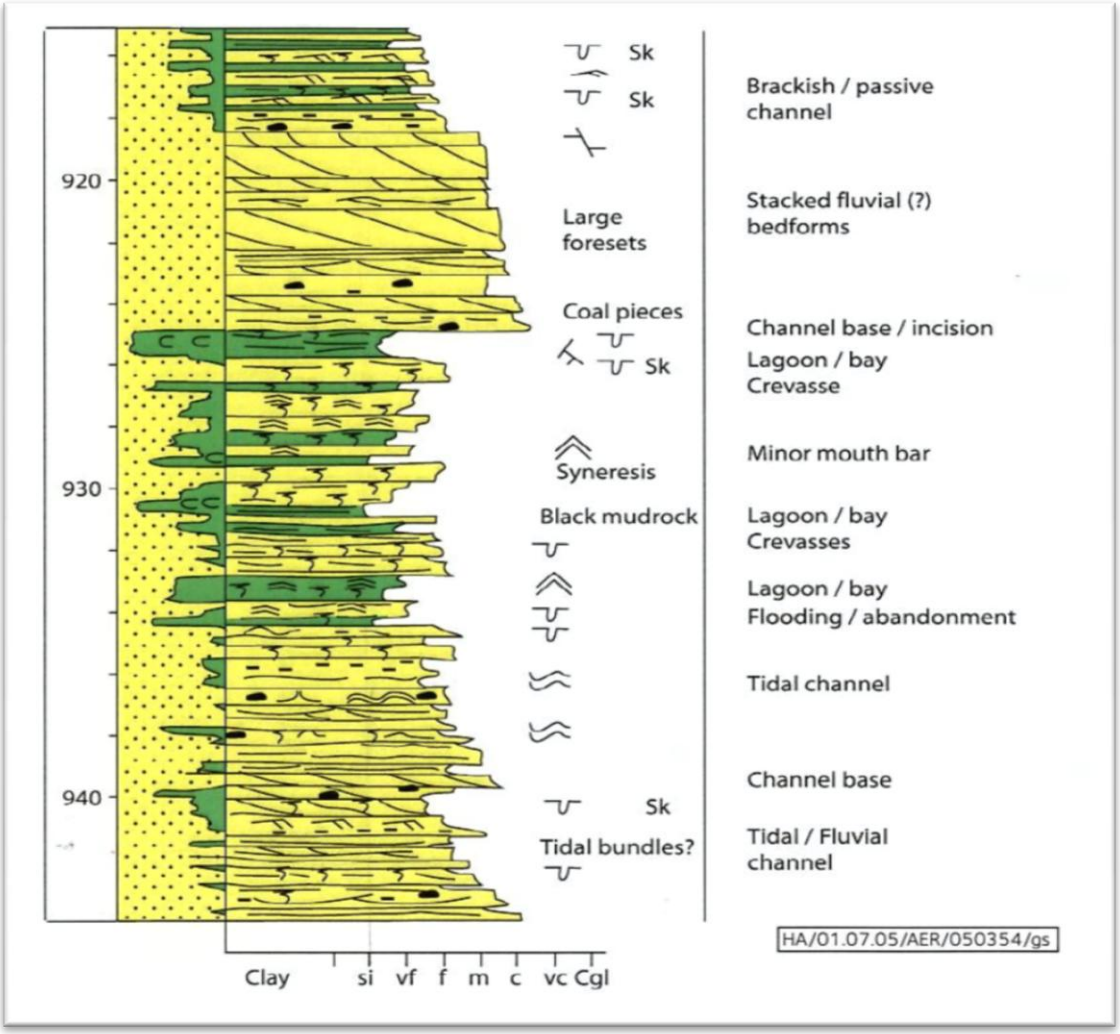

Figure 3.1.1a: Core description, Fruholmen Formation, well 7131/4-1. Depths in mRKB. Figure provided by Statoil ASA.

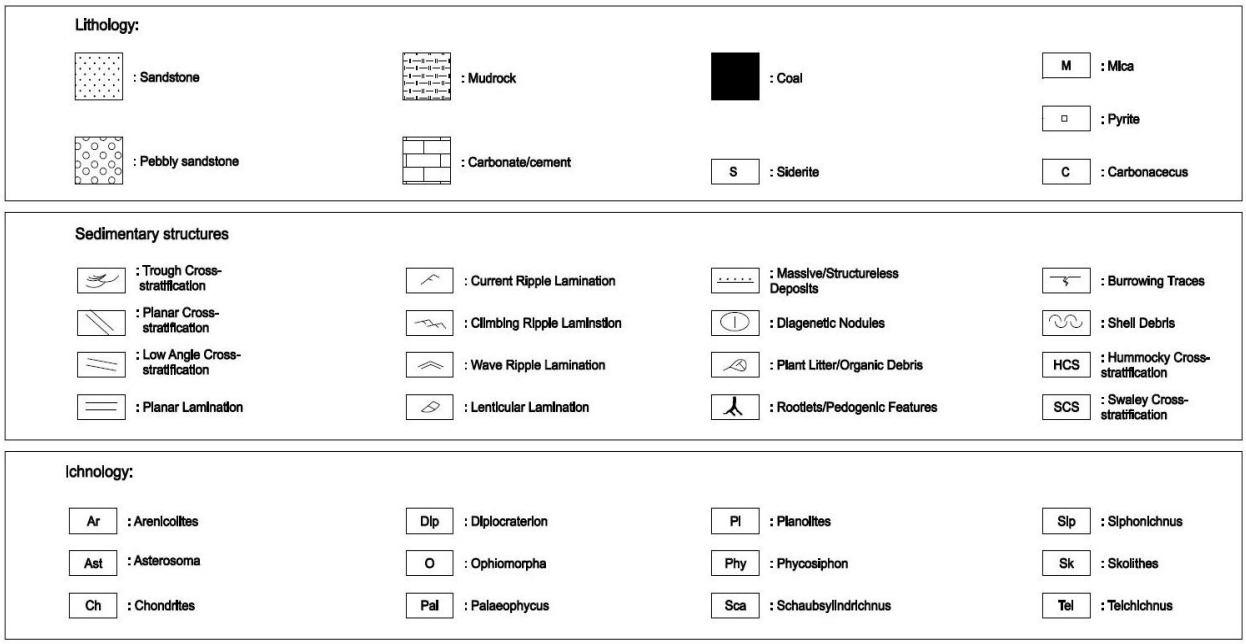

Figure 3.1.1b: Legend, core descriptions.

3.1.2 Petrographic composition

Lithology and texture

The shallowest ten thin-sections (915-924mRKB) from the Fruholmen Formation are from well sorted fine- and medium-grained, and more rarely coarse-grained sandstones that contain almost no detrital clay matrix. The following twelve samples (925.75-936.09mRKB) are fine-, medium- and coarse-grained siltstones with detrital clay contents being quite low for the most part. The remaining seven samples from the Fruholmen Formation (937-943mRKB) are moderately well to moderately sorted fine- and medium-grained sandstones with very little or no detrital clay. Grains are typically subangular (Figure 3.1.2).

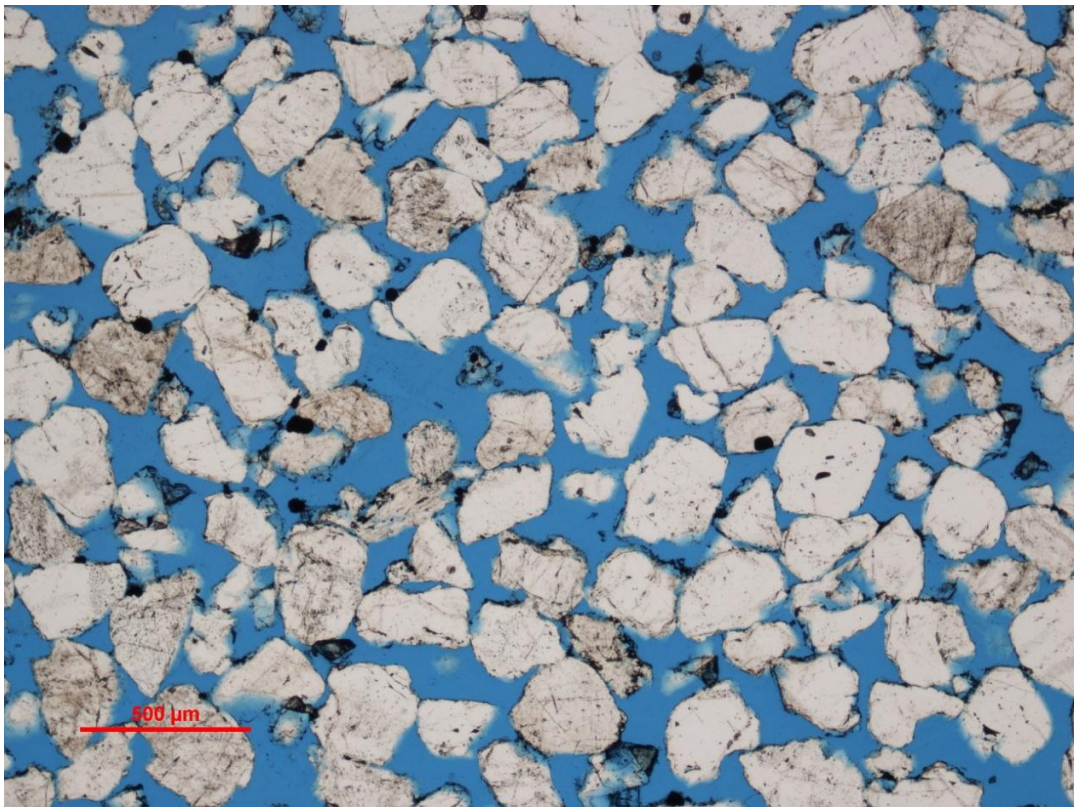

Figure 3.1.2: Medium-grained quartz arenite with 2% quartz cement and helium porosity 30.5%. Permeability was not measured. No detrital clay matrix is present. Scale bar is 500µm. Fruholmen Formation, 919.00mRKB.

Detrital grains

Quartz is the dominant detrital mineral and is present in volumes of 58.5-68.7% (Table 3.1.1). The detrital quartz consists mainly of monocrystalline grains. A few polycrystalline quartz grains are present, in addition to a few chert grains and quartz-rich fragments of metamorphic rocks.

Depth mRKB	Depth mRSF	Formation	Monocryst. quartz clasts	Polycryst. quartz clasts	Chert clasts	K-feldspar clasts	Plagioclase clasts	Muscovite clasts	Biotite clasts	Chlorite clasts	Heavy minerals	Plant fragm.	Clay clasts and mica rich rock fragm.	Qtz. rich meta fragm.	Detrital clay matrix	Quartz cement	Albite cement
915,00	559,00	Fruholmen	63,9	0,3	trace	0,7		0,3			trace	0,3	1,8	trace	3,0	0,7	
916,00	560,00	Fruholmen	58,5	trace		0,3		0,7		trace	trace	trace	5,3		18,3	0,3	
918,00	562,00	Fruholmen	67,7			0,3					trace		trace		trace	1,0	
919,00	563,00	Fruholmen	65,7	1,3	trace	0,3					trace					2,0	
921,00	565,00	Fruholmen	67,0	1,0	trace	0,3		trace			trace					0,7	
923,00	567,00	Fruholmen	65,0	1,3	trace	0,3					trace					1,3	
924,00	568,00	Fruholmen	61,7	1,3		0,3					trace			trace		trace	
937,00	581,00	Fruholmen	67,3	0,7	trace						trace					2,3	
939,00	583,00	Fruholmen	66,7	2,0		trace		trace			trace	trace	trace		3,3	0,3	
941,00	585,00	Fruholmen	63,7	0,3	trace	trace		trace			trace		0,7		6,0	0,7	
1073,00	717,00	Snadd	25,7	5,3	2,3	0,3				0,3	trace		16,0	2,0			
1075,00	719,00	Snadd	33,3	5,3	4,3	0,7		0,3			trace		8,3	4,7			
1081,00	725,00	Snadd	33,3	2,3	4,7	2,0	0,7				trace		6,7	11,0		trace	
1083,00	727,00	Snadd	36,6	4,0	4,3	1,0	1,3	trace		0,3	trace		5,7	9,7			
1087,00	731,00	Snadd	32,0	5,0	4,3	1,3	0,3	0,3		trace	trace		5,7	6,3			
1088,00	732,00	Snadd	46,7	5,7	3,7	1,0	0,3	trace			trace		3,0	9,0			
1094,00	738,00	Snadd	43,7	4,3	4,7	2,3	1,3	trace	trace		trace		5,7	5,0	0,3		
1097,00	741,00	Snadd	46,3	3,3	2,3	2,3	1,3	0,3		0,7	trace		6,0	5,3		trace	
1100,00	744,00	Snadd	36,3	2,3	1,3	1,3	1,0	0,7	trace	trace	trace		13,0	5,3		trace	
1102,00	746,00	Snadd	32,0	0,3	1,0	1,0	0,3	0,3		0,3	0,3		9,7	7,7			
1103,00	747,00	Snadd	41,3	2,7	2,3	4,3	0,7	0,3			trace		7,7	3,7			
1107,00	751,00	Snadd	34,3	3,0	3,0	2,7	1,0				trace		12,7	3,7			
1111,05	755,05	Snadd	27,7	3,7	4,3	2,3	1,7	0,3		0,3	trace		14,3	3,0		trace	

Depth mRKB	Depth mRSF	Formation	Chlorite cement	Kaolin cement	Siderite cement	Calcite cement	Pyrite cement	Porosity, primary	Porosity, dissol.	Grain size mm	Sorting (coef. of var.)	Sorting verbal scale	Porosity % (He)	KhL mD
915,00	559,00	Fruholmen		1,7			0,3	27,0	trace	0,17	0,33	Well sorted	22,9	1032,0
916,00	560,00	Fruholmen		1,0			0,3	15,3		0,19	0,41	Moderately well sorted	19,4	125,0
918,00	562,00	Fruholmen					trace	31,0	trace	0,17	0,41	Moderately well sorted	28,9	4225,0
919,00	563,00	Fruholmen					trace	30,7	trace	0,27	0,40	Moderately well sorted	30,5	NMP
921,00	565,00	Fruholmen		trace			trace	31,0	trace	0,30	0,33	Well sorted	29,7	20246,0
923,00	567,00	Fruholmen					trace	32,0	trace	0,29	0,44	Moderately well sorted	28,6	3579,0
924,00	568,00	Fruholmen					trace	36,6	trace	0,66	0,34	Well sorted	28,6	7165,0
937,00	581,00	Fruholmen						29,7		0,17	0,25	Well sorted	29,4	3436,0
939,00	583,00	Fruholmen						27,7		0,20	0,51	Moderately well sorted	27,8	1456,0
941,00	585,00	Fruholmen		trace			trace	28,7	trace	0,21	0,53	Moderately sorted	29,0	2276,0
1073,00	717,00	Snadd	36,0		0,7			11,0	0,3	0,31	0,36	Moderately well sorted	29,0	NMP
1075,00	719,00	Snadd	33,3		5,7			2,3	1,7	0,33	0,39	Moderately well sorted	32,7	0,36
1081,00	725,00	Snadd	9,3		2,3			23,0	4,7	0,24	0,37	Moderately well sorted	32,1	1480
1083,00	727,00	Snadd	7,3		0,7			25,0	4,0	0,29	0,41	Moderately well sorted	34,5	3902
1087,00	731,00	Snadd	6,7	0,7	1,7			32,3	3,3	0,24	0,34	Well sorted	35,4	3812
1088,00	732,00	Snadd	4,0	0,7				24,0	2,0	0,28	0,39	Moderately well sorted	36,0	3468
1094,00	738,00	Snadd	7,0	1,0	0,3			20,7	3,7	0,28	0,36	Moderately well sorted	29,6	1283
1097,00	741,00	Snadd	5,7	0,3	0,3			22,3	3,3	0,28	0,32	Well sorted	28,7	1067
1100,00	744,00	Snadd	7,0	0,7	1,0			27,0	3,0	0,23	0,35	Well sorted	30,4	517
1102,00	746,00	Snadd	0,3		0,7	34,7		10,7	0,7	0,24	0,22	Very well sorted	8,0	0,028
1103,00	747,00	Snadd	7,7	0,3			trace	24,7	4,3	0,29	0,30	Well sorted	33,4	2325
1107,00	751,00	Snadd	10,3	0,3	1,7			23,0	4,3	0,28	0,31	Well sorted	30,9	215
1111,05	755,05	Snadd	5,3			0,7		32,3	4,0	0,24	0,32	Well sorted	34,2	1111,05

Table 3.1.1: Modal analyses, well 7131/4-1. NMP: No measurement possible.

K-feldspar, commonly with microcline twins, accounts for up to 0.7% of sample volumes (Figures 3.1.3a and b). Many of the grains are partly dissolved, however, it is difficult to say whether this dissolution took place before or after deposition. No plagioclase was found in the Fruholmen samples.

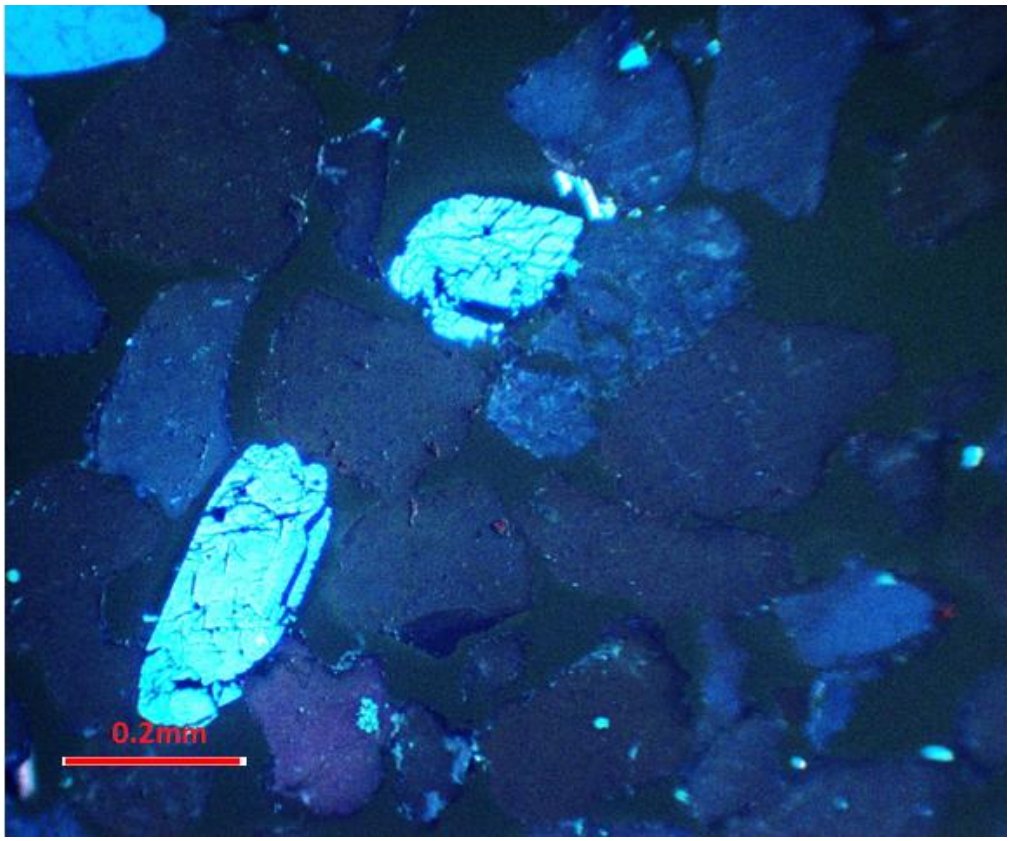

Figure 3.1.3a: Cathodoluminescence micrograph showing K-feldspar grains (light blue with fractures). Dark blue to almost black grains are quartz. The light blue grain without fractures in the upper left corner is also quartz. Note absence of plagioclase with yellow or orange cathodoluminescence colours (Amieux, 1982; Marshall, 1988). Scale bar is 200µm. Fruholmen Formation, 921.00mRKB.

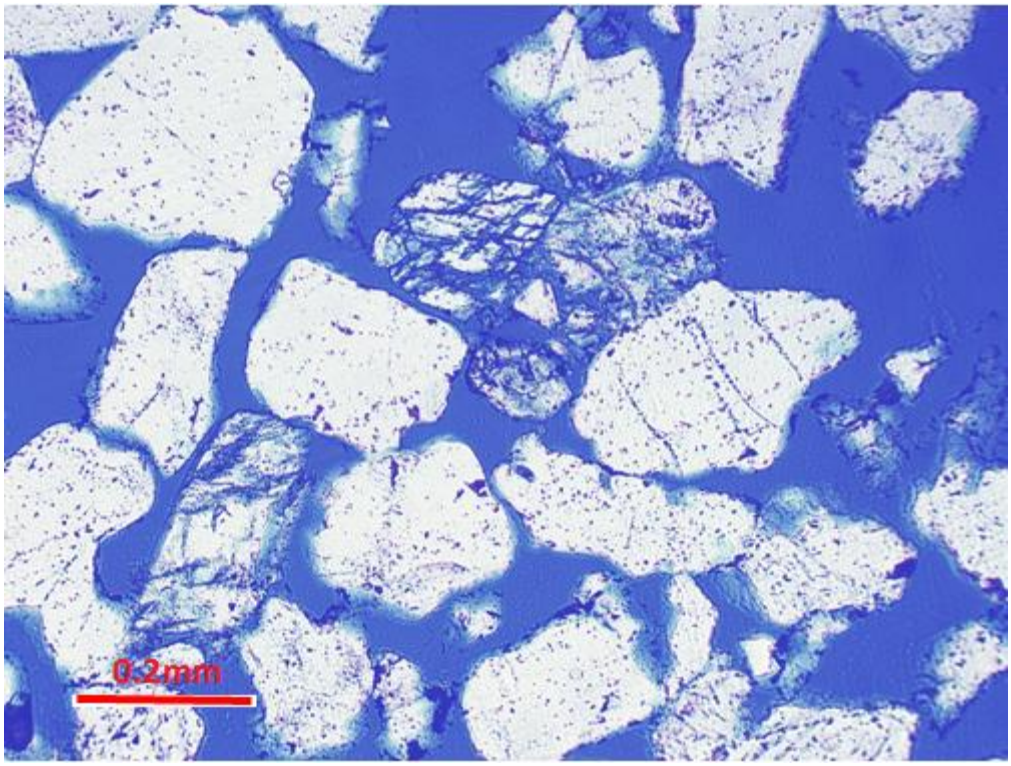

Figure 3.1.3b: Micrograph of the same area as in Figure 3.1.2a taken with plane-polarized light. Scale bar is 200µm.

Half of the samples contain up to 0.7% muscovite grains. A few green detrital chlorite grains were found in one sample, while no biotite was seen in the Fruholmen Formation.

Heavy minerals occur in all samples, but in trace amounts only. Heavy minerals seen in the Fruholmen Formation are zircon, yellow and green tourmaline, rutile, monazite with brown to black coatings characteristic of this mineral (Rasmussen et al., 1989; Walderhaug and Porten, 2007), and opaque iron-titanium oxides. The most common heavy minerals are opaques, zircon being second most common.

Small amounts (up to 0.3%) of plant fragments are present in a few samples.

Contents of clay clasts reach up to 5.3% in some samples. Many of the Fruholmen Formation sandstones are practically free of detrital clay matrix, with the exception of the sample from 916mRKB where the content of detrital clay matrix is 18%. The siltstones in the Fruholmen Formation typically contain clay-rich laminae and patches (Figure 3.1.4). Drilling mud is present in trace amounts in the sample from 919mRKB, and in the sample from 924mRKB drilling mud accounts for 6.6% of sample volume (Figure 3.1.5). This volume of drilling mud is included in the porosity value given in Table 3.1.1.

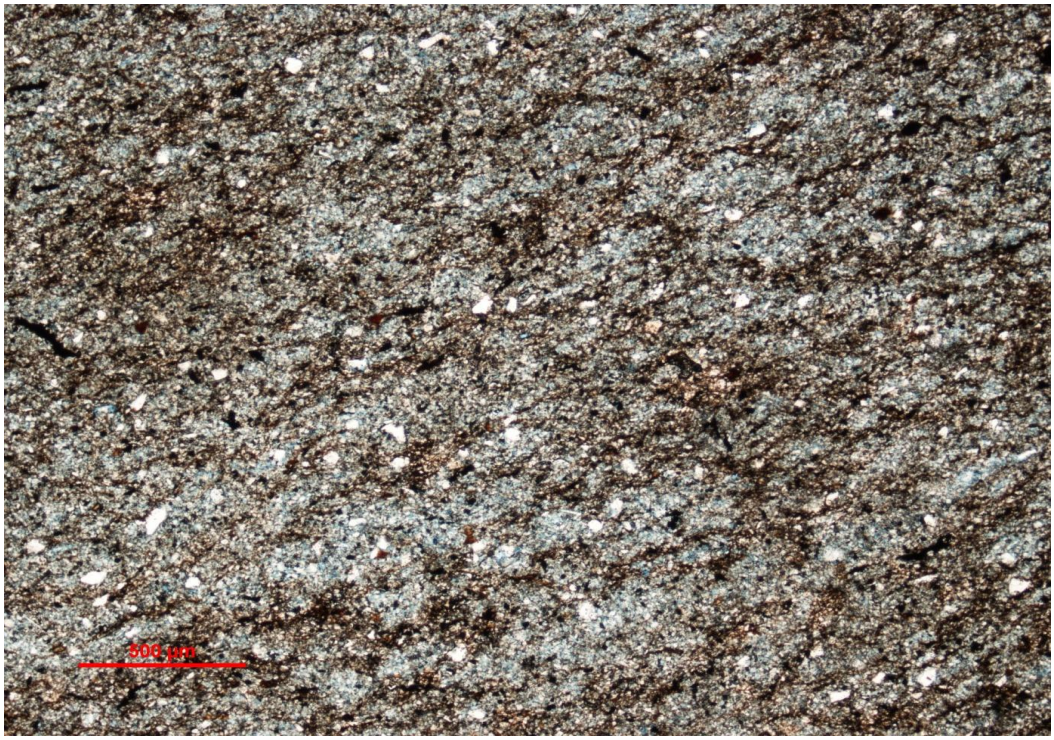

Figure 3.1.4: The Fruholmen Formation is more matrix-rich in the interval 925-934.5mRKB. Siltstone with helium porosity 21.8%. Scale bar is 500µm. 931.00mRKB.

Diagenetic minerals

Quartz overgrowths are the most common diagenetic cement in the Fruholmen Formation and are present in volumes of up to 2.3% (Table 3.1.1). Some of the overgrowths appear as rounded and irregular, indicating that they are inherited overgrowths formed in older sandstones (Figure 3.1.5). A very small amount of planar regular overgrowths that seem to have precipitated on quartz grains after deposition is also present (Figure 3.1.6).

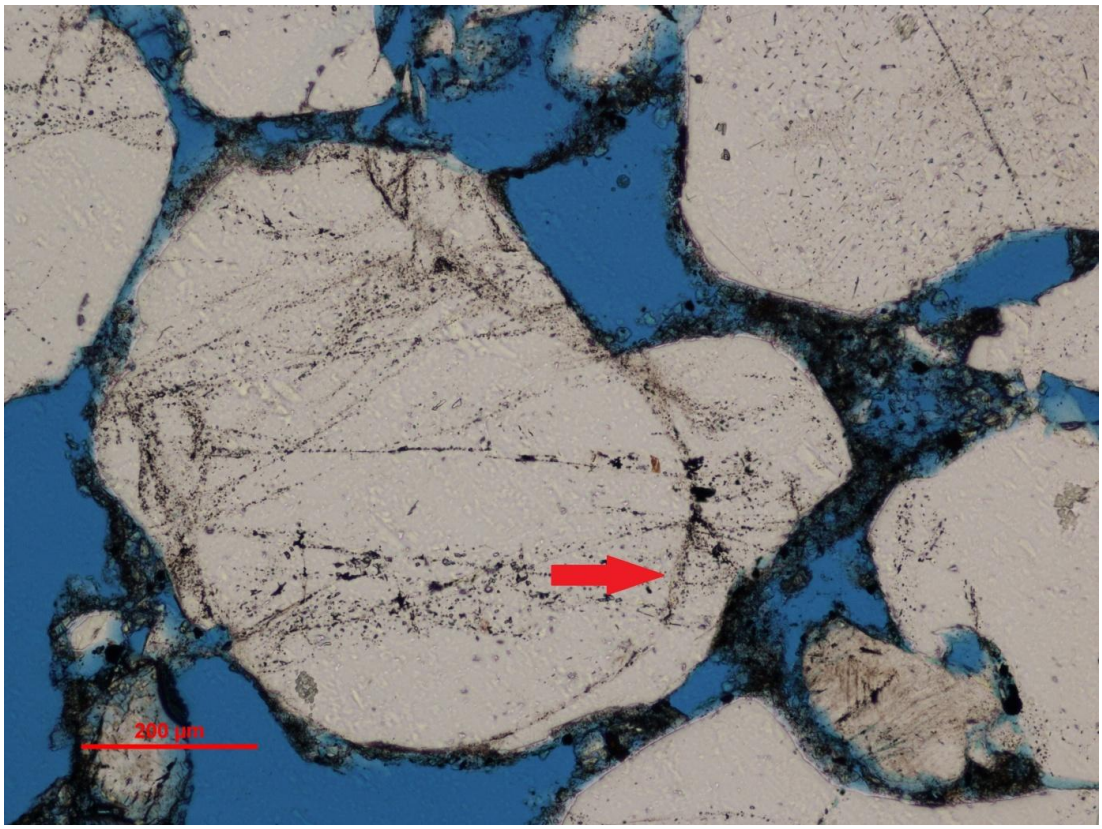

Figure 3.1.5: Quartz overgrowth indicated by dust rim (red arrow). The overgrowth does not have planar surfaces, but shows very large thickness variation which indicates that the overgrowth has been eroded from an older quartz-cemented sandstone and was present at the time of deposition. The dark material in the pores is drilling mud. The drilling mud consists of small fragments of barite and dark clay-like material. It can be recognized as drilling mud by its occurrence on top of late diagenetic minerals such as quartz overgrowths. Scale bar is 200µm. Fruholmen Formation, 924.00mRKB.

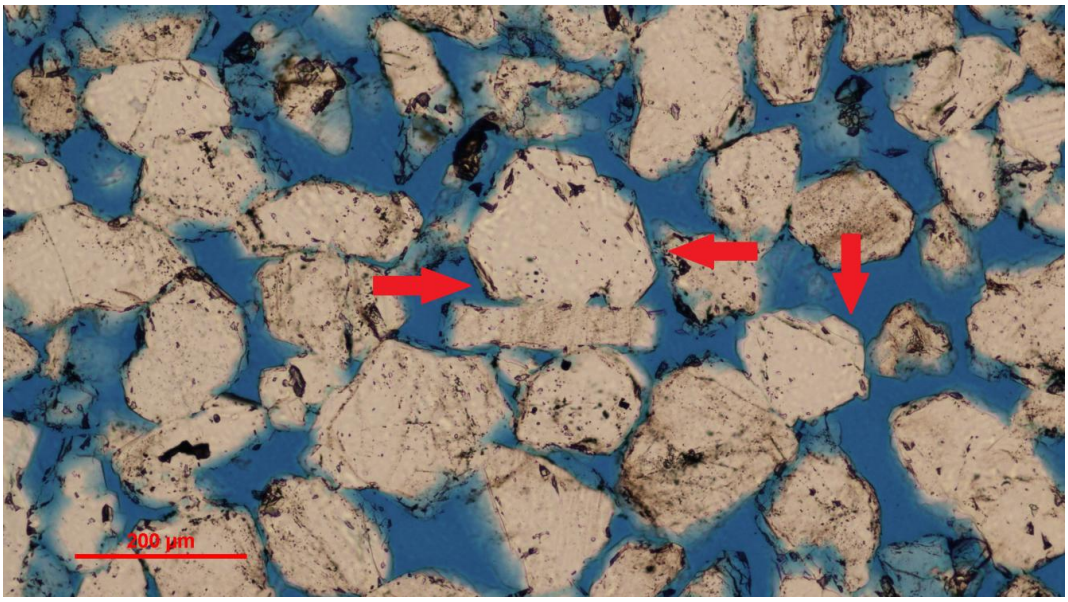

Figure 3.1.6: Quartz cement seen as planar overgrowths, indicated with red arrows. Scale bar is 200µm. Fruholmen Formation, 917.00mRKB.

Authigenic kaolin in the form of microporous aggregates built up of stacks of pseudohexagonal platelets occurs in some of the samples and reaches amounts of up to 1.7%.

Pyrite cement occurs as framboids and cement patches and is found in trace amounts in most samples (Figure 3.1.7).

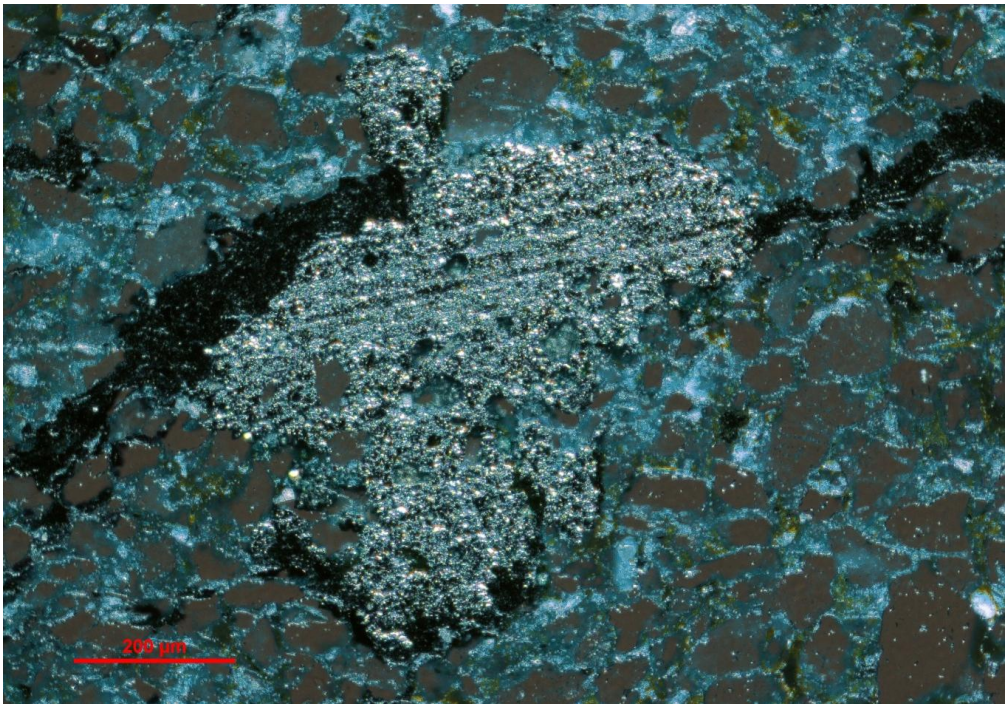

Figure 3.1.7: Patch of pyrite cement (golden colours). Micrograph taken with crossed nichols and a light beam perpendicular on the thin-section. Scale bar is 200µm. Fruholmen Formation, 942.00mRKB.

Porosity and permeability

Porosities determined by point-counting are in the range 15.3-36.6% whereas measured helium porosities for the same samples range from 19.4 to 30.5% (Table 3.1.1). The pore system in the sandstones is dominated by primary interconnected macropores. Minor dissolution porosity from feldspar dissolution is also seen.

Horizontal air permeabilities are ca. 0.1mD in the finest siltstones with the most clay, whereas permeabilities reach almost 38 000mD in the sandstones with highest porosities (Figure 3.1.8). The uppermost ten metres of the cores (915-925mRKB) have helium porosities around 30%. They are almost clay-free and have permeabilities of several Darcies to tens of Darcies. In the siltstone interval below (925-935mRKB) porosities are usually between 13 and 25% and permeabilities are also much lower, commonly between 0.3mD and 30mD. Below this siltstone interval a permeable sandstone zone is seen, with porosities and permeabilities reaching high values similar to the uppermost ten metre interval.

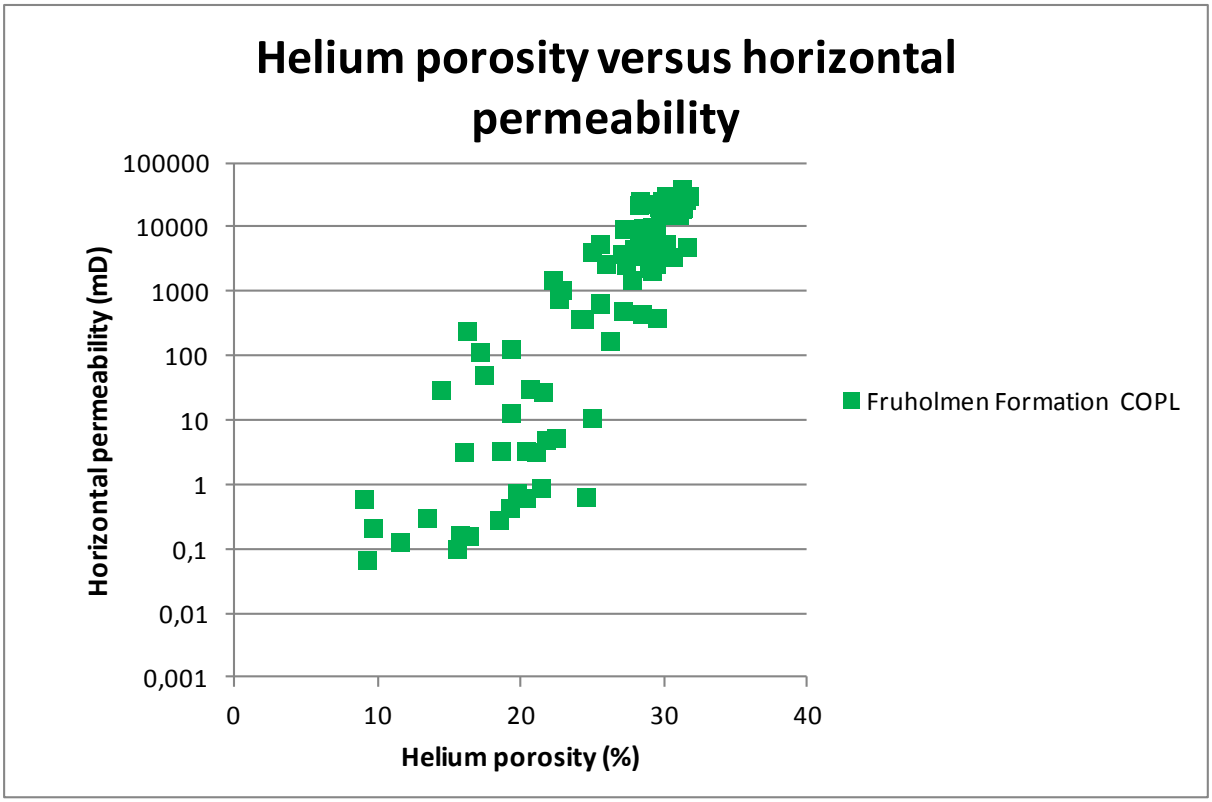

Figure 3.1.8: Helium porosity versus horizontal permeability for all Fruholmen Formation core plugs (COPL). A positive correlation is seen, and a cluster of points shows very good porosity and permeability values, 25-34% and 100-38 000mD, respectively. The points with permeability below 1mD correspond to the siltstone interval (925-936mRKB).

3.2 The Snadd Formation

3.2.1 Depositional environment

Statoil's core description of the Snadd Formation in well 7131/4-1 (Figures 3.2.1 and 3.1.1b) shows that the lower part of the cored Snadd Formation interval in this well is characterized by a 5m thick zone of mudstone and muddy sandstone with siderite concretions representing water saturated paleosol and lake floor swamp environments. Above there is an erosive-based thin coarse to very coarse sandstone with intraclasts, probably a channel lag deposit. The section passes into a 4m thick trough cross-bedded medium-grained sandstone sequence interpreted as a channelized dune field. Further upwards (1108-1104mRKB) medium-grained sandstone with carbonaceous lamination is seen, followed by a 20m section (1104-1084mRKB) of medium and coarse-grained sandstone with some planar and trough cross-bedding, a lot of muddy and sandy clasts, and some current ripples. The uppermost 14 metres consist of medium and occasionally coarse-grained planar and trough cross-bedded sandstone with some siderite and calcite cements. The intervals 1108-1104mRKB, 1104-1084mRKB and 1084-1070mRKB were deposited in a channel environment, possibly within an estuarine setting, including in-channel bars and dunes.

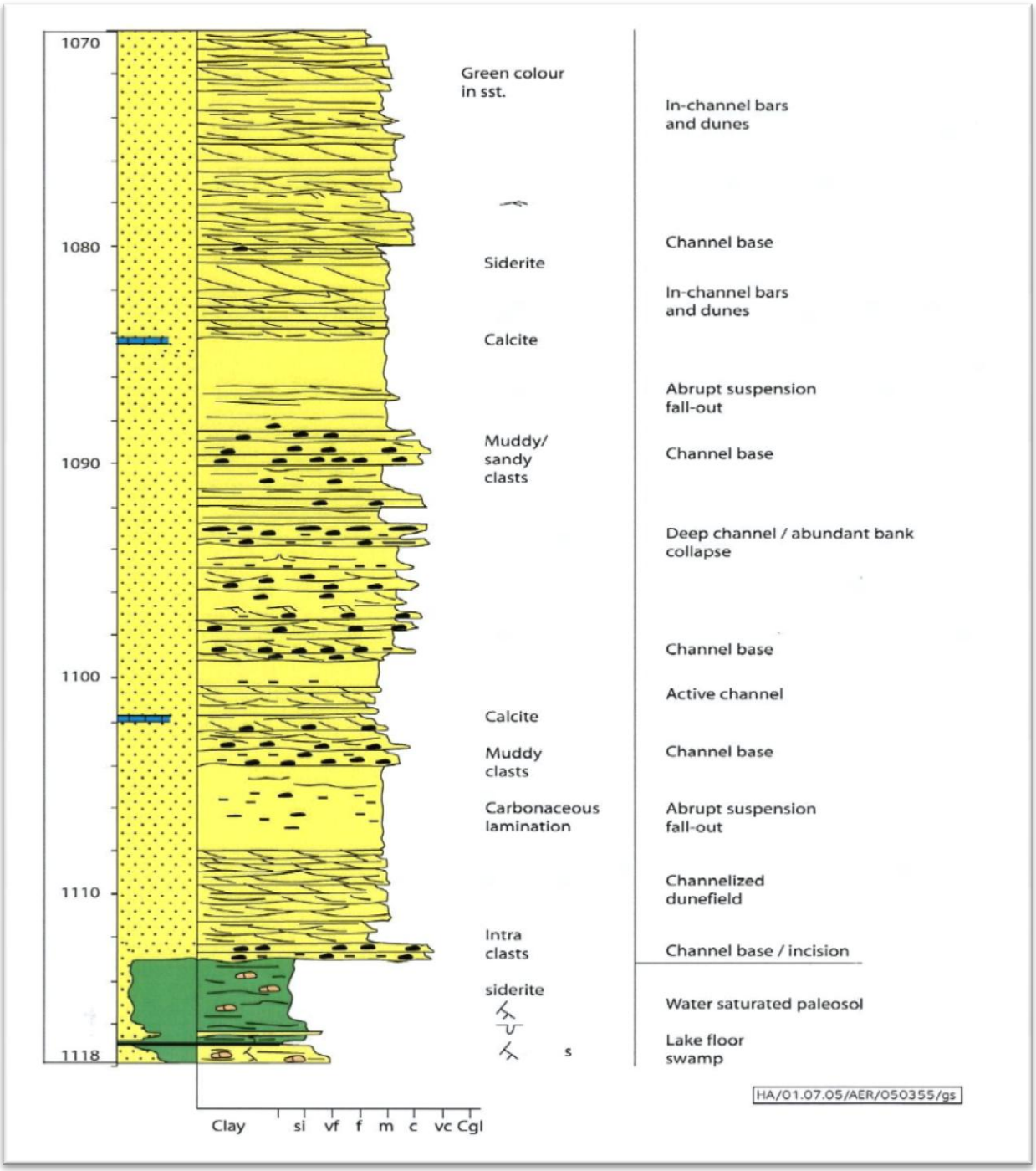

Figure 3.2.1: Core description, Snadd Formation, well 7131/4-1. Depths in mRKB. Figure provided by Statoil ASA.

3.2.2 Petrographic composition

Lithology and texture

The Snadd Formation cores (1070-1118mRKB) comprise moderately well, well and rarely very well sorted fine- and medium-grained sandstones and minor clay-rich siltstone. Up to 1cm clasts of matrix-supported sandstone and siltstone are present in some sandstone samples,

whereas detrital clay matrix contents typically do not exceed a few per cent and are often zero. Grains are mostly subangular (Figures 3.2.2 and 3.2.3).

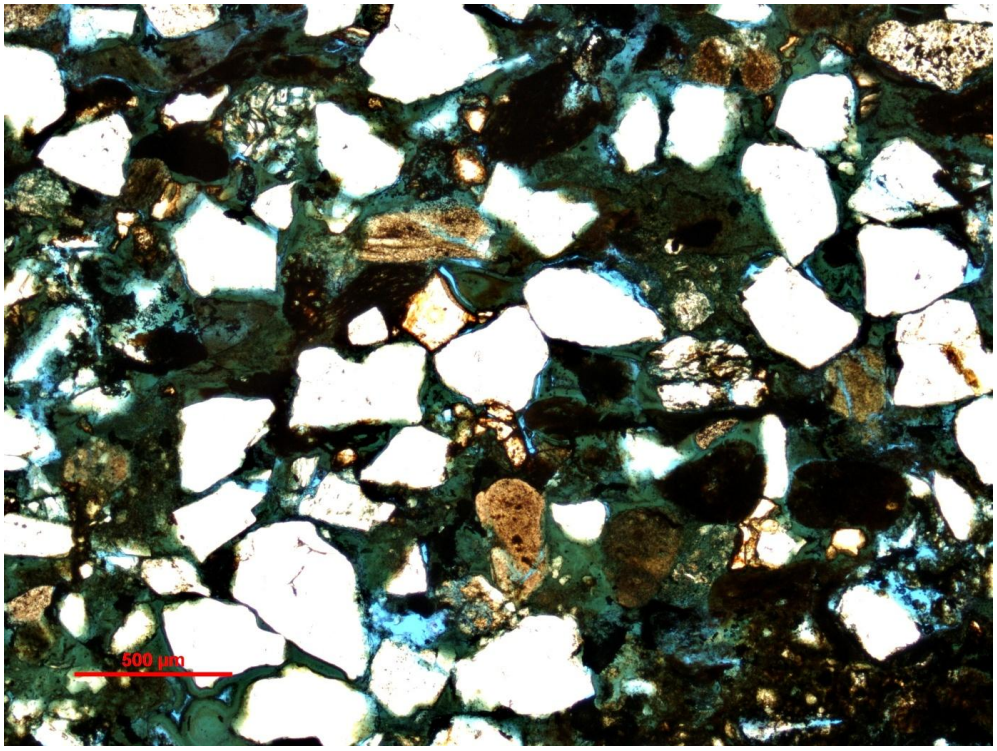

Figure 3.2.2: Fine-grained sandstone where microporous diagenetic chlorite (green, almost black) fills the majority of the pores. White grains are quartz. Scale bar is 500µm. Snadd Formation, 1070.00mRKB.

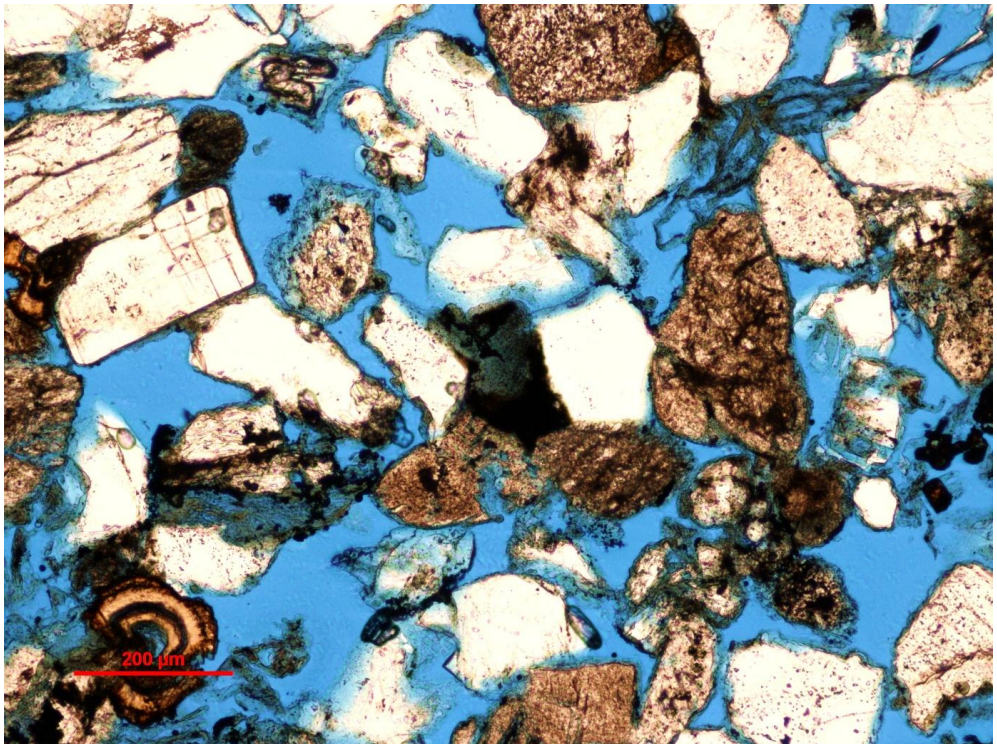

Figure 3.2.3: Medium-grained sandstone where thin rims of diagenetic chlorite cover all grains and prevent quartz cementation. Helium porosity is 32.1% and permeability is 1480mD. Scale bar is 200µm. Snadd Formation, 1081.00mRKB.

Detrital grains

Quartz is the most common detrital mineral and is found in volumes of 32.3-52.7% of sample volumes (Table 3.1.1). The quartz grains are usually monocrystalline, but volumes of polycrystalline quartz occasionally reach almost 6%. Chert clasts are found in all samples and account for 1-5% of the volumes of the point-counted samples. Some of the chert clasts are brown or reddish brown (Figure 3.2.4).

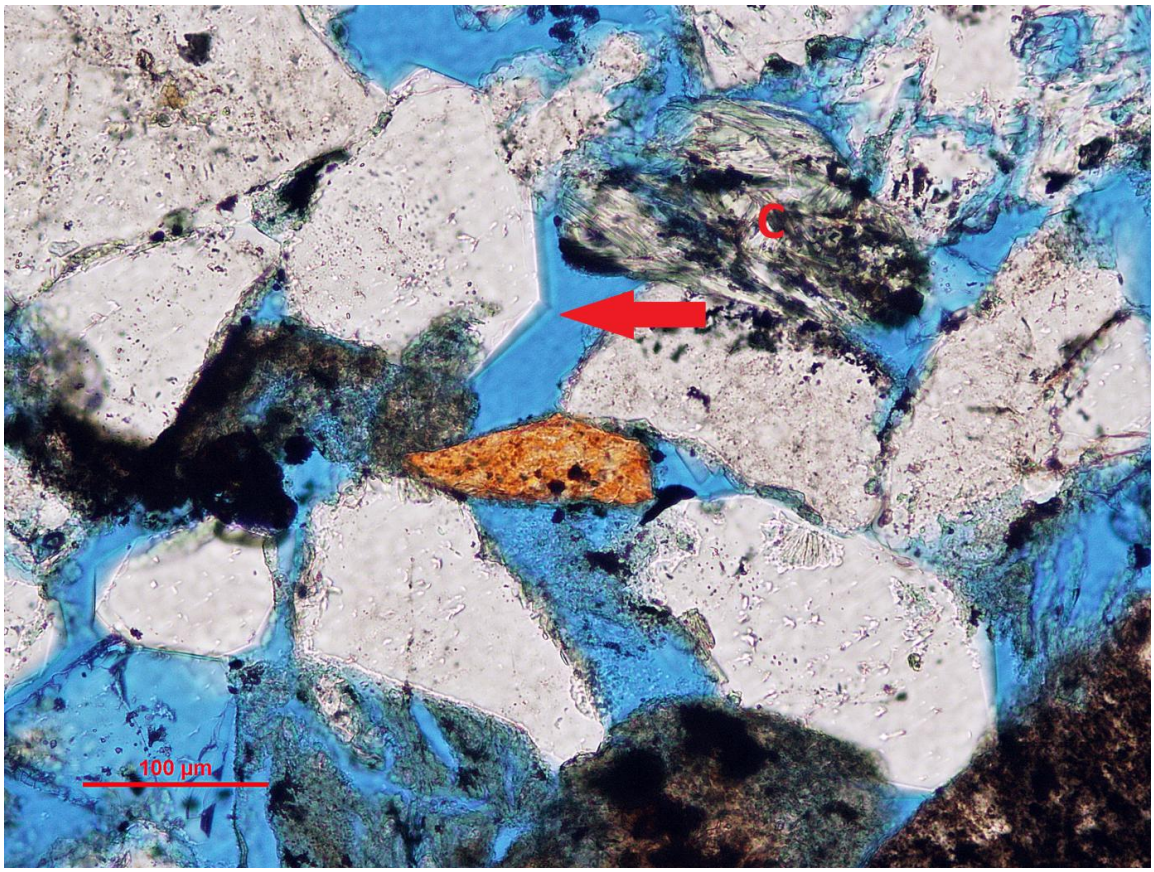

Figure 3.2.4: Thin rims of diagenetic chlorite cover almost all grains, but where chlorite coatings are incomplete development of quartz overgrowths is seen (indicated with red arrow). C=foliated metamorphic rock fragment (mica schist?) consisting of chlorite and quartz. Reddish-brown grain is chert. Scale bar is 100µm. Snadd Formation, 1089.05mRKB.

K-feldspar, partly with microcline twinning, is seen in volumes of up to 4.3%. Plagioclase contents are similar to K-feldspar contents. Albite twinning (Figure 3.2.9) and sericitization is found in some plagioclase grains. Feldspar grains are in some cases partly dissolved, and rare dissolution pores that do not contain any minerals may possibly have formed by feldspar dissolution (Figure 3.2.5). K-feldspar and plagioclase grains are easily distinguished from quartz and from each other by their cathodoluminescence colours. K-feldspar is intense light

blue, plagioclase is yellow and more rarely orange, whereas quartz appears darker blue, brown and almost black (Figures 3.2.6a and b).

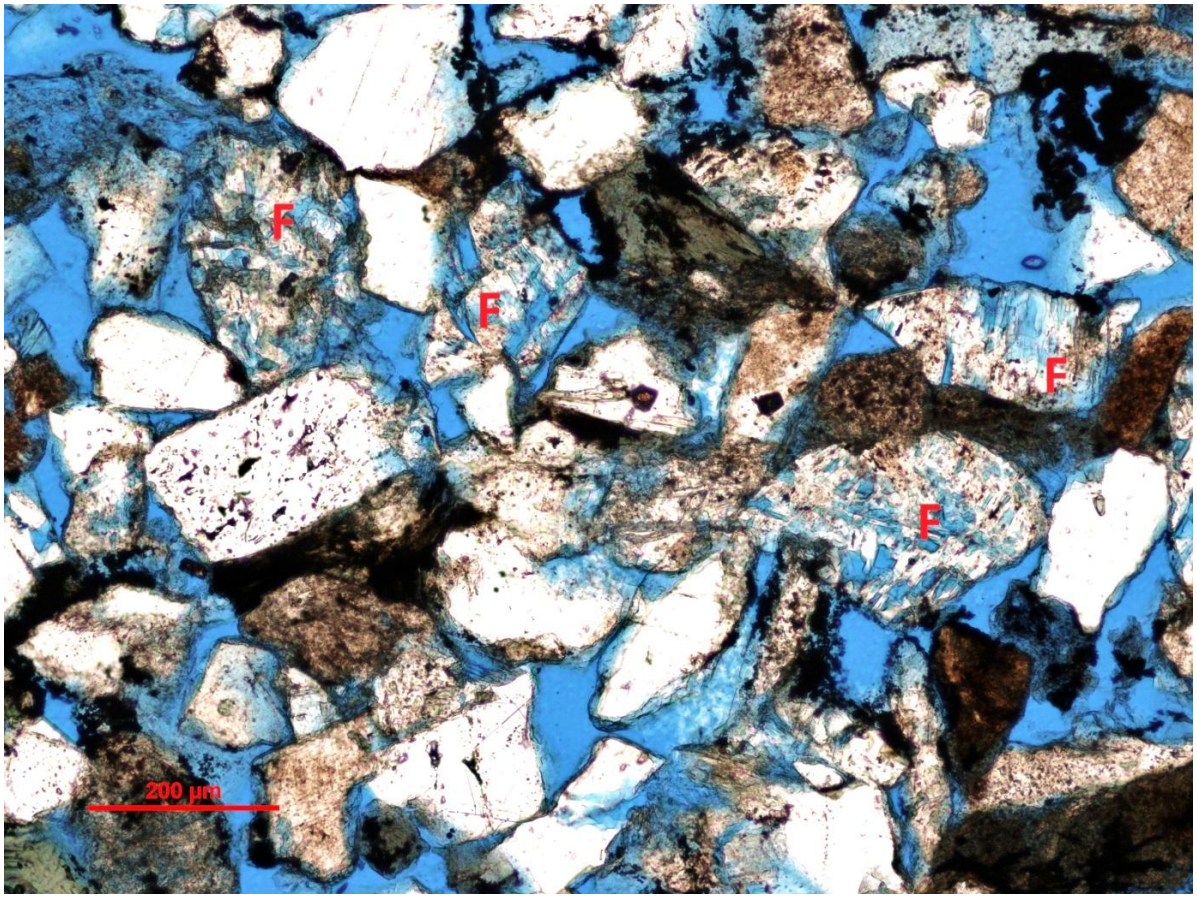

Figure 3.2.5: Partly dissolved feldspar grains (F) with dissolution pores. Dark grains are rock fragments and clay clasts. Diagenetic chlorite rims coat all grains. Scale bar is 200µm. Snadd Formation, 1100.00mRKB.

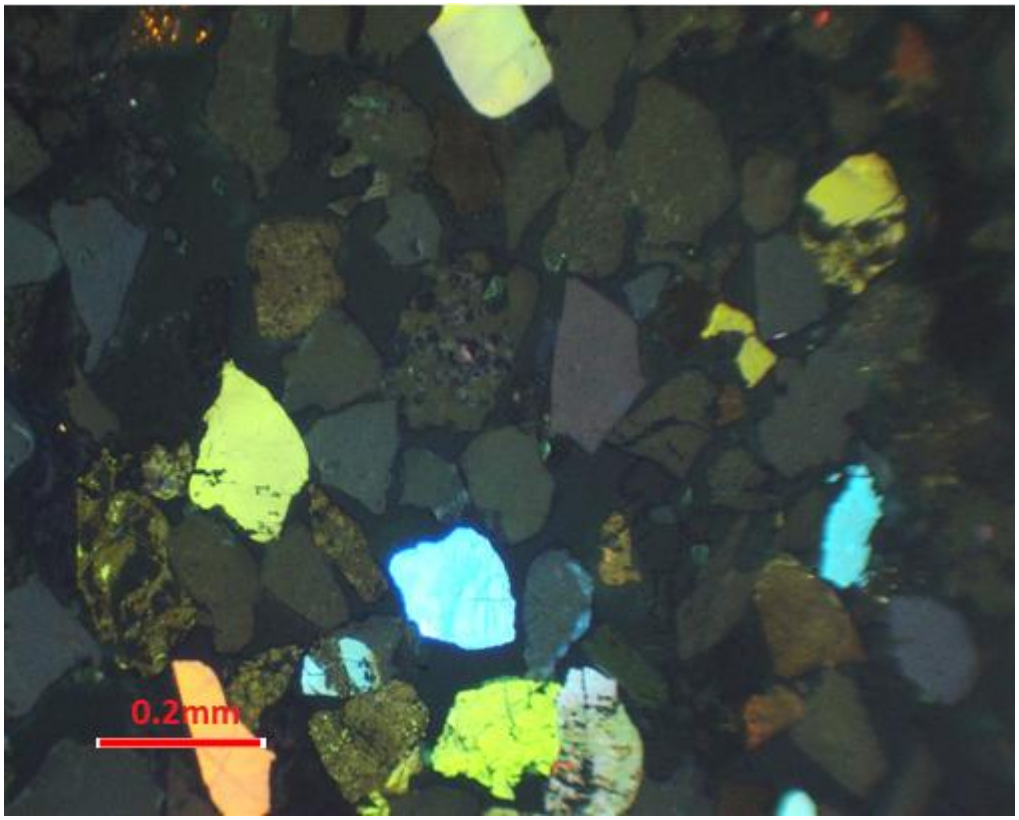

Figure 3.2.6a: Cathodoluminescence micrograph showing yellow and orange plagioclase, light blue K-feldspar and quartz with dark blue to almost black colours (Amieux, 1982; Marshall, 1988). Scale bar is 200µm. Snadd Formation, 1103.00mRKB.

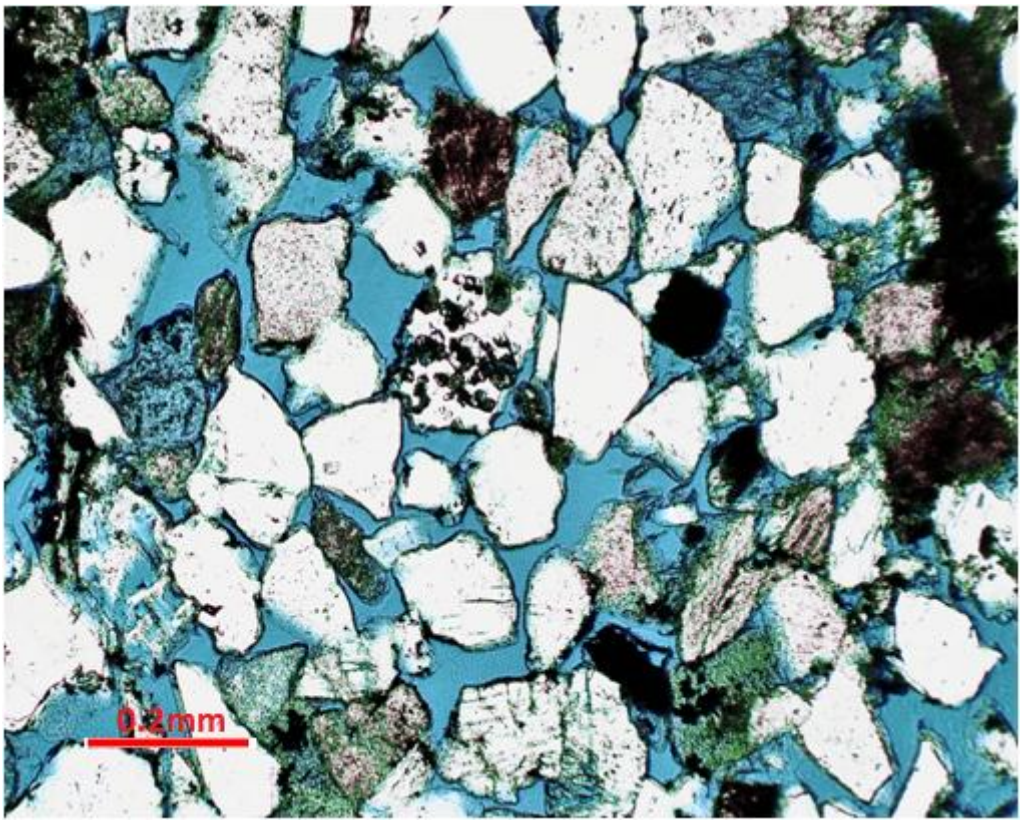

Figure 3.2.6b: Micrograph of the same area as in Figure 3.2.6a taken with plane-polarized light. Scale bar is 200µm.

Muscovite is usually found in amounts up to 0.7% (Figure 3.2.9). A few biotite flakes occur in a few samples, while green chlorite flakes occur in many of the samples in amounts of up to 0.7%.

Heavy minerals are present in all samples, normally in trace amounts. The heavy mineral suite comprises zircon, yellow, green and brown tourmaline (Figure 3.2.7a), rutile, apatite, red, brown and reddish-brown spinel (Figure 3.2.7b), slightly dissolved garnet, chloritoid (Figures 3.2.8a and b) and opaque iron-titanium oxides.

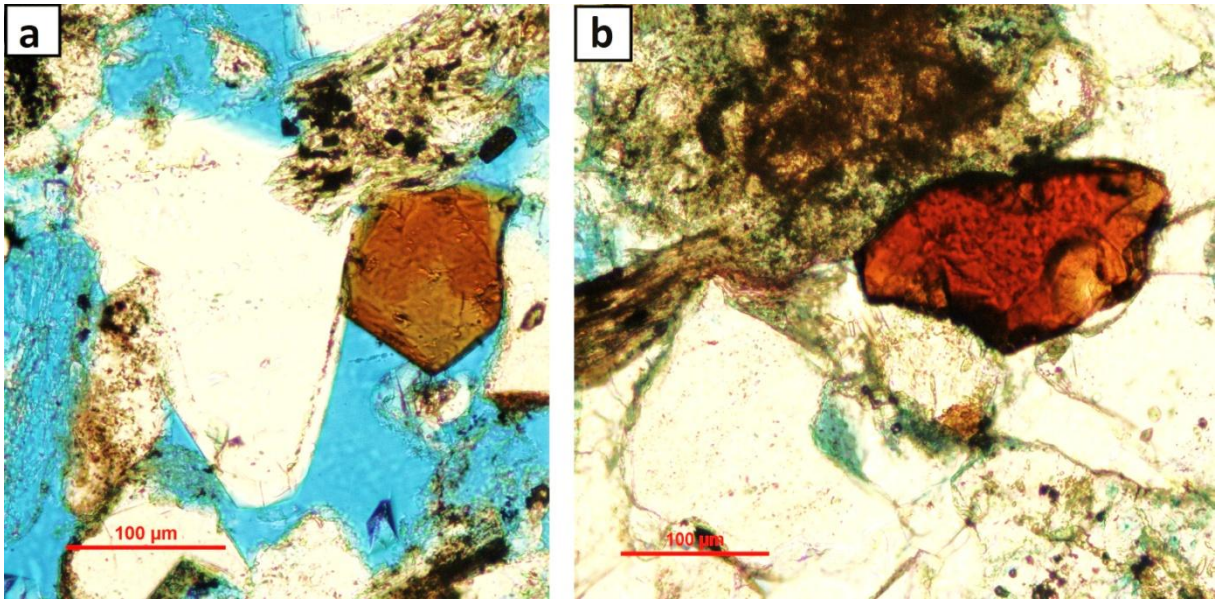

Figures 3.2.7: a: Greenish-brown tourmaline. Snadd Formation, 1091.00mRKB. b: Reddish-brown spinel. Scale bar is 100µm. Snadd Formation, 1102.00mRKB.

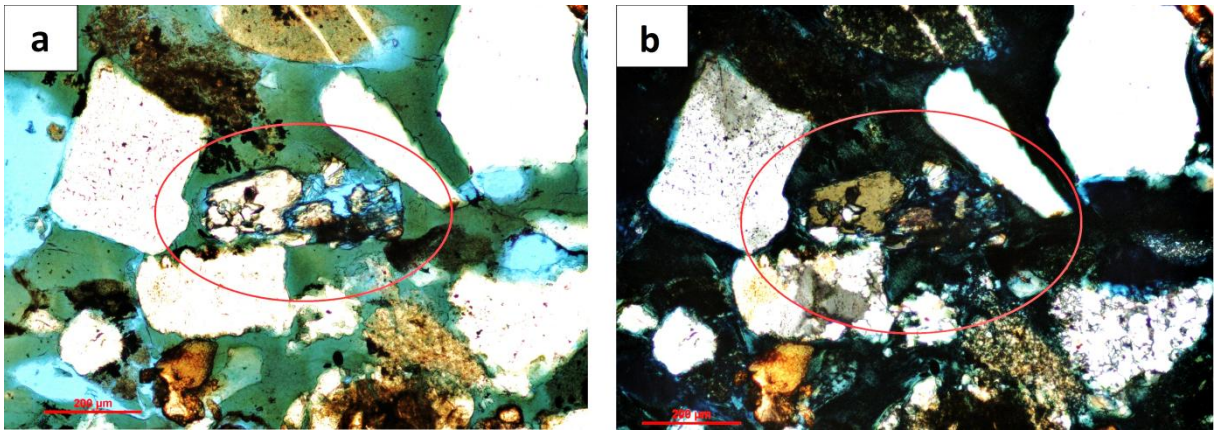

Figures 3.2.8: a: Chloritoid marked by red circle, b taken with crossed nichols. Scale bar is 200µm. Snadd Formation, 1075.00mRKB.

Green and brown clay clasts are abundant in the Snadd Formation and are seen in all samples in volumes from 3 to 16%. In addition, some mica-rich rock fragments such as polycrystalline

quartz with large amounts of mica and mica schists are seen in about half of the samples (Figure 3.2.9).

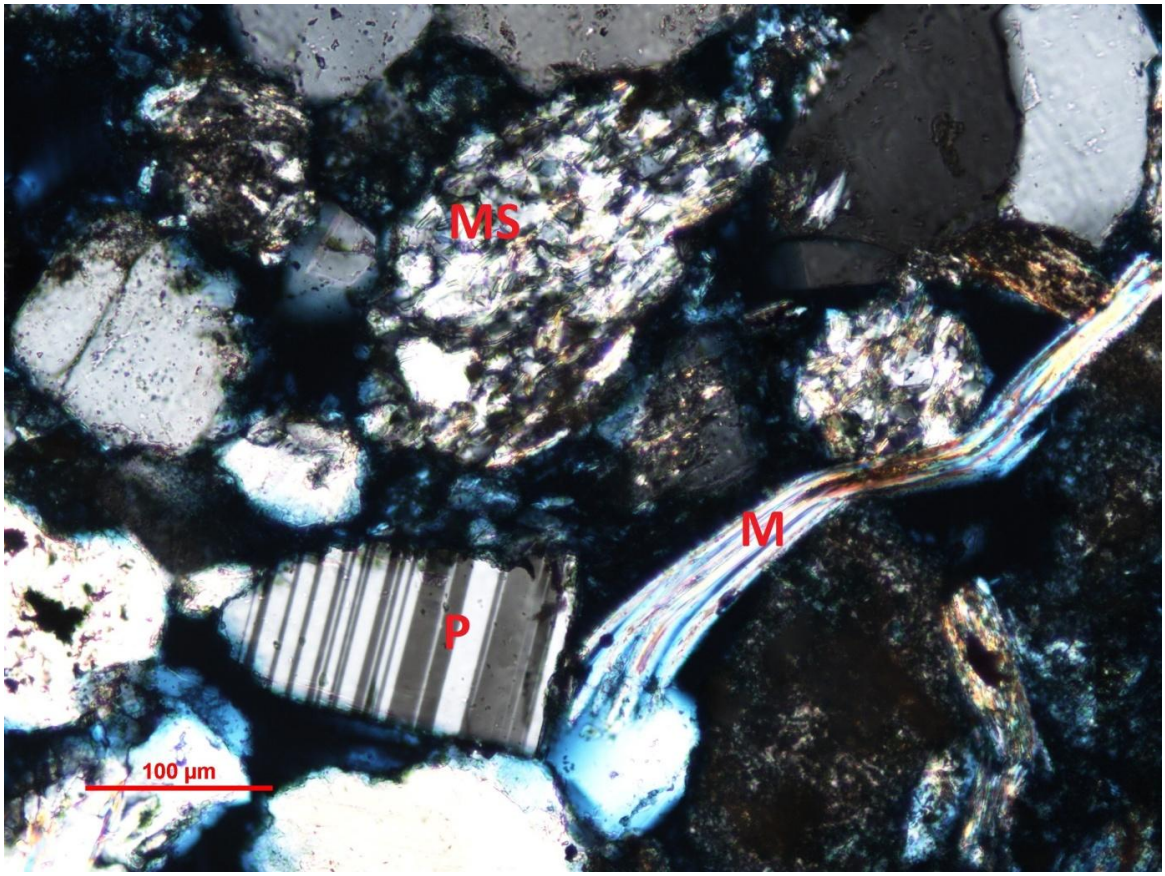

Figure 3.2.9: Mica schist fragment (MS), muscovite grain (M) and plagioclase grain with albite twinning (P). Muscovite is bent due to mechanical compaction. Micrograph taken with crossed nichols. Scale bar is 100µm. Snadd Formation, 1091.00mRKB.

Diagenetic minerals

Quartz overgrowths are present in trace amounts in around half of the samples where chlorite coatings are incomplete (Figure 3.2.10).

Chlorite cement occurs in all Snadd Formation samples and accounts for 0.3-10% of sample volumes in most samples (Figure 3.2.3). However, in samples 1073 and 1075mRKB point-counted volumes of microporous chlorite cement are as high as 36 and 33.3% respectively. The upper ten metres of the Snadd core are extremely rich in microporous chlorite which fills almost all pores (Figure 3.2.2). Below this interval the chlorite coatings are much thinner (<5µm) and of quite constant thickness. The chlorite coats all detrital grains, but not the cements pyrite, siderite, calcite and quartz overgrowths.

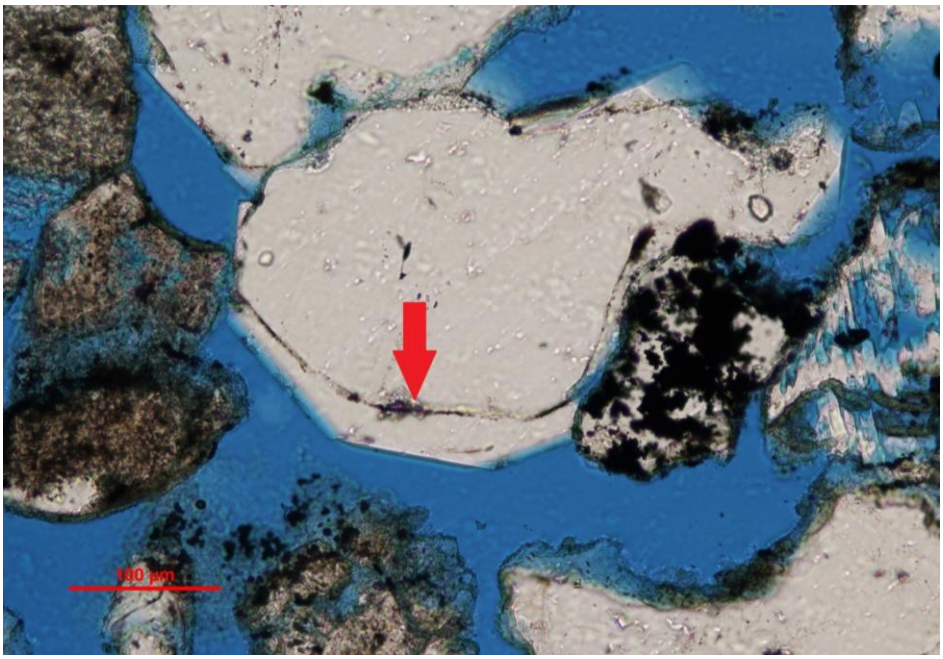

Figure 3.2.10: Thin rims of green diagenetic chlorite cement cover almost all grains. Precipitation of quartz cement with planar surfaces is seen (red arrow) where the chlorite coat is incomplete. Scale bar is 100µm. Snadd Formation, 1081.00mRKB.

Diagenetic kaolin in the form of microporous aggregates made up of stacks of pseudohexagonal platy crystals was found in many of the Snadd Formation samples (Figure 3.2.11). Point-counted volumes of kaolin are between 0.3 and 0.7%.

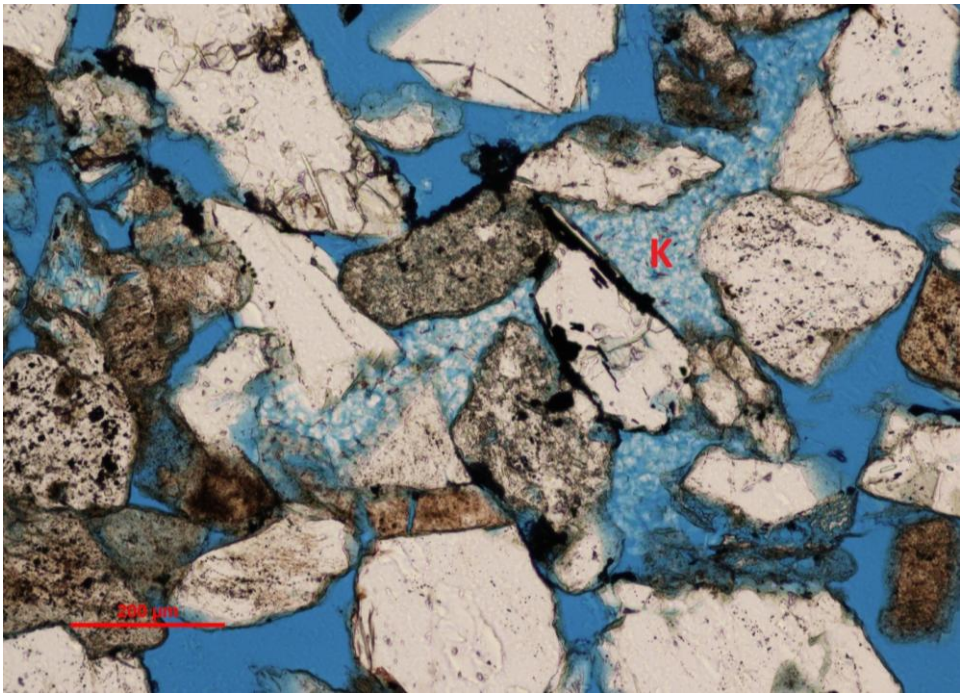

Figure 3.2.11: Diagenetic kaolin crystals (K) filling pores. Scale bar is 200µm. Snadd Formation, 1094.00mRKB.

Pyrite cement framboids and cement specks are seen in trace amounts in only a few samples.

Siderite cement was found in most Snadd Formation samples in volumes of 0.3% up to 6%. The siderite occurs as brown scattered cement patches with diameters up to 0.5mm. It consists of concentric layers of cement with varying colour (Figure 3.2.12). In addition, sideritic intraclasts occur engulfed within pervasive calcite cement.

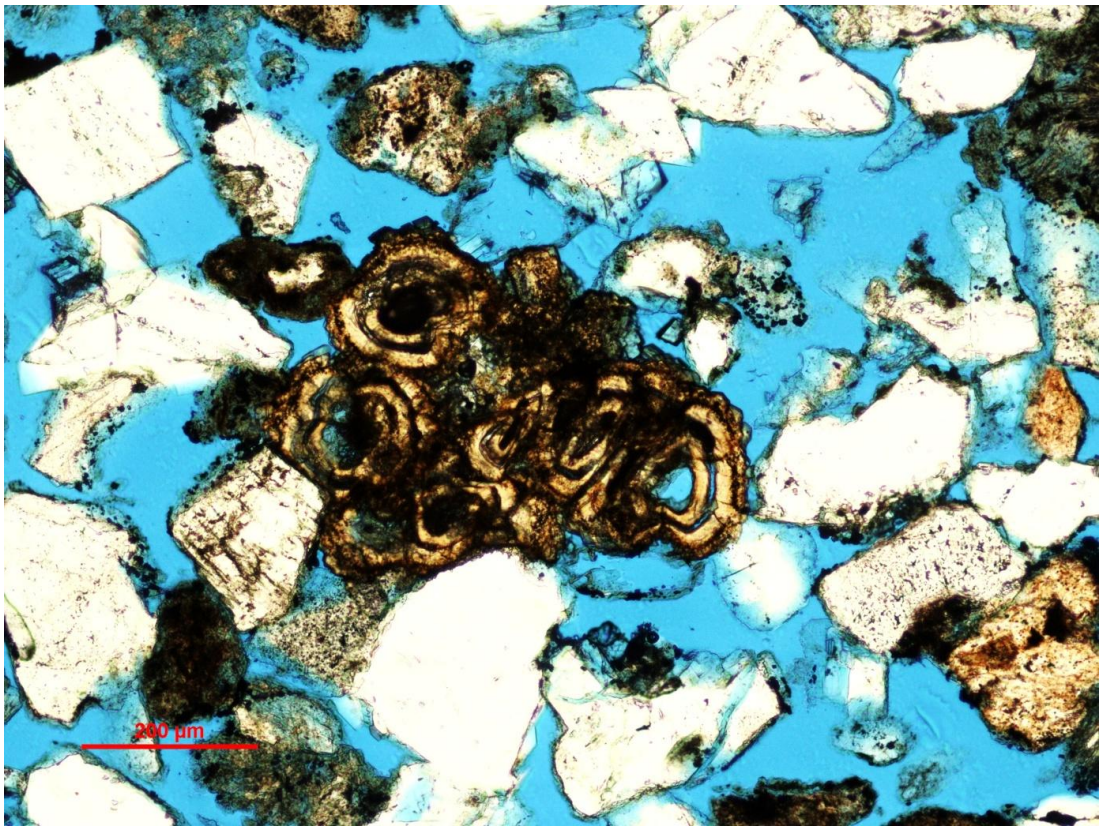

Figure 3.2.12: Orange-brown siderite with concentric layers. Scale bar is 200µm. Snadd Formation, 1081.00mRKB.

Calcite cement is an abundant pore-filling cement in some cases (1102.00, 1112.15 and 1113.00mRKB). In other samples calcite cement only appears in volumes of up to 0.3%. Where calcite is abundant it has precipitated on top of chlorite rims.

Porosity and permeability

Porosities determined by point-counting vary from 4% to 36.3% (Table 3.1.1) while helium porosities mostly range from 26 to 36% (Figure 3.2.13). Dissolution porosity is seen in all Snadd Formation samples, probably formed by dissolution of feldspar grains (Figure 3.2.5). The lowest point-counted porosities occur where chlorite cement almost totally fills pores

(1070-1075mRKB, Figure 3.2.2), but the chlorite is very microporous. Helium porosities for these samples may therefore be over 30% for samples with less than 5% point-counted porosity (Figure 3.2.13).

Snadd Formation permeabilities are only 0.1-20mD for the uppermost zone even though porosities mostly lie above 30%. The poor permeabilities are due to chlorite filling most pores and porosity mainly being poorly connected micropores. The samples with thin chlorite grain coats contain mostly primary macropores and typically have permeabilities of 200-5 000mD and porosities of 26-36%.

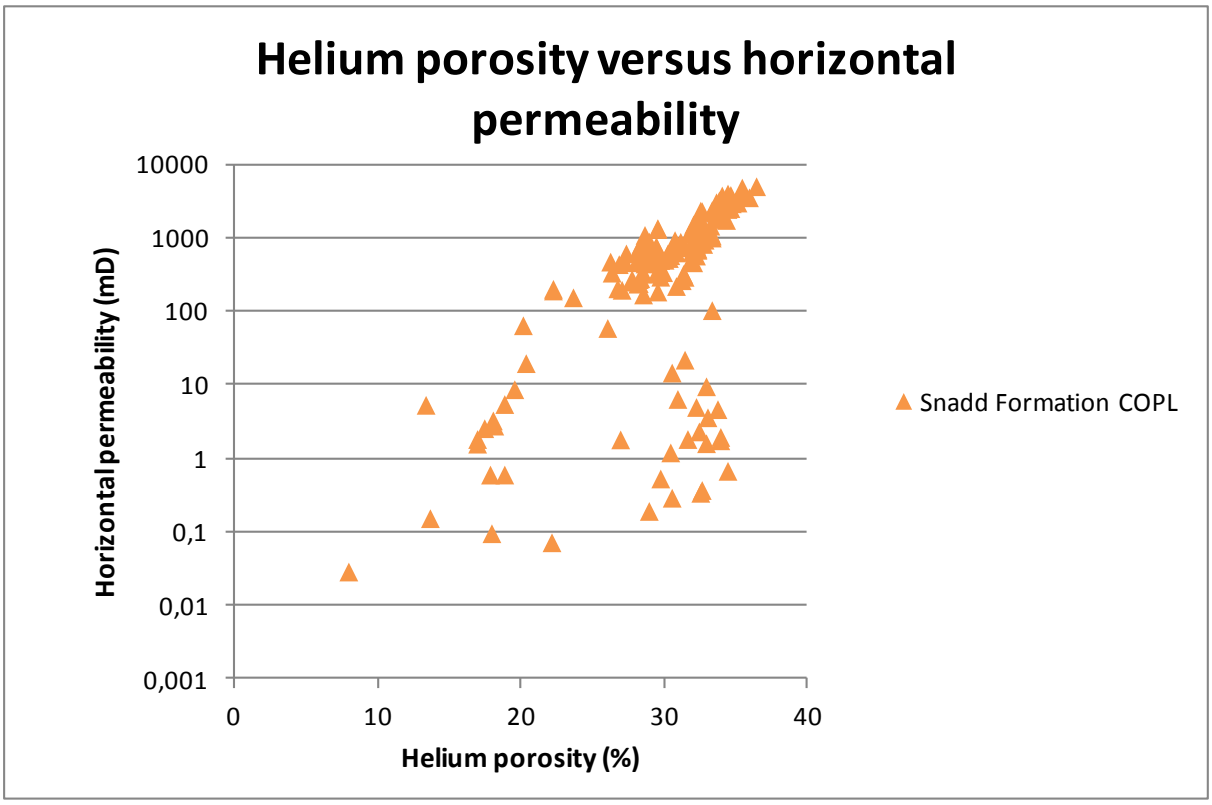

Figure 3.2.13: Helium porosity versus horizontal permeability for all Snadd Formation core plugs (COPL). Variable values are seen, but the majority of the porosity values lie in the interval 25-37%, permeabilities are largely between 100 and 5 000mD. The samples with porosities above 30% but permeabilities of only 0.1-20mD contain large amounts of very microporous diagenetic chlorite that fills almost all pores.

4 Well 7222/11-1

4.1 The Snadd Formation

4.1.1 Depositional environment

Three cores were retrieved from the Snadd Formation in well 7222/11-1 (Figures 4.1.1a and b and 3.1.1b). Cores 1 and 2 are taken from 778 to 807mRKB and Core 3 from 1287 to 1299.5mRKB. The lowermost core is dominated by sandstone with shale interbedding and coarsens upward from very fine- to fine- to medium-grained. The deepest ten metres are moderately bioturbated and contain some carbonate fossils and wave ripples. The uppermost five metres of Core 3 are partly cross-bedded. The core interpretation suggests that Core 3 represents a prograding shoreline comprising an offshore transition zone passing upward to a lower shoreface, and finally up to a mouth bar or beach ridge at the top.

The basal nine metres of Core 2 are characterized by interbedded siltstone and sandstone with current ripples, rootlets and traces of siderite. The section may represent interdistributary bays or lakes with crevasse splays. The rest of the cored section is medium-grained and often cross-bedded sandstone with some calcite cement. It is considered to be deposited as migrating dunes in a fluvial or tidal channel complex.

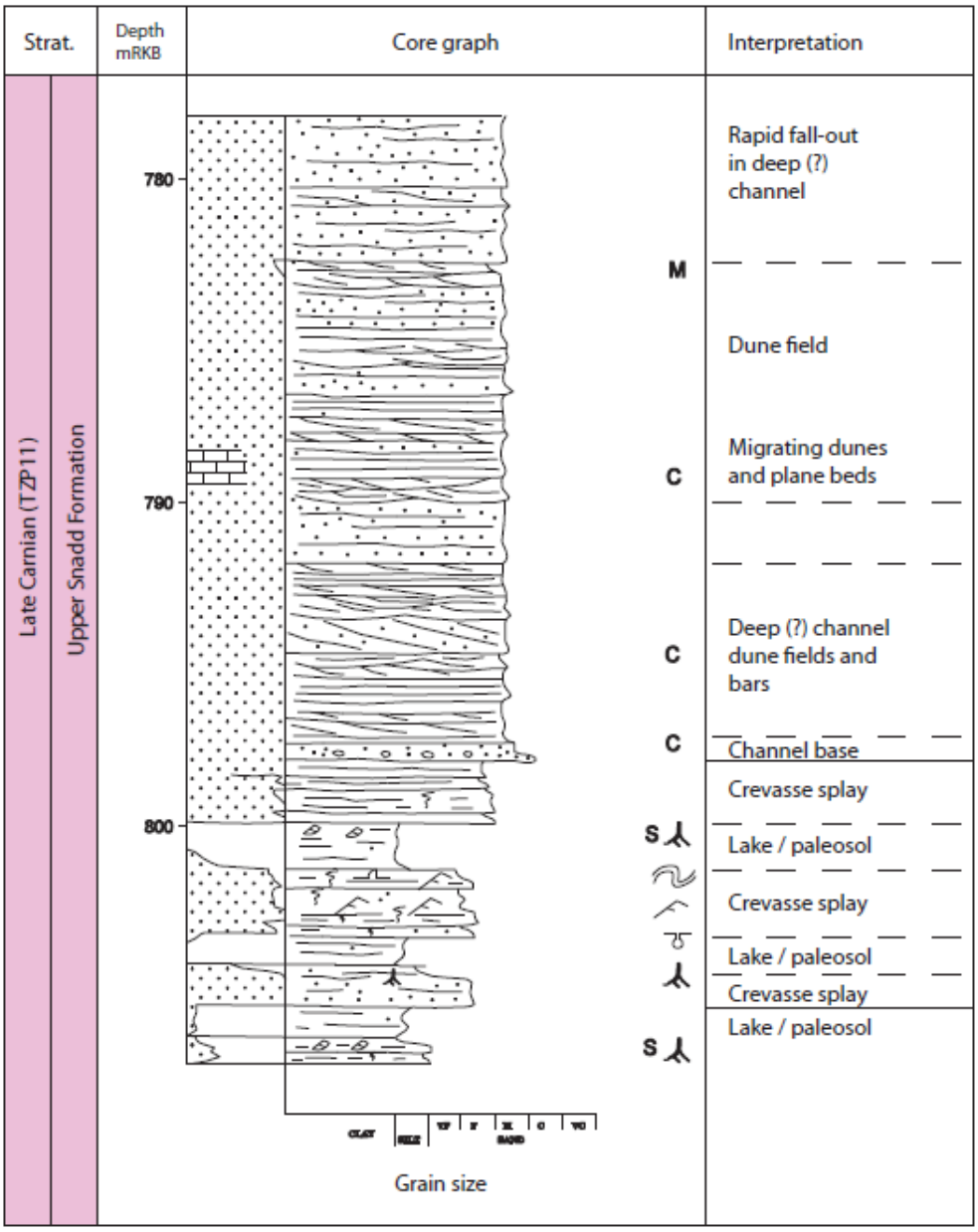

Figure 4.1.1a: Core description, Cores 1 and 2, Snadd Formation, well 7222/11-1. Depths in mRKB. Figure provided by Statoil ASA.

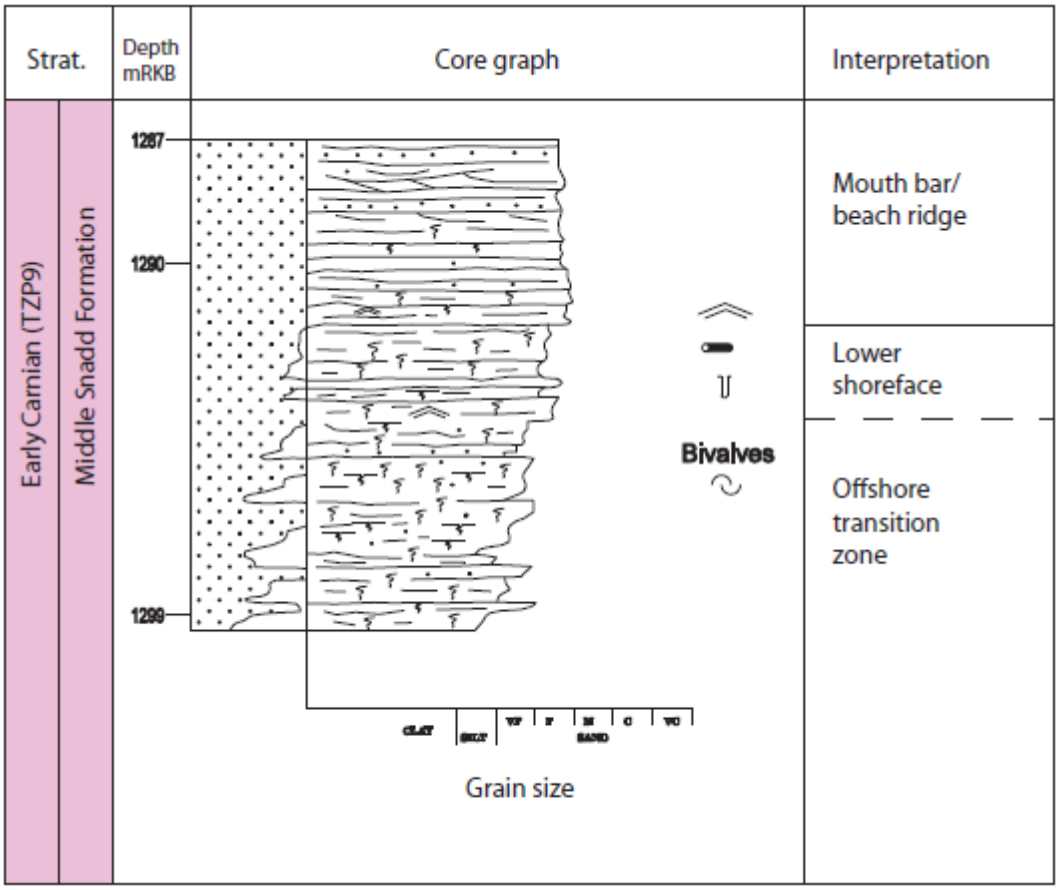

Figure 4.1.1b: Core description, Core 3, Snadd Formation, well 7222/11-1. Depths in mRKB. Figure provided by Statoil ASA.

4.1.2 Petrographic composition

Lithology and texture

The shallowest samples of the Snadd Formation (641.70-799.02mRKB) comprise well sorted and moderately well sorted fine-grained sandstone with low detrital clay content (Figure 4.1.2). The deeper samples (1287-1299.5mRKB) have a higher content of clay clasts, have a fine grain size and are slightly better sorted. Grains are dominantly subangular in the Snadd Formation in well 7222/11-1.

Detrital grains

The most abundant detrital mineral in the Snadd Formation is quartz. Quartz grains account for 32.4-58.3% of sample volumes (Table 4.1.1). The detrital quartz is mostly monocrystalline, but polycrystalline grains are also common (1.3-7.3% of sample volumes), and chert grains are seen in all samples (1.7-5% of sample volumes). Quartz-rich metamorphic rock fragments are common in all samples with point-counted volumes from 7

to 15.3% (Figure 4.1.5). In addition to quartz these fragments contain minor muscovite and sometimes chlorite.

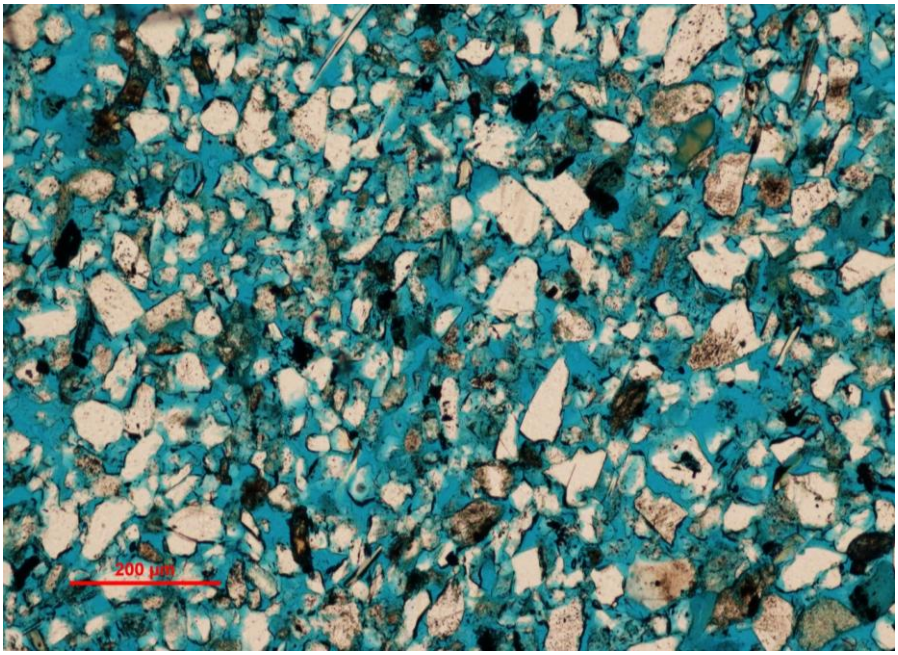

Figure 4.1.2: Very fine-grained quartz-rich sandstone. No quartz overgrowths are seen, and the sandstone is practically clay-free. Helium porosity is 34.3% and permeability is 213.3mD. The relatively low permeability value is due to the very fine grain size. Scale bar is 200µm. Snadd Formation, 641.70mRKB.

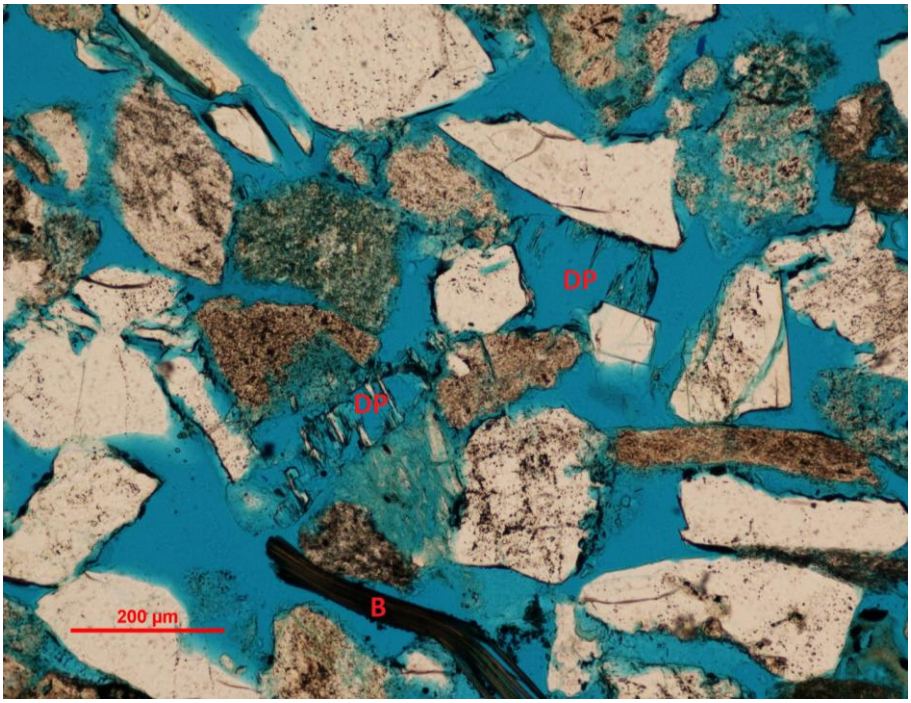

Figure 4.1.3: Fine to medium-grained quartz-rich sandstone with very good sorting. Several pale to dark brown rock fragments. The white grains are quartz and plagioclase, the dark and greenish grains are rock fragments and clay clasts, and brown biotite (B) is seen at the base of the micrograph. Note dissolved feldspar with dissolution pores (DP). Helium porosity is 33.9%, permeability is 1737mD. Scale bar is 200µm. Snadd Formation, 788.05mRKB.

Depth mRKB	Depth mRSF	Formation	Monocryst. quartz clasts	Polycryst. quartz clasts	Chert clasts	K-feldspar clasts	Plagioclase clasts	Muscovite clasts	Biotite clasts	Chlorite clasts	Heavy minerals	Plant fragm.	Clay clasts and mica rich rock fragm.	Qtz. rich meta fragm.	Detrital clay matrix	Quartz cement
778,03	399,03	Snadd	29,0	6,0	1,7	4,3	5,3	0,3	trace	0,7	trace		3,3	15,0		trace
782,02	403,02	Snadd	23,7	5,7	3,0	3,0	3,7	trace	0,7	0,7	trace		4,0	15,3	trace	trace
784,25	405,25	Snadd	30,3	4,7	3,7	6,0	2,7	0,3	1,0	trace	trace		3,7	11,0	1,6	trace
788,05	409,05	Snadd	25,0	5,7	4,7	3,6	6,3	0,7	trace	0,7	trace		4,0	9,0	1,3	trace
794,02	415,02	Snadd	31,0	3,7	5,0	4,3	3,7	0,7	trace	0,3	trace		5,7	7,0	1,0	trace
799,02	420,02	Snadd	35,3	1,3	2,0	3,0	5,0	0,3	0,7	trace	trace		8,3	8,0	1,3	trace
1102,00	723,00	Snadd	24,7	4,3	3,7	4,3	6,0	0,7	trace	0,7	trace	trace	11,7	12,0	0,3	trace
1287,00	908,00	Snadd	35,3	1,3	2,0	2,0	4,3	0,7		trace	trace	trace	7,0	11,3	3,6	
1291,00	912,00	Snadd	38,0	4,0	1,7	6,0	4,0	trace		trace	trace		5,3	8,0	1,6	
1495,40	1116,40	Snadd	30,0	4,7	2,3	2,3	12,7	0,3	trace	0,3	trace		10,3	8,3	1,0	trace
1617,30	1238,30	Snadd	36,3	2,7	2,7	1,0	7,0	0,3		1,0	trace		7,3	8,0	3,3	0,3
1800,60	1421,60	Snadd	47,0	7,3	4,0	1,3	4,7	1,0		0,7	trace		4,3	7,0	trace	0,7
2235,00	1856,00	Kobbe	25,0	13,7	3,0		10,3	1,7	0,3	trace	0,3	0,3	13,3	9,7	2,0	1,7
2235,52	1856,52	Kobbe	28,9	5,3	1,0		12,7	0,7		0,7	trace		10,3	18,0	1,0	0,7
2236,50	1857,50	Kobbe	27,7	12,7	1,7		8,0	1,7		trace	trace	0,7	13,0	9,6	4,6	0,7
2237,00	1858,00	Kobbe	25,0	13,0	1,0		12,7	2,7		trace	0,3	0,3	10,3	15,0	3,3	0,7
2238,50	1859,50	Kobbe	40,7	7,3	1,7		12,3	1,0		0,3	trace		6,0	7,7	4,7	0,3

Depth mRKB	Depth mRSF	Formation	Albite cement	Chlorite cement	Kaolin cement	Siderite cement	Calcite cement	Pyrite cement	Porosity, primary	Porosity, dissol.	Grain size mm	Sorting (coef. of var.)	Sorting verbal scale	Porosity % (He)	KhL mD
778,03	399,03	Snadd		3,3	1,7	trace	trace	trace	29,7	trace	0,23	0,32	Well sorted	32,8	1732,0
782,02	403,02	Snadd		5,0	1,7	0,3		trace	32,3	0,7	0,23	0,34	Well sorted	31,8	1358,0
784,25	405,25	Snadd		2,7	0,7		1,0		29,7	1,0	0,26	0,33	Well sorted	31,7	1040,0
788,05	409,05	Snadd		1,7	2,7	0,7			32,3	1,7	0,24	0,34	Well sorted	33,9	1737,0
794,02	415,02	Snadd		6,3	0,3	trace	0,7		28,7	1,7	0,26	0,30	Well sorted	33,6	1802,0
799,02	420,02	Snadd		3,3	0,3	0,7		trace	30,3		0,14	0,40	Moderately well sorted	31,0	369
1102,00	723,00	Snadd		2,7	1,7		0,3	trace	26,7	0,3	0,22	0,36	Moderately well sorted	27,8	214,0
1287,00	908,00	Snadd		4,0		trace		trace	28,3		0,14	0,41	Moderately well sorted	33,7	91,3
1291,00	912,00	Snadd		2,7				trace	28,0	0,7	0,13	0,29	Well sorted	32,4	157,0
1495,40	1116,40	Snadd		1,0	2,0	0,3	5,0	trace	19,0	0,3	0,16	0,29	Well sorted	21,6	31,7
1617,30	1238,30	Snadd		5,3	1,3	6,0	trace	trace	15,0	2,3	0,18	0,31	Well sorted	6,8	0,078
1800,60	1421,60	Snadd		1,3	2,0	1,3	trace		15,0	2,3	0,23	0,23	Very well sorted	17,7	5,62
2235,00	1856,00	Kobbe	trace	trace	0,3	trace	3,3	trace	15,0	trace	0,14	0,31	Well sorted	19,1	2,76
2235,52	1856,52	Kobbe		trace	2,3	0,3	trace		18,1		0,15	0,35	Well sorted	19,8	13,2
2236,50	1857,50	Kobbe	0,3	0,7	0,3	trace	trace	0,7	17,6	trace	0,15	0,73	Moderately sorted	19,5	5,06
2237,00	1858,00	Kobbe	0,3	0,3	0,7	trace	trace	trace	13,7	0,7	0,14	0,35	Well sorted	18,7	3,55
2238,50	1859,50	Kobbe	trace	0,3	0,3				17,3		0,15	0,27	Well sorted	20,7	19,9

Table 4.1.1: Modal analyses, well 7222/11-1.

K-feldspar, partly with microcline twinning, makes up 1-6% of sample volumes and is seen in all Snadd Formation samples. Plagioclase is also seen in all samples with volumes ranging from 2.7 to 12.7%. Some plagioclase grains show albite twinning, and some grains are heavily sericitized. Some K-feldspar and plagioclase grains are partly dissolved (Figure 4.1.3), although it is difficult to tell if these grains dissolved before or after deposition.

Flaky muscovite is seen in all samples in trace amounts to volumes of 0.7%. A few grains of brown biotite are seen in some samples (Figure 4.1.3), and up to 1% green detrital chlorite is found in almost all Snadd Formation samples.

Heavy minerals (Figure 4.1.4) are present in all samples, usually only in trace amounts. The heavy mineral suite comprises zircon, yellow, green and occasionally grey tourmaline, rutile, apatite, garnet, brown, reddish-brown and orange spinel, monazite, chloritoid, staurolite and opaque iron-titanium oxides. Grey tourmaline, monazite, staurolite and chloritoid are rare.

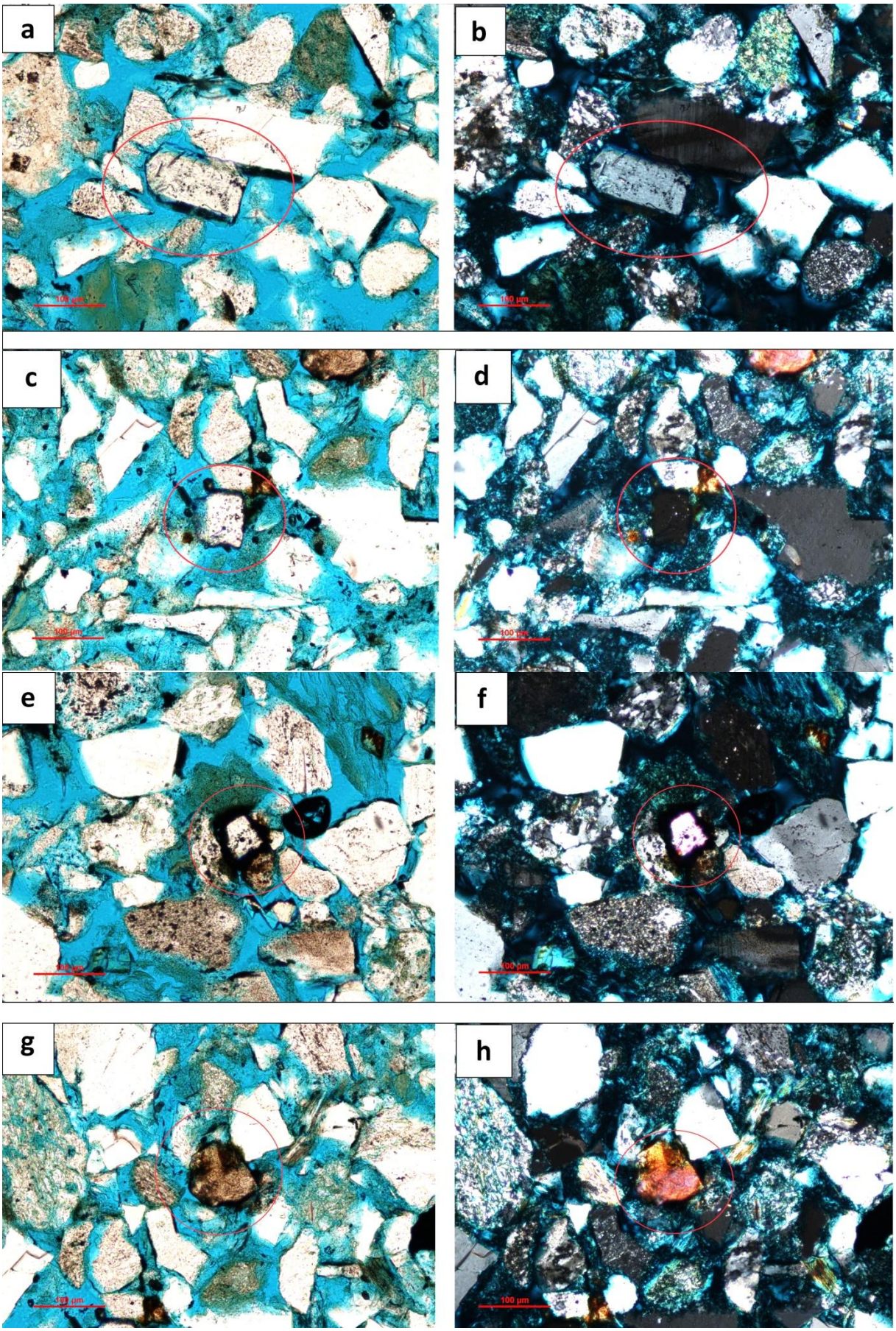
a
b
c
d
e
f
g
h
100 µm

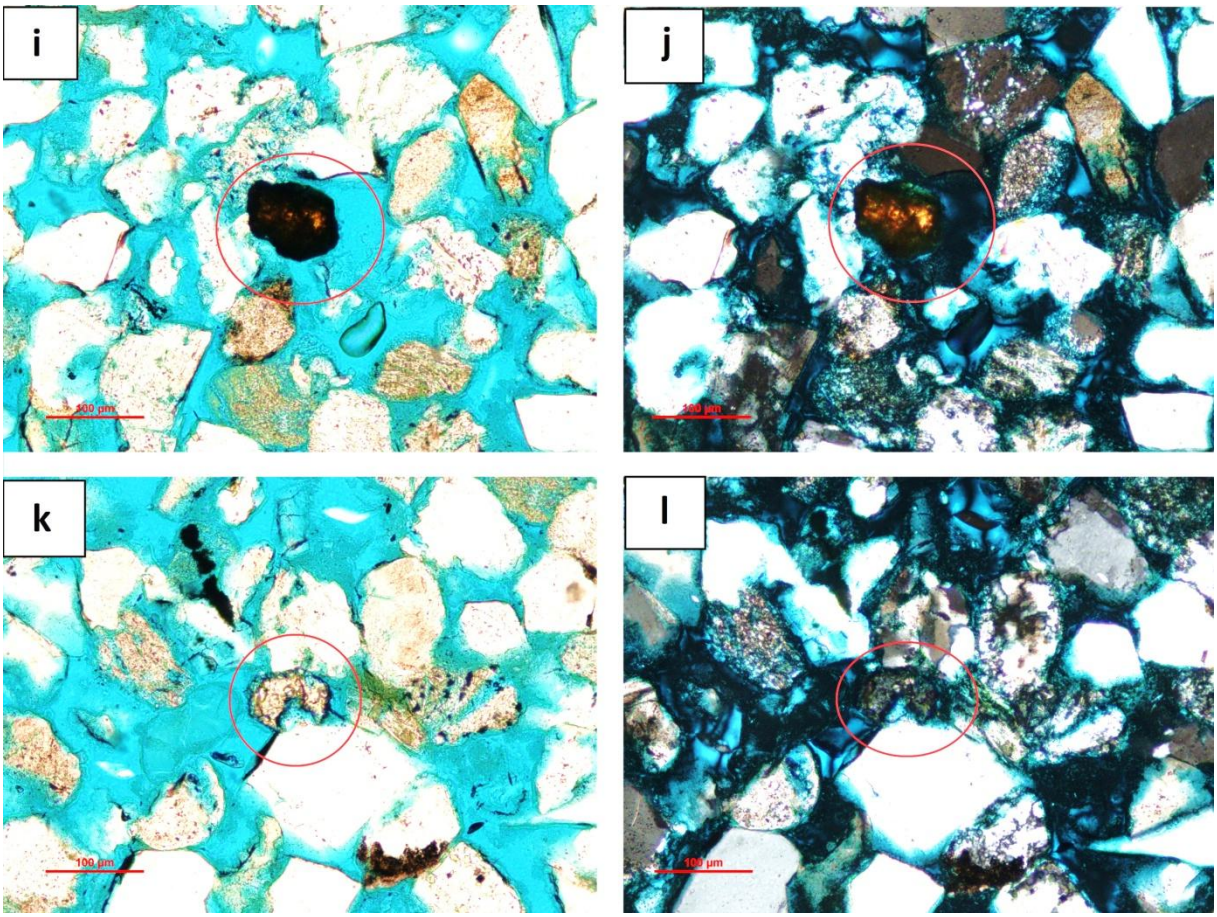

Figures 4.1.4: Heavy minerals in the Snadd Formation. a: Apatite, 799.02mRKB. b: Apatite with crossed nichols. c: Garnet, 799.02mRKB. d: Garnet with crossed nichols. e: Monazite, 799.02mRKB. f: Monazite with crossed nichols. g: Zirkon, 799.02mRKB. h: Zirkon with crossed nichols. i: Rutile, 1291.00mRKB. j: Rutile with crossed nichols. k: Staurolite, 1291.00mRKB. l: Staurolite with crossed nichols. Scale bar is 100µm.

Plant fragments are seen in trace amounts only in a few samples.

Clay clasts and mica-rich rock fragments are found in all samples in volumes ranging from 3.3 to 11.7%. Fragments include mica schists (Figure 4.1.5), probable phyllite, slate, and possible intraclasts. A few volcanic rock fragments consisting of elongate plagioclase crystals in a brown matrix also occur (Figure 4.1.6). Detrital clay matrix is seen in all samples but only accounts for up to 3.6% of sample volumes.

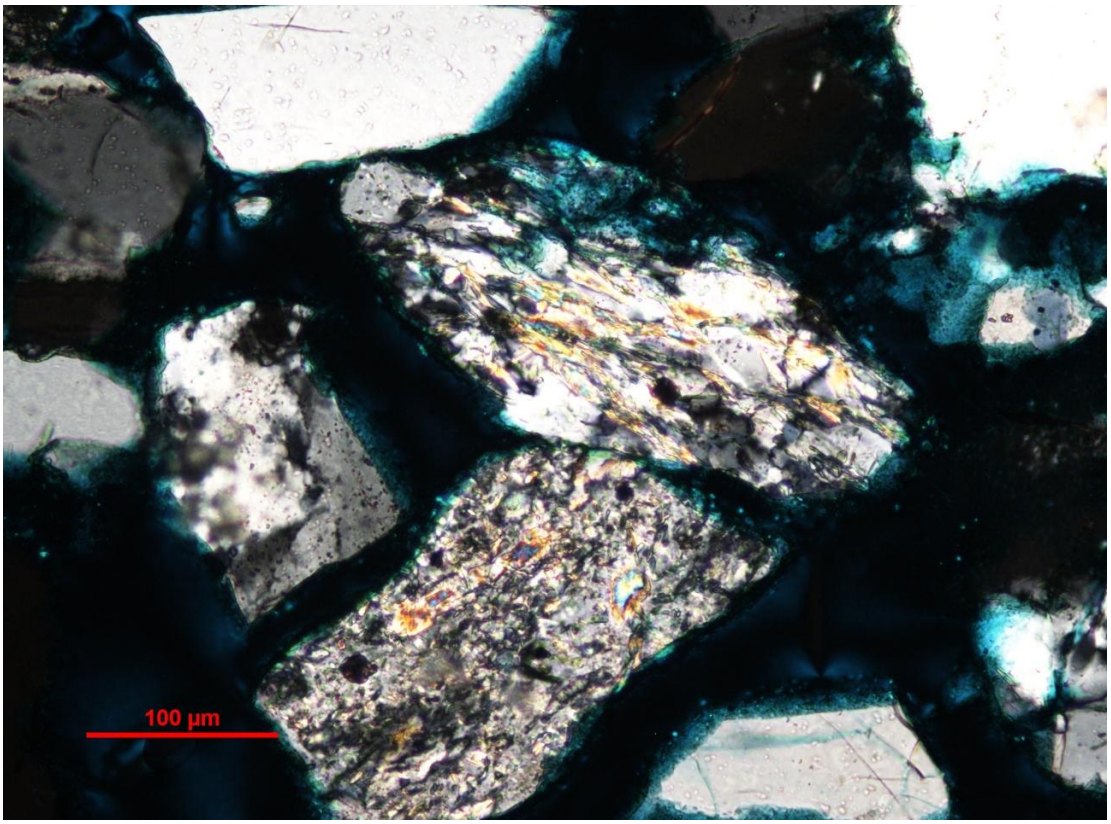

Figure 4.1.5: Mica schist fragments. Micrograph taken with crossed nichols. Scale bar is 100µm. Snadd Formation, 796.02mRKB.

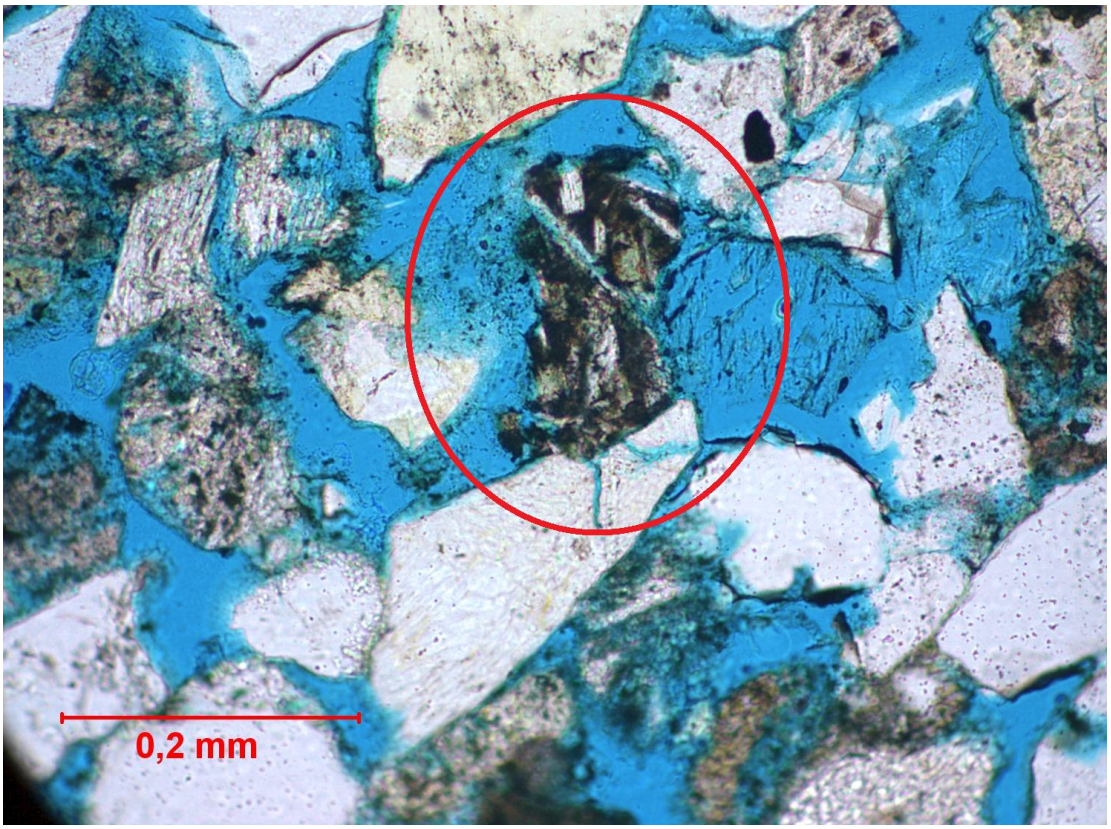

Figure 4.1.6: Volcanic rock fragment (red circle) made up of plagioclase crystals in a dark matrix. Scale bar is 200µm. Snadd Formation, 778.03mRKB.

Diagenetic minerals

Quartz overgrowths are seen in trace amounts in almost all samples (Figure 4.1.7). The overgrowths appear on clean quartz grains as planar surfaces and the boundaries are sometimes defined by dust rims. The low content of quartz overgrowths in the Snadd Formation is mostly due to chlorite coatings covering almost all grains. Quartz overgrowths are seen where chlorite coats are incomplete.

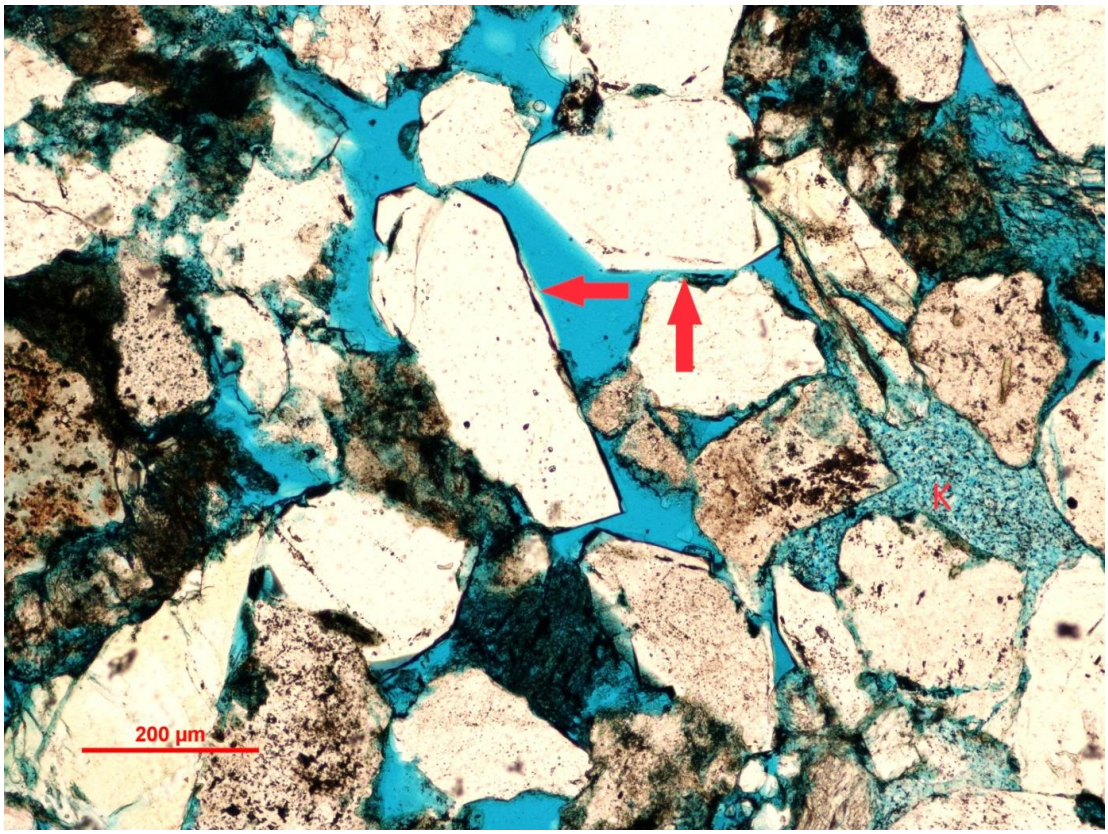

Figure 4.1.7: Micrograph showing quartz grains with planar quartz overgrowths (red arrows). Authigenic kaolin indicated with a red K. Scale bar is 200µm. Snadd Formation, 1800.80mRKB.

Microporous authigenic kaolin aggregates built up of stacks of pseudohexagonal platelets are usually present in volumes of up to 2.7% (Figure 4.1.7).

Diagenetic chlorite coats almost all grain surfaces in most of the thin-sections from the cores from the shallowest depths (778-1291mRKB, Figure 4.1.8). The other samples from these depths have chlorite coats on some of the grains, however, no diagenetic chlorite was seen in the side wall cores.

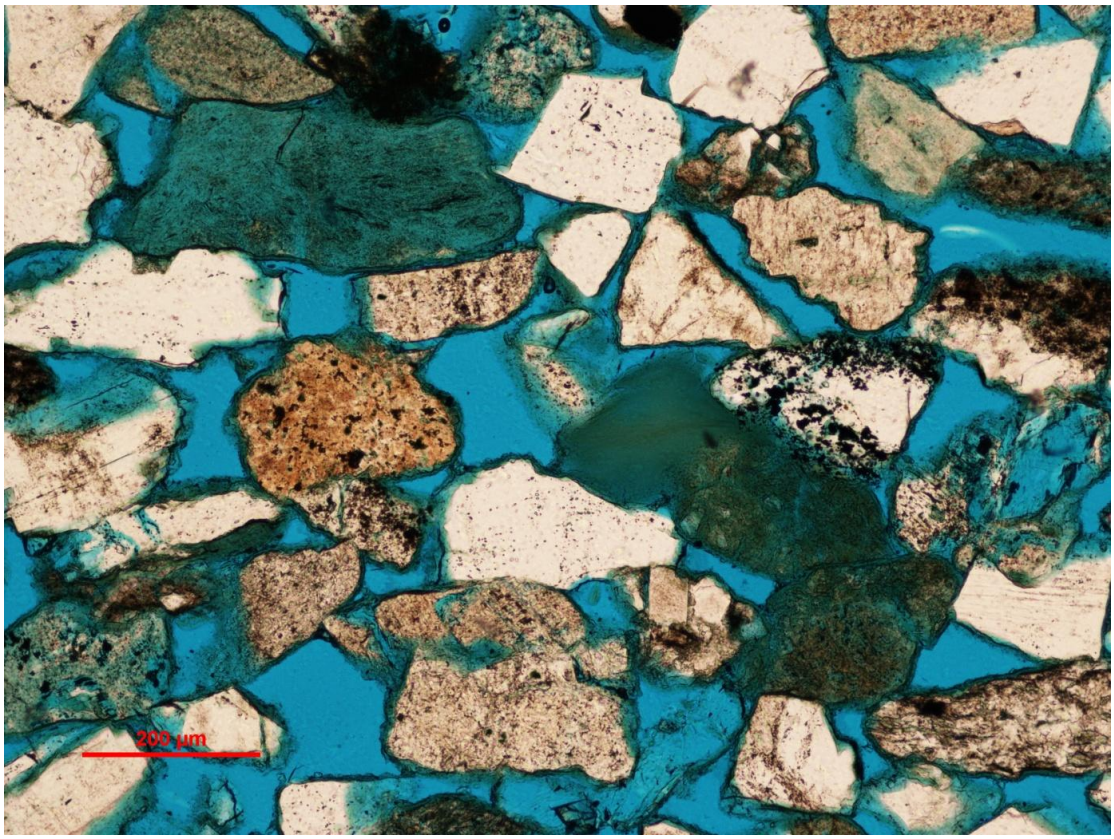

Figure 4.1.8: Thin rims of diagenetic chlorite covering all grains and preventing quartz cementation. Scale bar is 200µm. Snadd Formation, 796.02mRKB.

Small amounts (trace to 0.7%) of siderite cement were seen in around half of the Snadd Formation samples. The siderite forms composite grains of brown rhombic crystals and also occurs within clay clasts and expanded biotite grains. Some sideritic grains may be detrital. Small amounts (trace amounts to 1%) of blue-stained ferroan calcite cement occur as scattered cement patches in several samples, although some of the side wall cores are strongly calcite-cemented (Figure 4.1.9).

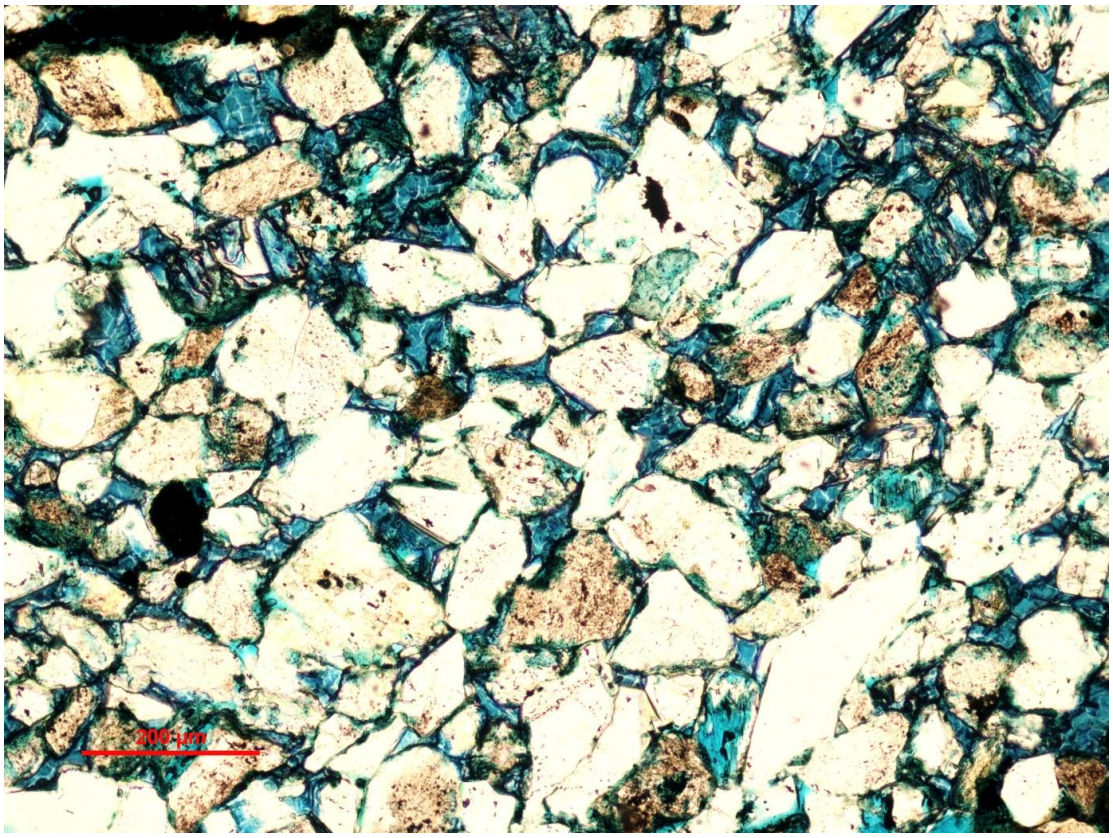

Figure 4.1.9: Ferroan calcite with blue staining filling most pores. Scale bar is 200µm. Snadd Formation, 1297.00mRKB.

Pyrite framboids and cement patches are seen in almost all samples, but are present in trace amounts only.

Porosity and permeability

Point-counted porosities vary from 17.3% to 34% (Table 4.1.1) in the samples that are not strongly calcite-cemented, which, with one exception, is very close to the measured helium porosities for the same Snadd Formation samples, (17.7 to 33.9%). For the side wall core sample 1617.30mRKB point-counted porosity is 17.3% and helium porosity is 6.8%. This may possibly be due to the side wall core being inhomogeneous. Point-counted porosity values are for some of the samples a few per cent lower than helium porosities, probably due to the presence of micropores in grains such as clay clasts and rock fragments.

Most of the examined Snadd Formation samples have pore systems that mainly consist of primary intergranular macropores. Their original size has been reduced by mechanical compaction and precipitation of diagenetic chlorite and quartz. Dissolution porosity formed by dissolution of feldspar and carbonate fossils is seen in the majority of the samples from

trace amounts up to 2.7%. It is, however, difficult to determine whether some feldspar grains were already partly dissolved when they were deposited. Micropores are present in clay clasts and rock fragments, and are therefore present in all samples but are more abundant in the more clay-rich and micaceous samples.

Very variable horizontal permeability is measured. In the cleaner and more clay-free samples permeability reaches almost 5 000mD, whereas in the clay-rich and micaceous samples permeabilities are as low as 0.008mD (Figure 4.1.10).

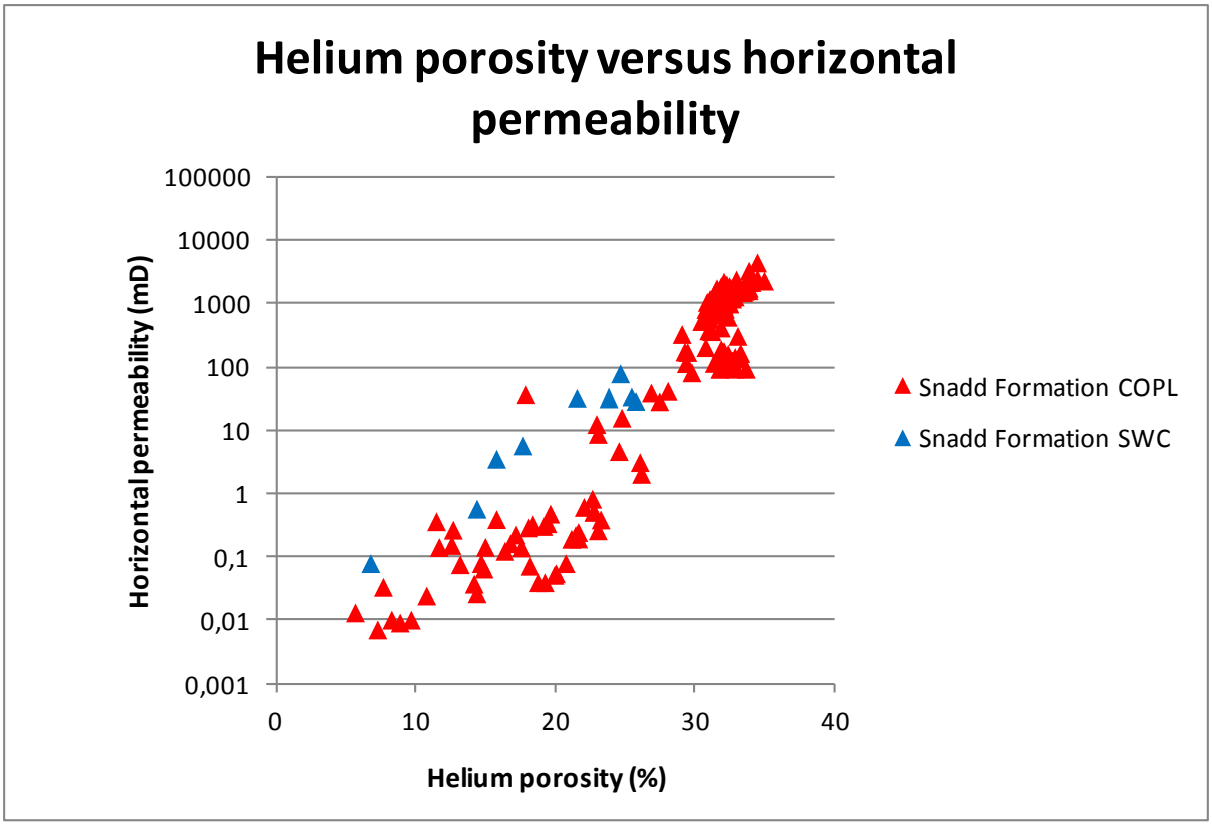

Figure 4.1.10: Helium porosity versus horizontal permeability for all Snadd Formation core plugs (COPL) and side wall cores (SWC). A positive correlation is seen. The values are very variable, but the core plugs show a cluster from Cores 1 and 2 with especially good porosity and permeability values, 29-34% and 80-4 400mD, respectively.

4.2 The Kobbe Formation

4.2.1 Depositional environment

Cores 4 and 5 from the Kobbe Formation are cut from 2209.5 to 2224.8mRKB and from 2227.1 to 2243.4mRKB, respectively (Figures 4.2.1 and 3.1.1b). The lowermost part of Core 5 contains a 1m thick mudstone layer deposited in an offshore marine setting. The next

approximately 10m thick section is dominated by dm-m thick beds of very fine- to fine-grained sandstone with current ripples, slight bioturbation and a few bivalves. This interval is interpreted as estuarine tidal channel and sandy tidal flat deposits. The uppermost 5m of Core 5 and lowermost 2m of Core 4 are more muddy with interbeds of mudstone and fine-grained sandstone and were deposited on a mixed sandy and muddy tidal flat. Above there is a thin layer of laminated fine-grained sandstone with some calcite cement that probably marks a rise of relative sea level. Above this transgressive layer the remaining eleven metres of Core 4 comprise moderately muddy and somewhat bioturbated very fine- and occasionally fine-grained outer estuarine mouth bar sandstones with wave ripples and horizontal lamination and an uppermost 4m thick unit of offshore mudstones.

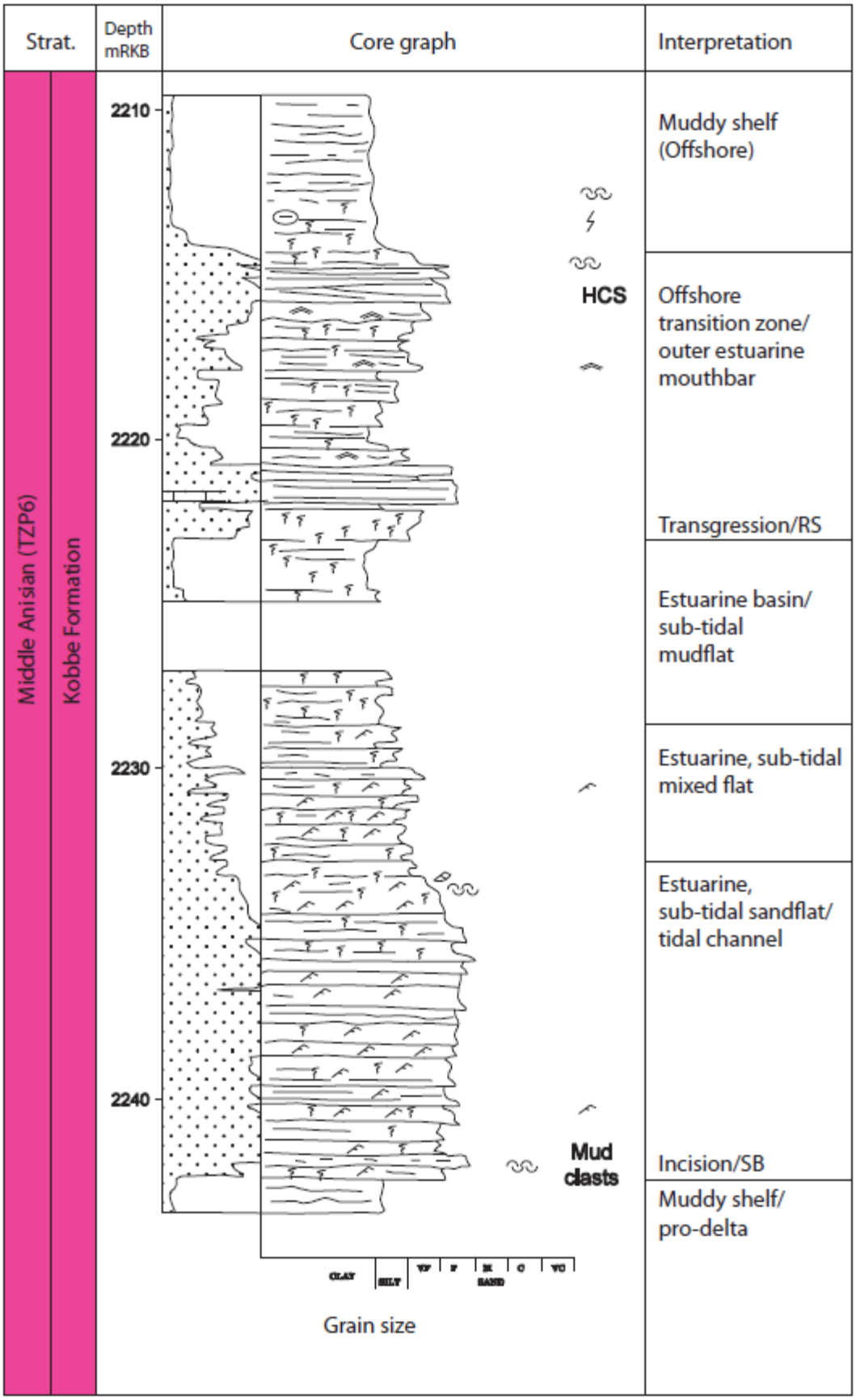

Figure 4.2.1: Core description, Cores 4 and 5, Kobbe Formation, well 7222/11-1. Depth in mRKB. Figure provided by Statoil ASA.

4.2.2 Petrographic composition

Lithology and texture

Samples from the Kobbe Formation are mainly very fine- and fine-grained well sorted sandstones with low to moderate contents of detrital clay (Figures 4.2.2, 4.2.3a and b). In addition, some samples are clay-rich very fine-grained and very well sorted sandstone. Interlaminated clay-rich siltstone and very fine-grained well sorted sandstone also occur. Grains are typically subangular.

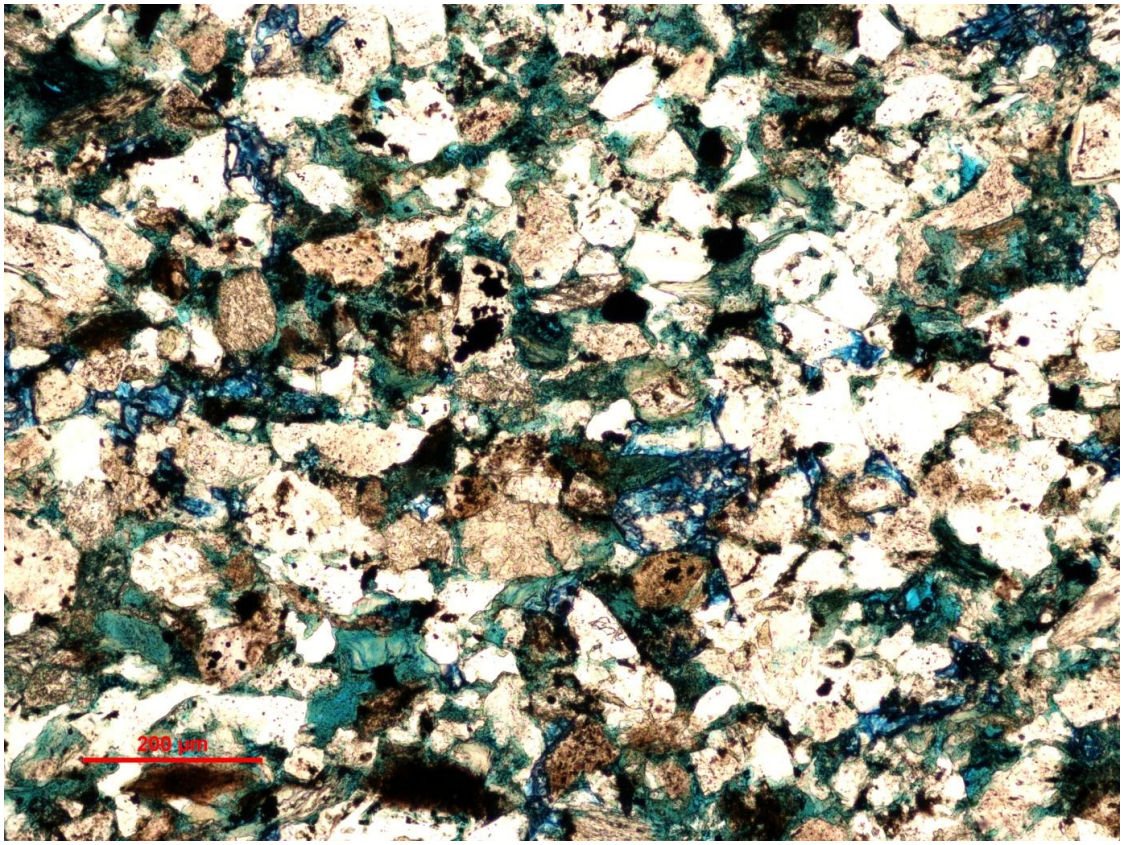

Figure 4.2.2: Very well sorted fine-grained quartz-rich sandstone with common plagioclase (dusty white to brown) and rock fragments. Green clay clasts and blue-stained ferroan calcite fill the pores. Helium porosity is 12.5% and permeability is 0.037mD. Scale bar is 200µm. Kobbe Formation, 2215.25mRKB.

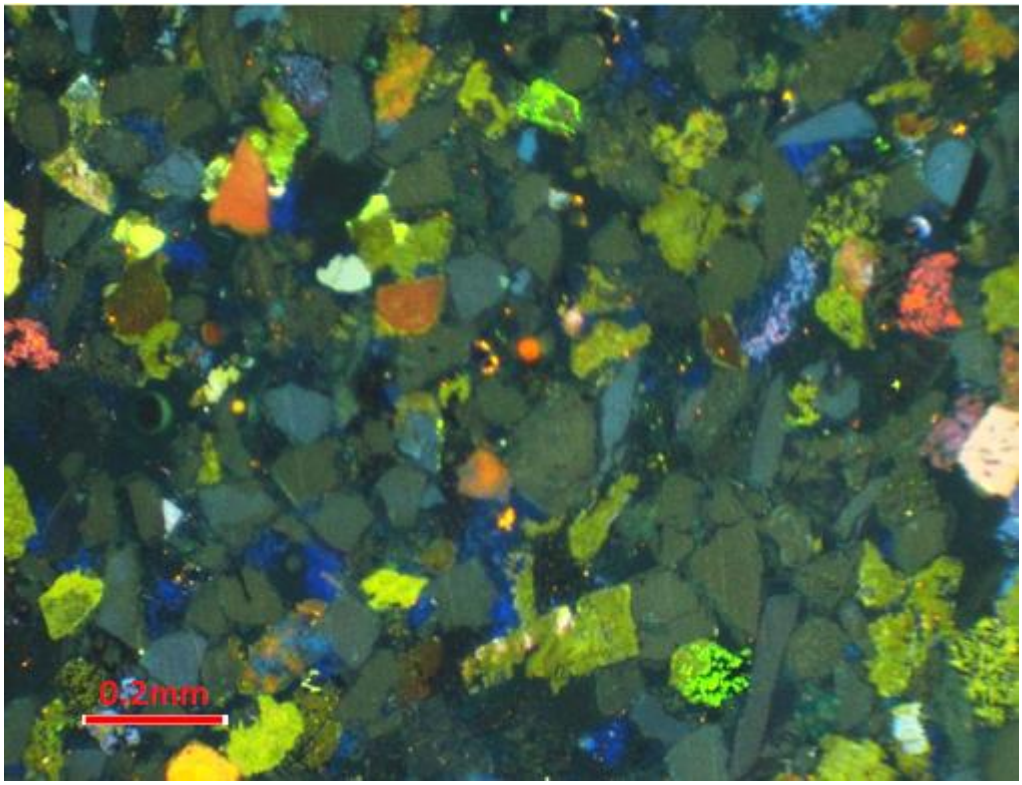

Figure 4.2.3a: Cathodoluminescence micrograph showing yellow and orange plagioclase grains. The other grains are dominantly quartz. Authigenic kaolin is dark blue. Note absence of K-feldspar with intense light blue cathodoluminescence colours (Amieux, 1982; Marshall, 1988). Scale bar is 200µm. Kobbe Formation, 2236.50mRKB.

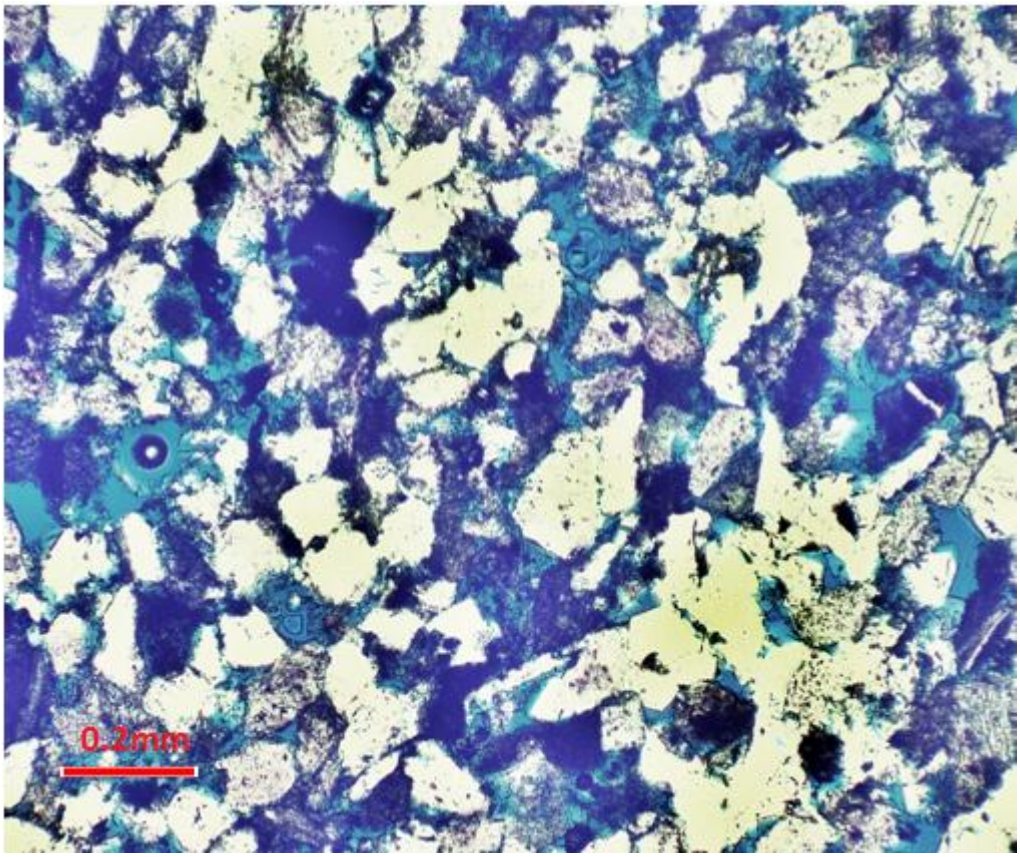

Figure 4.2.3b: Micrograph of the same area as in 4.2.3a taken with plane-polarized light. Scale bar is 200µm.

Detrital grains

Quartz is the most abundant detrital mineral in the Kobbe Formation and monocrystalline quartz accounts for 25 to 40.7% of sample volumes (Table 4.1.1). Polycrystalline quartz is also common and makes up 5.3 to 13.7% of samples volumes. Chert grains are found in all Kobbe Formation samples (1-3% of sample volumes), and quartz-rich metamorphic rock fragments are also abundant in all Kobbe Formation samples (9.6-18% of sample volumes). The chert grains are normally grey, but also appear as brown or orange.

K-feldspar is not present in samples from the Kobbe Formation, but plagioclase contents are relatively high, ranging from 8 to 12.7% of sample volumes (Table 4.1.1). Some of the plagioclase grains are inclusion-free with albite twinning, while some grains contain abundant tiny fluid inclusions and/or sericite. Some of the inclusion-rich grains are seen to have albite twinning as well.

Small amounts of flaky muscovite are seen in all Kobbe Formation samples (0.7 to 2.7% of sample volumes). Biotite only occurs in small amounts in a few samples, and appears as brown flakes. Green detrital chlorite is seen in trace amounts in all samples.

Heavy minerals in amounts up to 0.3% of sample volumes are seen in all Kobbe Formation samples. Heavy minerals from the Kobbe Formation are zircon, yellow, green, blue and grey tourmaline, rutile, apatite, reddish-brown and brown spinel, monazite, chloritoid and opaque iron-titanium oxides. Opaques, rutile, apatite and spinels are most often seen, while grey tourmaline, monazite and chloritoid are very rare.

Plant fragments appear in around half of the samples, most often in amounts of 0.3 to 0.7% (Figure 4.2.4). The fragments may reach 5mm in length and commonly have a cellular structure. Carbonate fossils are rarer than plant fragments in the Kobbe Formation, and are probably the source of carbonate cement in some of the samples. Most of the carbonate fossils are not identified, but some fragments can be recognized as parts of bivalve or brachiopod shells (Figure 4.2.5).

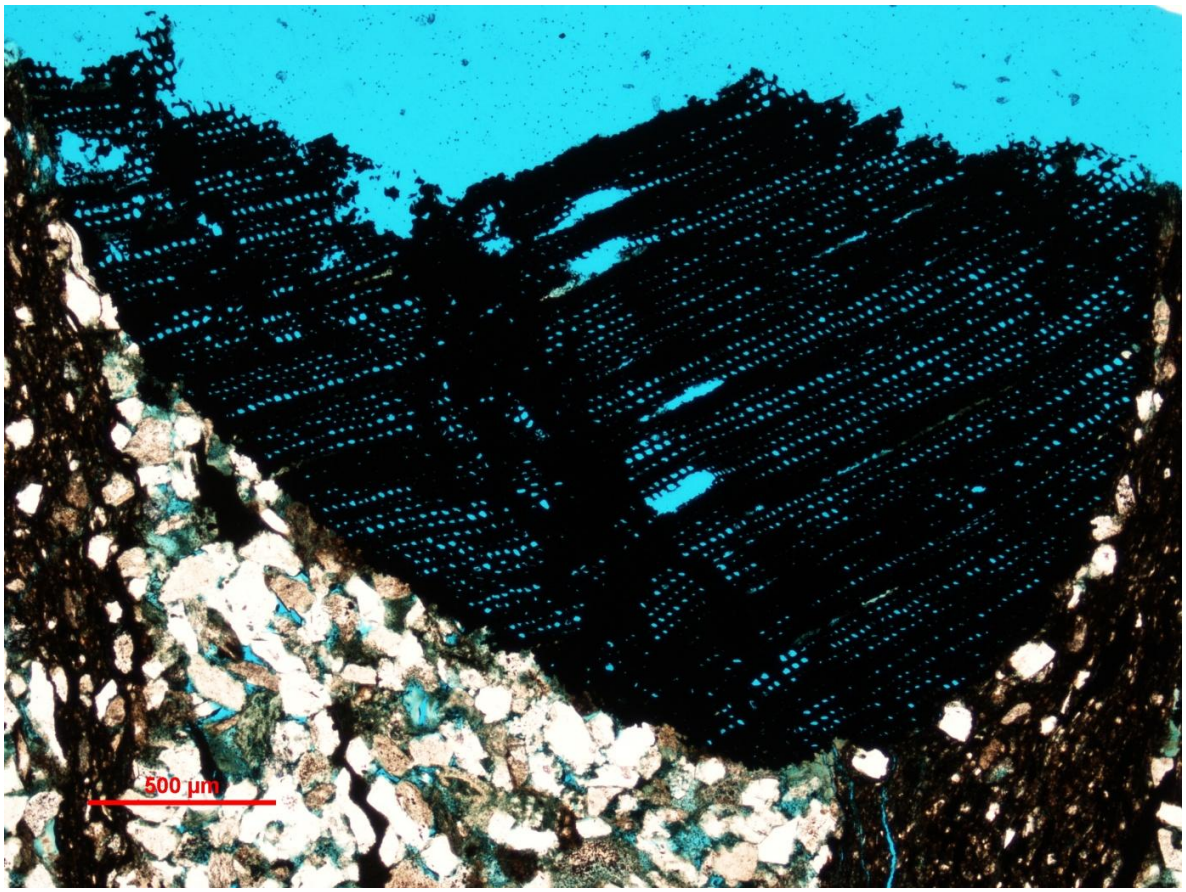

Figure 4.2.4: Plant fragment with cell structure. Scale bar is 500µm. Kobbe Formation, 2241.10mRKB.

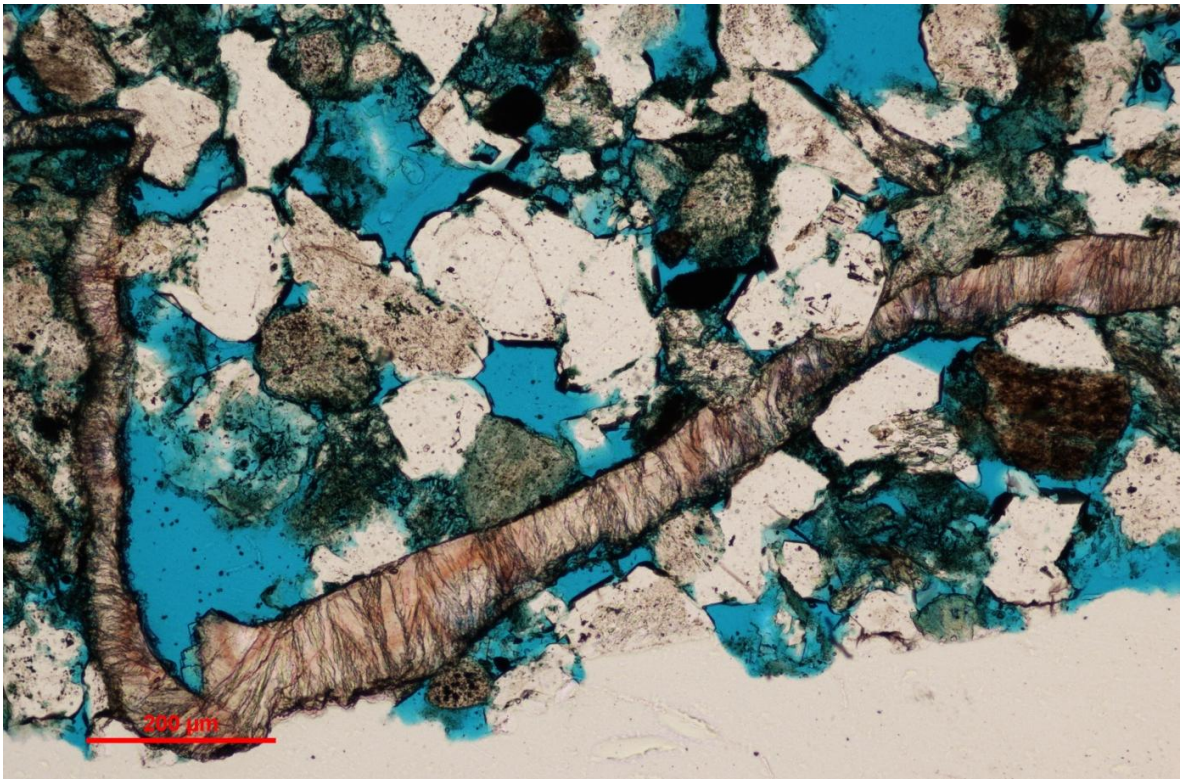

Figure 4.2.5: Bivalve. Scale bar is 200µm. Kobbe Formation, 2238.50mRKB.

Clay clasts and mica-rich rock fragments such as mica schist, phyllite and slate are common in the Kobbe Formation and account for 6 to 13.3% of sample volumes. A few volcanic rock fragments consisting of elongate plagioclase crystals in a brown matrix also occur.

Detrital clay matrix accounts for up to 4.7% of point-counted sample volumes, but volumes of detrital clay matrix are higher in some of the other samples.

Diagenetic minerals

Quartz overgrowths are present in small volumes (0.3 to 1.7%) in all Kobbe Formation samples (Figure 4.2.6). The volumes of quartz overgrowths would have been higher if volumes of monocrystalline quartz were higher and the quartz grains were not quite often coated by clay.

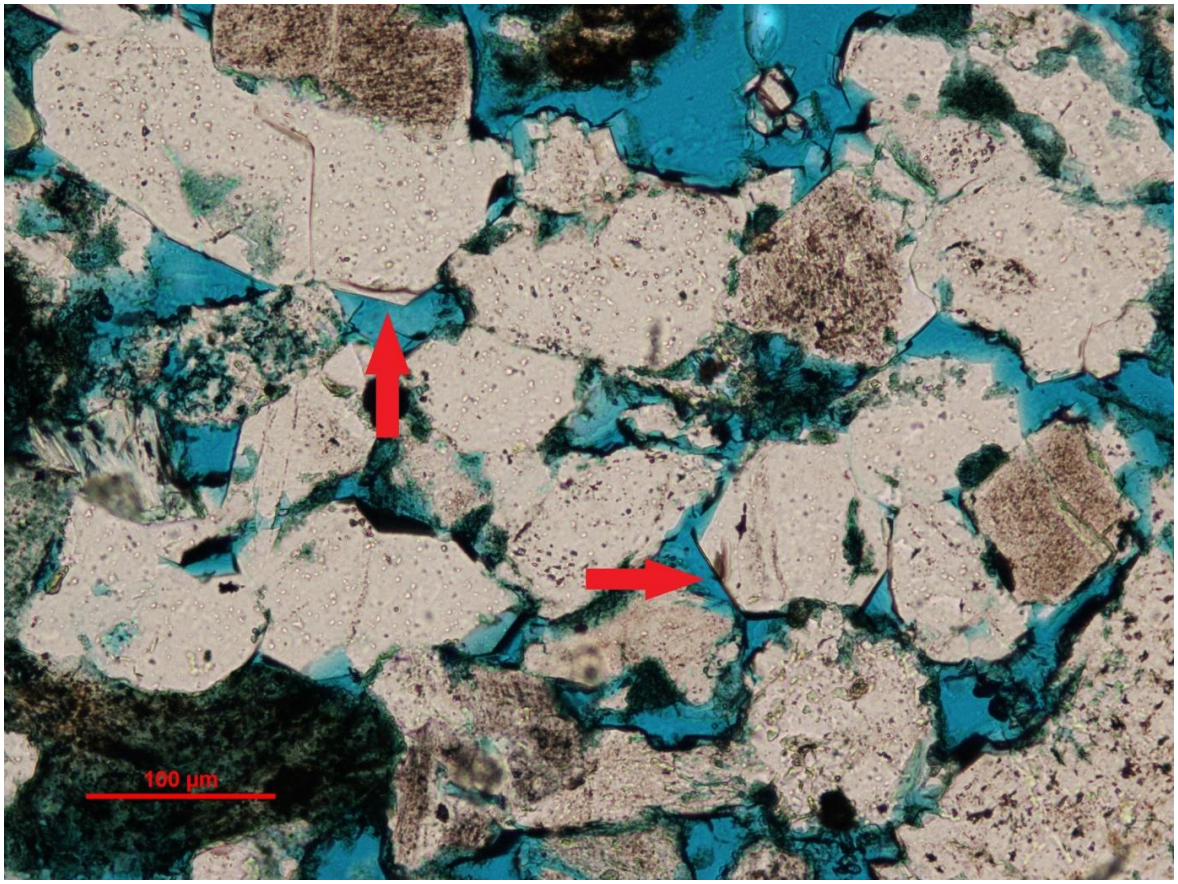

Figure 4.2.6: Quartz grains with planar quartz overgrowths, indicated with red arrows. White grains with numerous brown specks are plagioclase. Scale bar is 100µm. Kobbe Formation, 2238.50mRKB.

Kaolin cement in the form of microporous aggregates made up of stacks of pseudohexagonal platy crystals is seen in all Kobbe Formation samples in volumes of 0.3 to 2.3%. Partial grain

coatings of authigenic chlorite are found on some grains in around half of the Kobbe Formation samples. The chlorite coatings are rare and not so well developed as in the Snadd Formation.

Siderite is present in trace amounts in most of the samples. The siderite is normally developed as scattered very small (3-10µm) pale brown rhombic crystals (Figure 4.2.7). Some larger polycrystalline sideritic aggregates are also seen, but they may be intraclasts or grains eroded from older sandstones.

Blue-stained ferroan calcite cement forms small cement patches in most of the Kobbe Formation samples (Figure 4.2.7). Calcite cement is usually seen in trace amounts, maximum content of calcite cement is 3.3%.

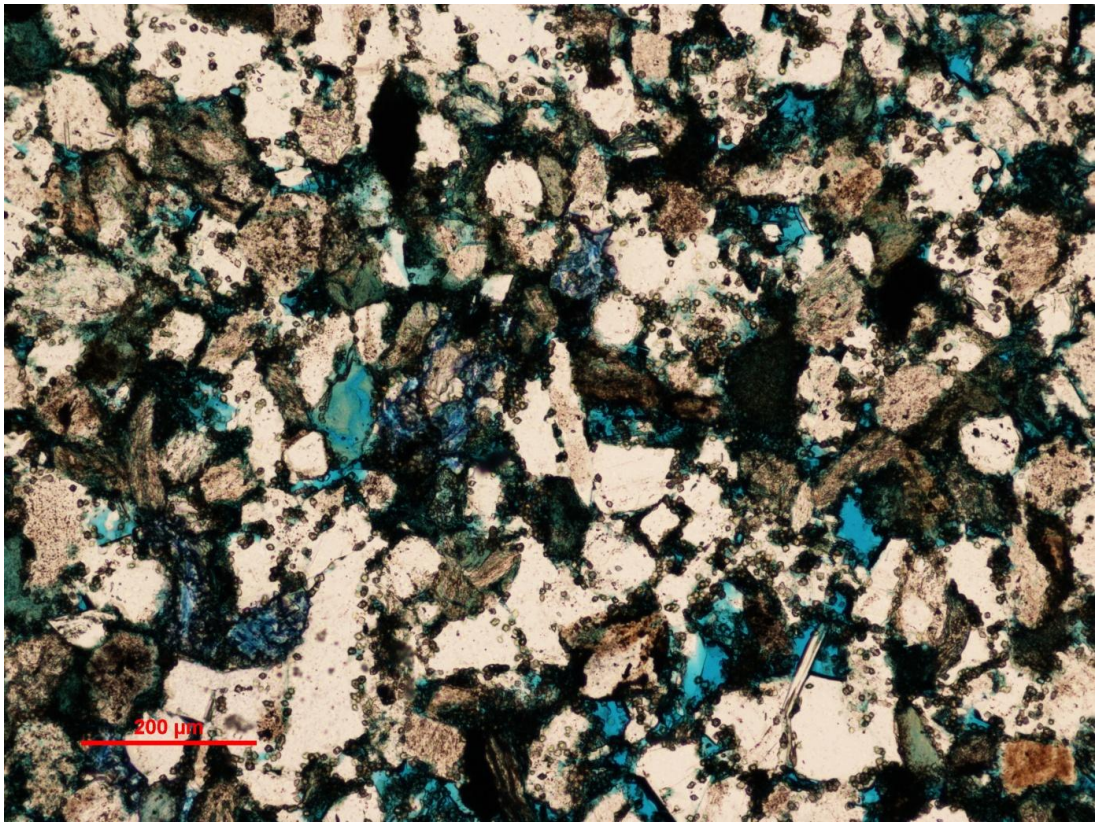

Figure 4.2.7: Tiny grains of brown siderite scattered over the whole thin-section. Blue-stained ferroan calcite is seen in some of the pores. Scale bar is 200µm. Kobbe Formation, 2221.50mRKB.

Pyrite cement is present in trace amounts in most of the Kobbe Formation samples. The pyrite cement occurs as framboids and cement patches. The pyrite cement is often integrated with plant fragments, and occasionally pyrite partly replaces the plant fragments.

Albite cement is present in most of the samples in amounts up to 0.3% (Figure 4.2.8). The albite cement occurs as overgrowths on plagioclase grains, and albite cement crystals also partly fill dissolution pores.

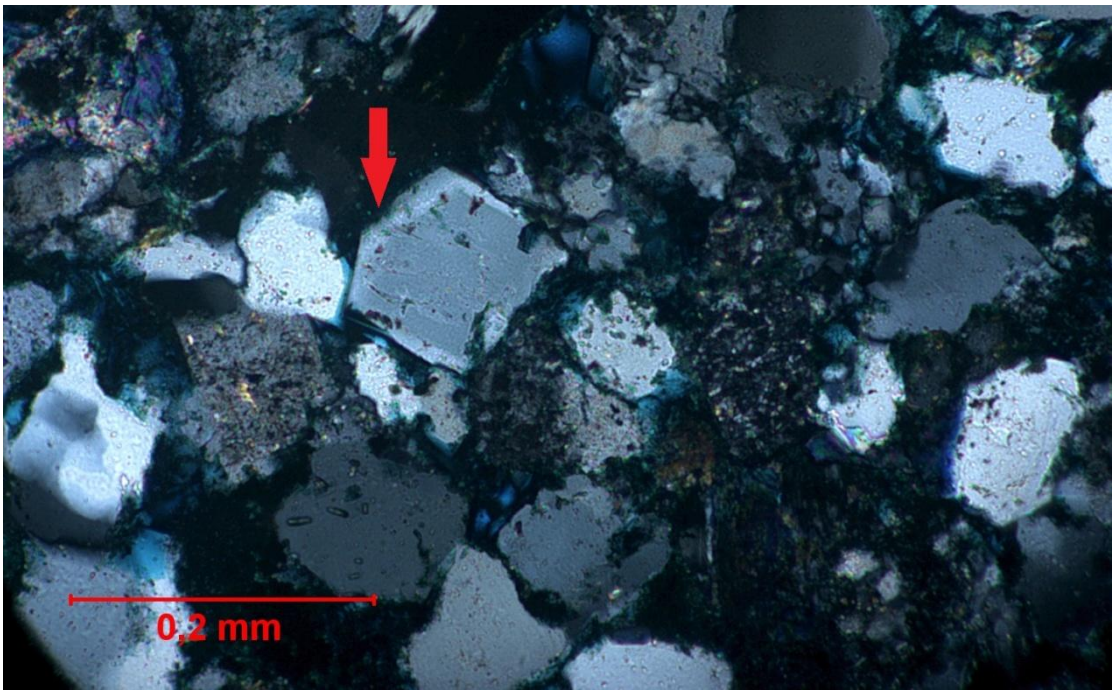

Figure 4.2.8: Albite overgrowth on plagioclase grain, indicated with red arrow. The overgrowth shows a lighter colour than the original grain with crossed nichols. Scale bar is 200µm. Kobbe Formation, 2235.00mRKB.

Porosity and permeability

Point-counted porosities are 14.3 to 18.1% (Table 4.1.1) and are very close to helium porosities which range from 18.7 to 20.7% for the point-counted samples. The pore system in the Kobbe Formation sandstones mostly consists of primary intergranular macropores. Their original size has been modified by mechanical compaction and precipitation of quartz overgrowths and to a smaller degree other diagenetic cements. Micropores within detrital and authigenic clay and within some of the rock fragments also account for a substantial fraction of the total porosity. A few dissolution pores formed by dissolution of feldspar are present in trace amounts in some samples.

Horizontal permeability for the core plugs varies from 0.037 to 19.9mD, and there is a trend that permeability increases with helium porosity (Figure 4.2.9). Permeability is highest in the sandstones that contain the least clay.

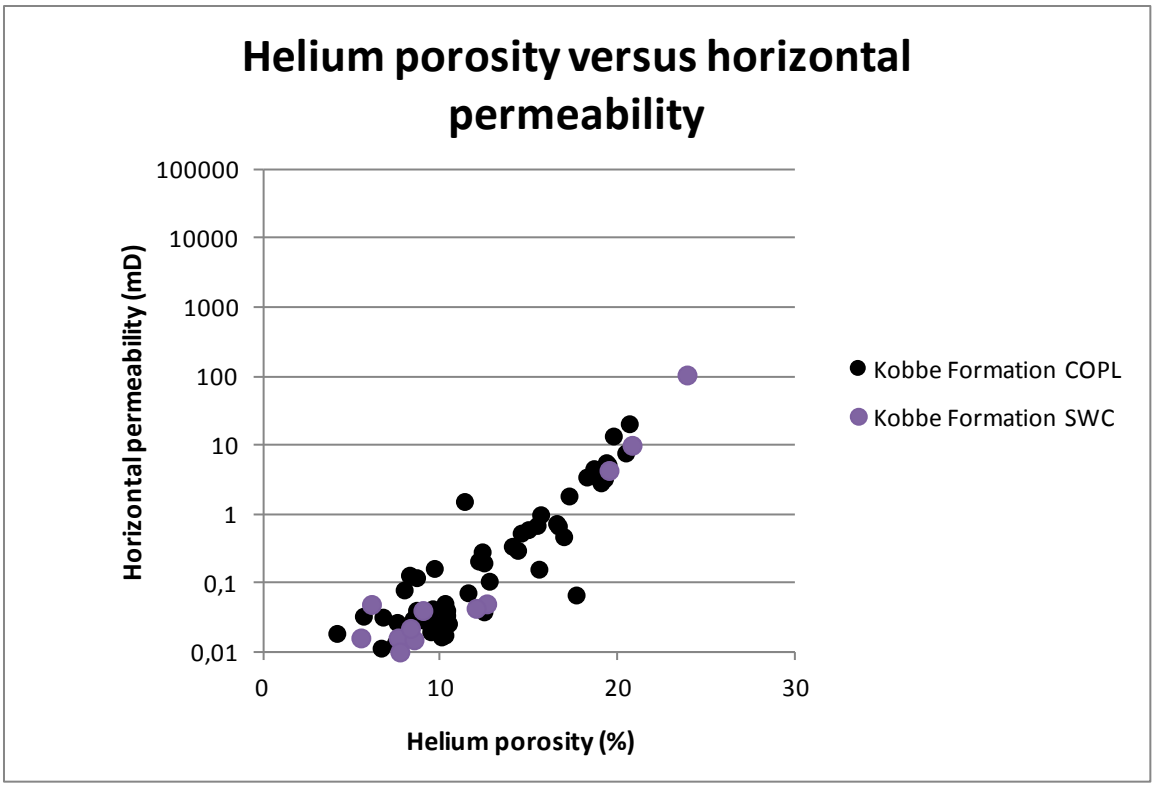

Figure 4.2.9: Helium porosity versus horizontal permeability for Kobbe Formation core plugs (COPL) and side wall cores (SWC). A positive correlation is seen. Porosity and permeability values are generally poorer in the Kobbe Formation, with a cluster of points with porosities of 4-13% and permeabilities below 1mD. Values rarely exceed 20% and 10mD.

5 Discussion

5.1 Sandstone composition and provenance

The Fruholmen Formation sandstones in well 7131/4-1 comprise well and moderately well sorted fine- to coarse-grained very quartz-rich sandstones with hardly any detrital clay (Figure 5.1.1). No plagioclase is present, K-feldspar contents are very low, less than 1%, and trace volumes of chert are present in around half of the samples. Nearly all Fruholmen Formation sandstones classify as quartz arenites. Quartz grains with inherited quartz overgrowths from older quartz-cemented sandstones occur. Together with the very high quartz contents this suggests a source area containing at least some older sediments and/or metasediments.

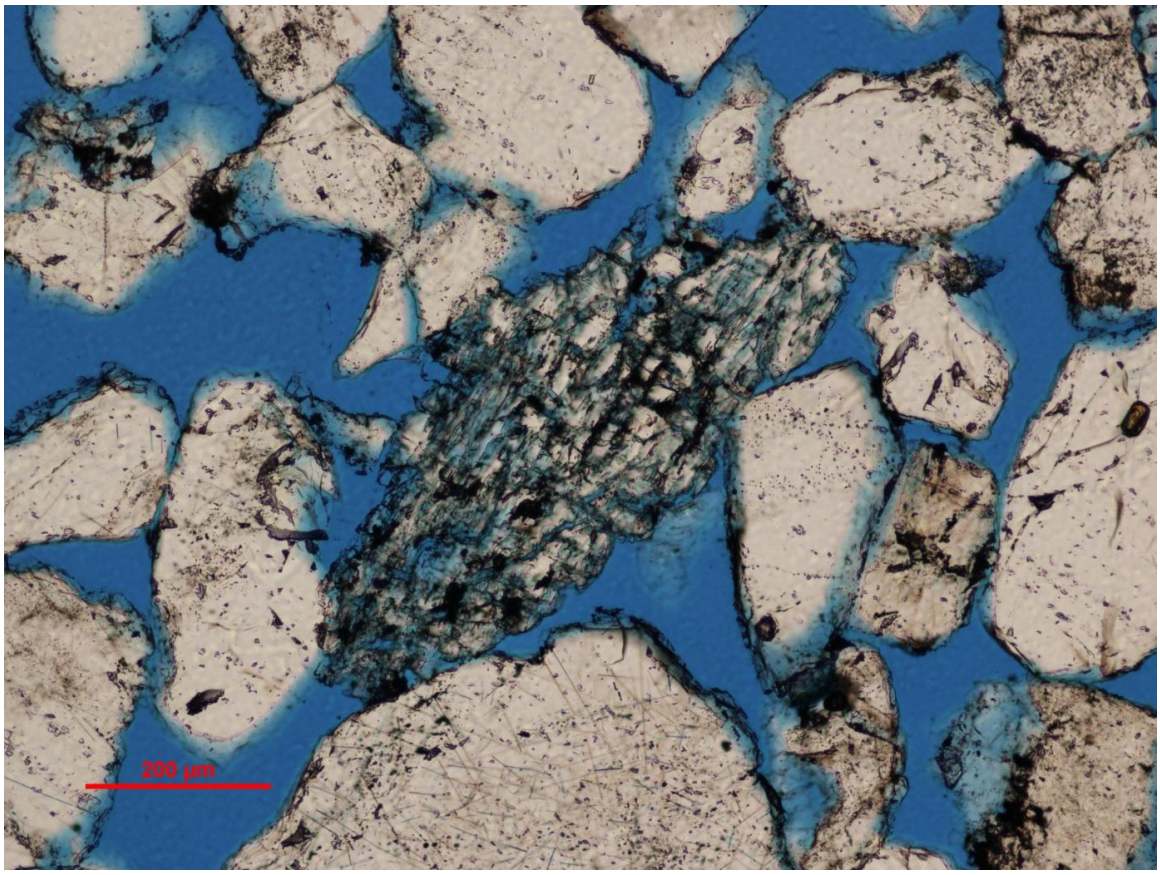

Figure 5.1.1: One of only a very few K-feldspar grains observed in the Fruholmen Formation. The grain is partly dissolved. Nearly all sand grains in the Fruholmen Formation consist of quartz. Scale bar is 200µm. Fruholmen Formation, well 7131/4-1, 920.00mRKB.

The well and moderately well sorted fine- and medium-grained clay matrix-free sandstones of the Snadd Formation in well 7131/4-1 have a detrital composition very different from the Fruholmen Formation sandstones and are classified as sublitharenites and lithic arenites (Figure 5.1.2). Plagioclase grains are present in all samples in volumes of 0.3-2%, K-feldspar is more common (up to 4%) than in the Fruholmen Formation, and large volumes of chert (1-

5%) and abundant mica-rich and quartz-rich metamorphic rock fragments are present (typically 10-18%). The metamorphic rock fragments are mostly difficult to classify, but include foliated mica schist and probable phyllite made up of quartz, muscovite and more rarely chlorite; metamorphic sandstone and siltstone mostly consisting of quartz grains, quartz cement, muscovite and occasionally chlorite; probable slate fragments; and possibly volcanic fragments that are difficult to distinguish from other clay mineral-rich metamorphic fragments and clay clasts. A few quartz grains with inherited quartz cement beneath early diagenetic chlorite grain coats were also seen. Together with the abundant metasedimentary rock fragments this suggests a source area rich in metasedimentary and possibly sedimentary rocks.

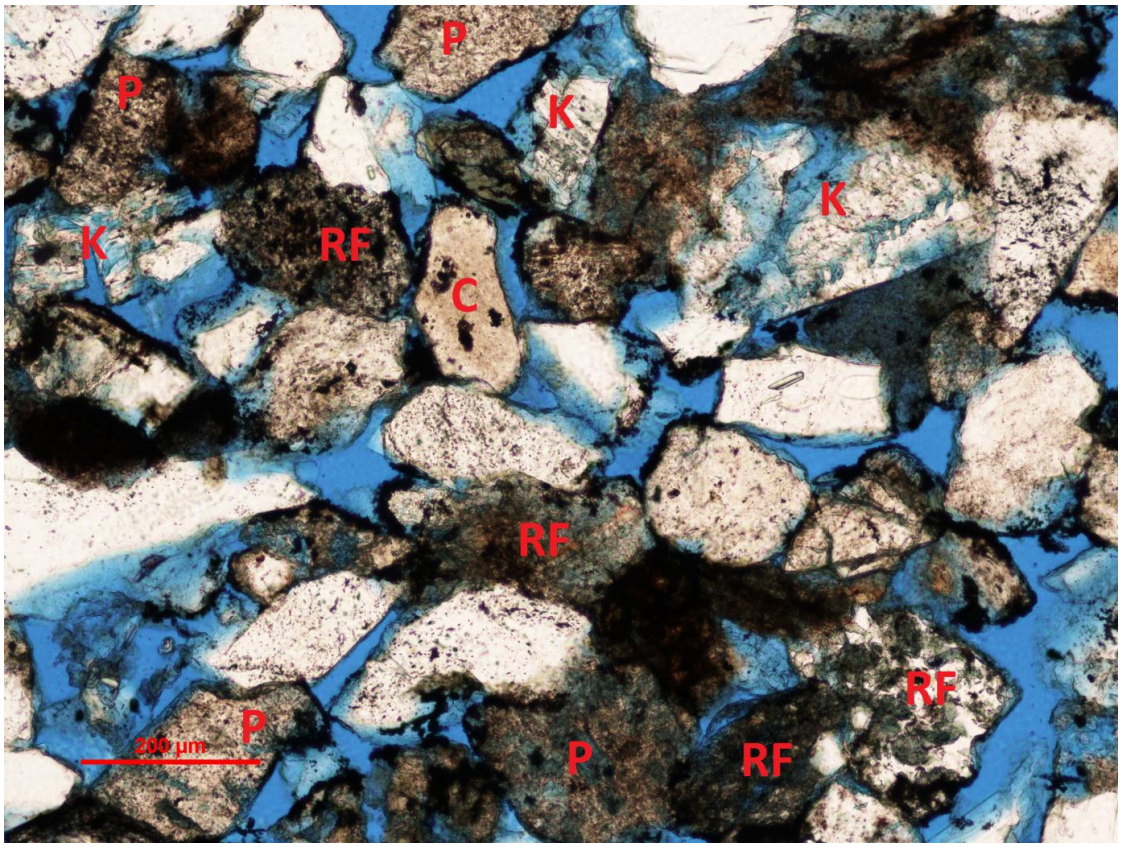

Figure 5.1.2: Snadd Formation sandstone containing quartz grains (white), chert (C), other rock fragments (RF), clay clasts (dark brown), plagioclase (P) and K-feldspar (K). Scale bar is 200µm. Snadd Formation, well 7131/4-1, 1100.00mRKB.

The composition of the Snadd Formation sandstone samples from well 7222/11-1 is very similar to the composition of the Snadd Formation sandstones in well 7131/4-1 (Figure 5.1.4) although plagioclase contents are higher (3-7% and in one case 13%). Types of rock fragments present are the same as described for the Snadd Formation in well 7131/4-1, although a few more easily identified plagioclase-rich volcanic rock fragments were also

found. Detrital clay matrix contents are low, zero to 4%, but higher than in well 7131/4-1, whereas grain size is on average slightly finer in well 7222/11-1, dominantly fine-grained and only rarely medium-grained. Sorting is as in well 7131/4-1, well and moderately well.

The Kobbe Formation sandstones in well 7222/11-1 are well- and moderately well sorted and fine-grained, finer grained than the Snadd Formation in the same well, and have detrital clay matrix contents of 1-5%. The Kobbe Formation samples plot in the same area of a quartz-feldspar-lithics plot as the Snadd Formation samples from well 7222/11-1 (Figure 5.1.4), but although the total feldspar contents are approximately the same for the two formations in this well, only plagioclase is present in the Kobbe Formation (Figure 5.1.3). The same types and amounts of rock fragments are present in the Kobbe Formation and the Snadd Formation in well 7222/11-1, suggesting a source area with abundant metasediments and possibly sedimentary rocks and some volcanics. The high plagioclase contents may, however, possibly point to some plutonic rocks in the source area, although Bergan and Knarud (1992) suggest that plagioclase may be derived from basaltic rocks.

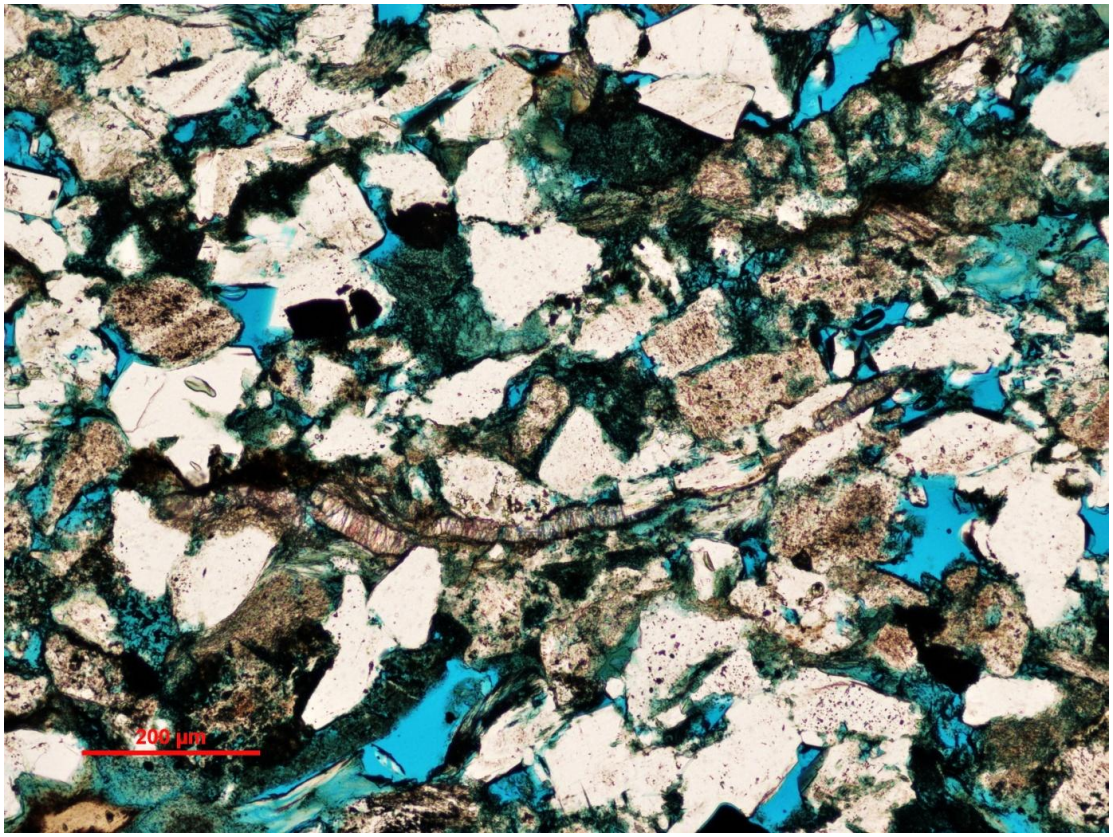

Figure 5.1.3: Kobbe Formation sandstone with 12.3% plagioclase. Most plagioclase grains contain numerous small brown inclusions, quartz grains are white. Dark grains are mostly clay clasts and rock fragments. A partly dissolved bivalve is present at the centre of the micrograph. Scale bar is 200µm. Kobbe Formation, well 7222/11-1, 2238.50mRKB.

There is also a difference between the three studied formations with regard to the heavy minerals present. All three formations contain zircon, yellow and green tourmaline, rutile, monazite and opaque iron-titanium oxides. Apatite, chloritoid and spinels are found in the Snadd and Kobbe formations but not in the Fruholmen Formation. Garnet was seen in the Snadd Formation in both wells, but not in the Kobbe and Fruholmen formations. Rare staurolite was seen in the Snadd Formation in well 7222/11-1, and grey and blue tourmalines are present in the Kobbe Formation. Chloritoid and staurolite are typical of metamorphic rocks (Deer et al., 1966), supporting that metasediments were present in the source area.

The change in composition between the different formations could have various explanations. Different depositional settings could explain differences in sorting, grain size and detrital clay contents, and a shift in climate in the upper Triassic could have led to more intense weathering and more quartz-rich sediments (Bergan and Knarud, 1992; Nystuen et al., 2007). However, although different energy levels in the depositional environments and climate change may contribute to explaining some of the observed differences in sandstone composition, the differences are very marked and also apply to chemically stable components, which indicates that there must also have been changes in the types of rocks that were eroded in the source areas. For instance, chert consists of chemically stable quartz, and it is difficult to see how the near absence of chert in the Fruholmen Formation versus its abundance in the Snadd and Kobbe formations could be a result only of more intense weathering during deposition of the Fruholmen Formation. It is possible that sediments sourced from the same area vary in composition with time due to erosion of different types of rocks at different times, but the studied deposits may also have been sourced from different geographical areas, which could have led to varying compositions. Previous studies have shown that Triassic sandstones from the eastern Barents Sea which have eastern source areas have high contents of rock fragments whereas sands sourced from Scandinavia may be more quartz-rich (Mørk, 1999). This could suggest that the sublitharenites and lithic arenites of the Kobbe and Snadd formations were largely sourced from the east whereas the quartz arenites of the Fruholmen Formation may possibly have a Scandinavian source. However, study of additional wells would be necessary before it is possible to settle these questions, and there is also a possibility that local highs could have been sources of sand (Mørk, 1999).

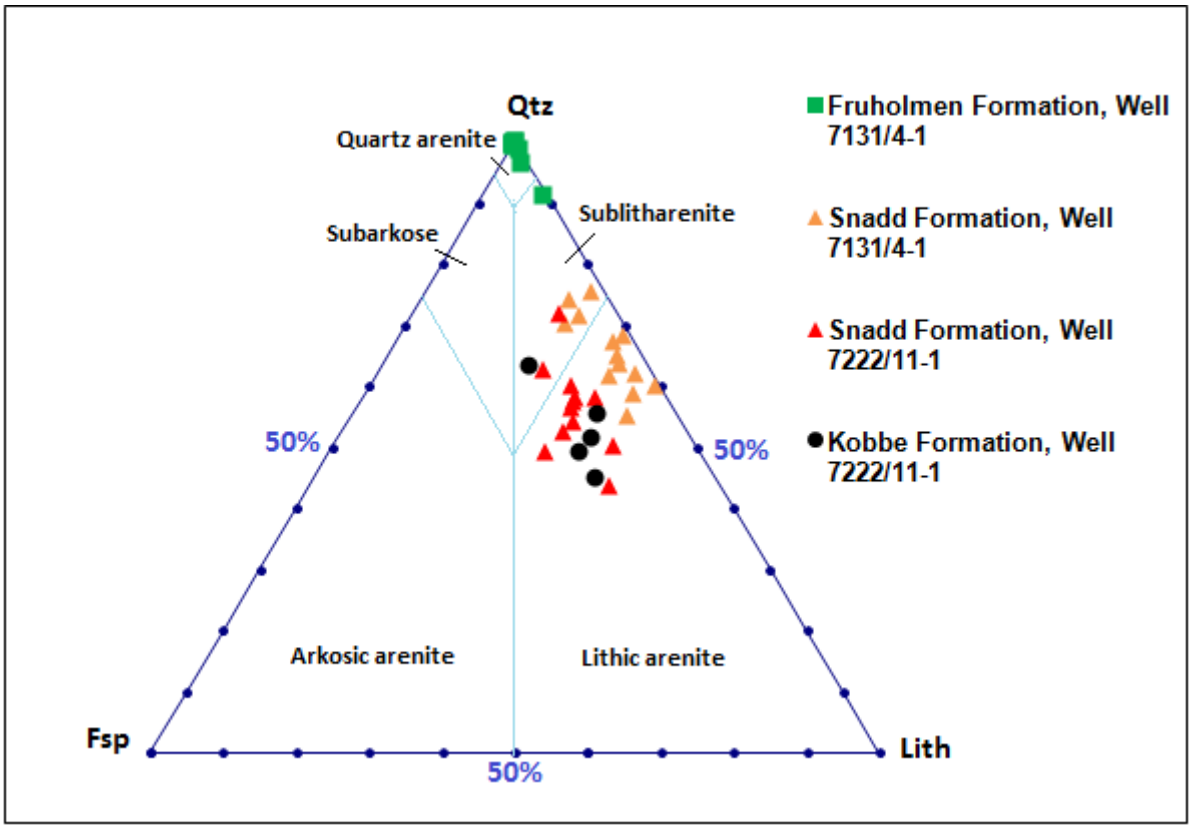

Figure 5.1.4: Plot showing sandstone composition based on modal analysis. The Fruholmen Formation is very mature and hardly contains any feldspar or rock fragments, whereas the Snadd and Kobbe formations are less quartz-rich and contain more feldspar, even though they are quartz-dominated. The Kobbe Formation contains only plagioclase feldspar, whereas the feldspar in the Snadd Formation is both K-feldspar and plagioclase. Qtz: Monocrystalline and polycrystalline quartz, Fsp: K-feldspar and plagioclase, Lith: Chert, clay clasts, mica-rich rock fragments and quartz-rich metamorphic fragments. Modified from Pettijohn et al. (1972).

5.2 Sandstone diagenesis

5.2.1 The Fruholmen Formation

The small observed volumes of framboidal pyrite were probably formed by an early diagenetic process in marine environments where sulphate reducing bacteria use sulphate from sea water to consume organic material in the sediment and form dihydrogen sulphide, H_2S. H_2S then reacts with iron to firstly make monosulphides that later react with sulphur and create pyrite (Berner, 1970; 1981).

The traces of kaolin and dissolved feldspar in some samples could indicate meteoric water infiltration during or shortly after deposition that led to feldspar dissolution and precipitation of authigenic kaolin (Bjørlykke et al., 1979). However, it is also possible that minor amounts of amorphous silica- and alumina-rich gels precipitated in the mixing zone between fluvial and marine water, and that this material crystallized to kaolinite during burial (Walderhaug,

2000). As the kaolin has not been illitized, there is no reason to believe that the K-feldspar has been dissolved as a result of illitization (Bjørlykke, 1980).

Quartz overgrowths are typically late diagenetic and precipitate at temperatures exceeding 70°C (Bjørlykke et al., 1986; Ehrenberg, 1990; Giles et al., 1992; Walderhaug, 1994a). The main source for quartz cement is normally dissolution of quartz grains at stylolites (Bjørlykke et al., 1986; Ehrenberg, 1990; Walderhaug, 1994a; Bjørkum, 1996). Dissolution of quartz at stylolites formed from clay-rich laminae is seen in some samples, especially siltstones (Figure 5.2.1).

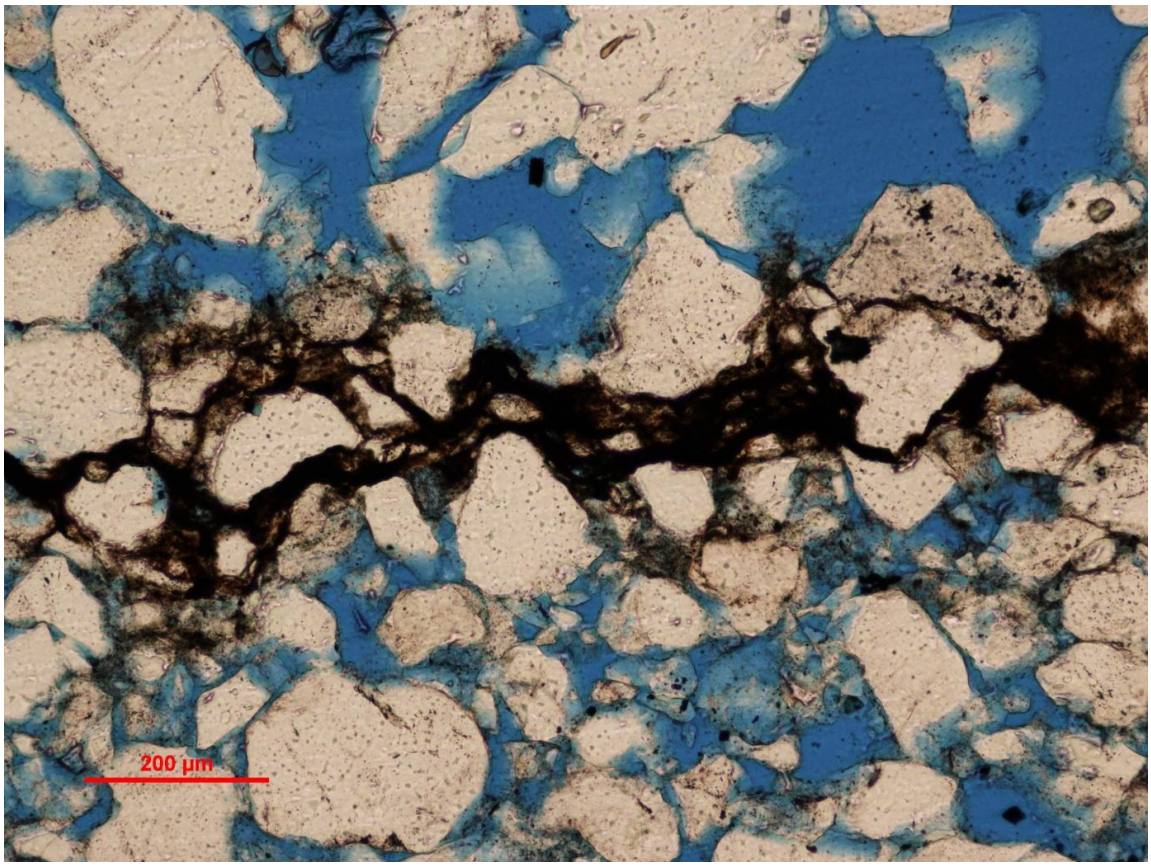

Figure 5.2.1: Stylolite evolved from clay-rich lamina. Scale bar is 200µm. Fruholmen Formation, well 7131/4-1, 942.00mRKB.

A variation in volumes of quartz cement was observed. This is probably due to the difference in quartz surface area available for quartz cementation (Heald and Larese, 1974; Walderhaug, 1996). These variations in available quartz surface area are largely caused by variable grain size which explains why most quartz cement is found in the most fine-grained samples.

Almost all grain surfaces are coated with detrital clay in the sample 916mRKB. Otherwise there are few grain coatings on quartz grains.

5.2.2 The Snadd Formation

Chlorite, or an amorphous or poorly crystalline chlorite precursor, formed at very shallow depth as an early diagenetic phase, which is indicated by early diagenetic siderite and pyrite not being coated by chlorite. The chlorite coatings formed before quartz cementation because they prevent quartz overgrowth precipitation where the chlorite is present (Figure 5.2.2). Chlorite is also covered by calcite in both wells. The early chlorite or chlorite precursor probably formed well-crystallized chlorite as burial and temperature increased and may have formed from amorphous Si-, Al- and Fe-rich colloids supplied by rivers and flocculated by saline marine waters in the fluvial-marine mixing zone (Ehrenberg, 1993).

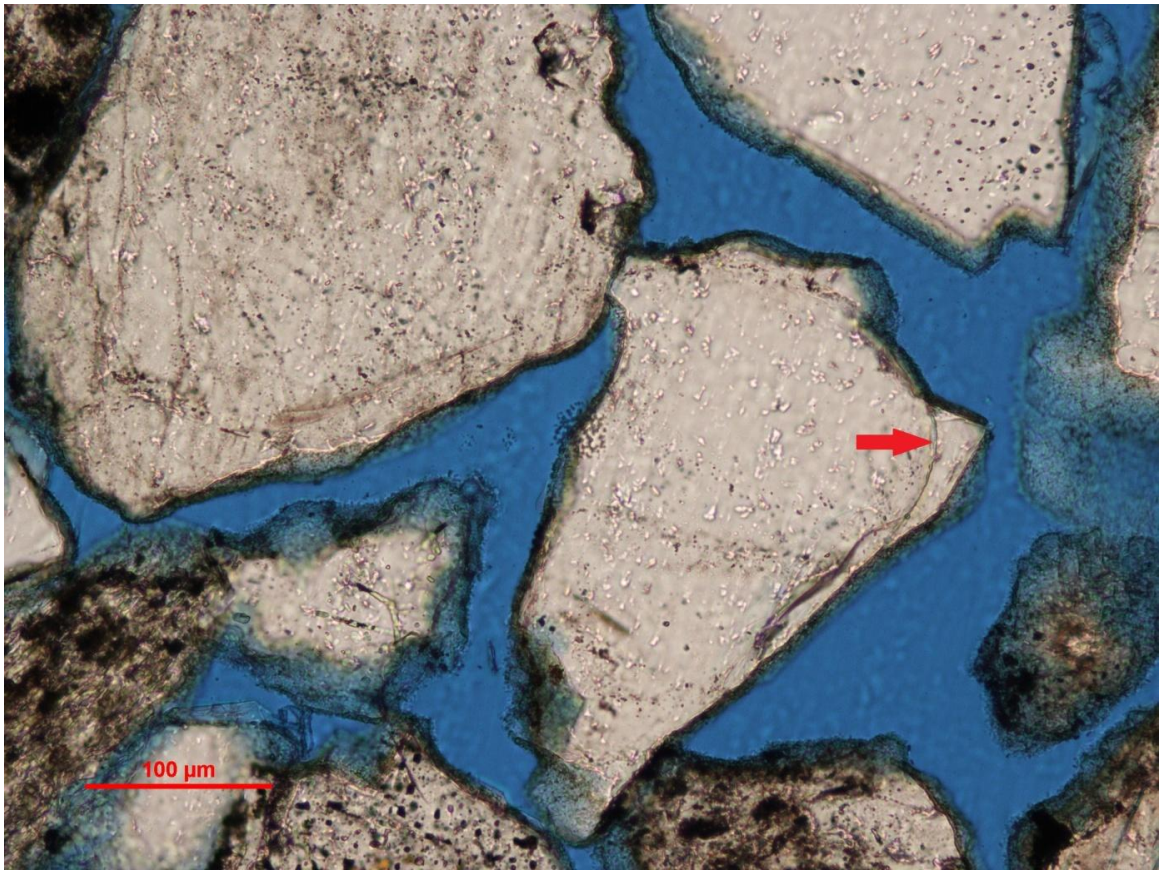

Figure 5.2.2: Chlorite coatings covering all grains. Here a thin rim of diagenetic chlorite is seen covering a possible inherited quartz overgrowth (red arrow) and preventing further quartz cementation. Scale bar is 100µm. Snadd Formation, well 7131/4-1, 1110.00mRKB.

The framboidal morphology of the pyrite suggests that pyrite probably formed very close to the sediment surface due to microbiological sulphate reduction (Berner 1970; 1981). In

addition, some of the pyrite in the Snadd Formation in well 7222/11-1 is engulfed by calcite cement, which also indicates early pyrite precipitation.

The siderite cement occurs engulfed in calcite and therefore predates calcite. There is otherwise very little evidence for constraining when siderite precipitated, but siderite often forms at shallow burial depths (Berner, 1981). Siderite and chlorite formation may be linked to a depositional setting where river waters transported colloidal iron into marine waters where the iron-bearing particles flocculated (Ehrenberg, 1993).

The small amounts of authigenic kaolin observed in the thin-sections may have formed as a consequence of the above mentioned flocculation mechanism. However, as dissolved feldspar is also seen in the Snadd Formation samples, kaolin may also have formed from dissolved feldspar as a result of meteoric water flushing (Bjørlykke et al., 1979).

Calcite cement probably formed from carbonate fossils originally present within the Snadd Formation (Bjørkum and Walderhaug, 1990). Some carbonate fossil fragments are still present in the Snadd Formation in well 7222/11-1, and minor calcite cementation may therefore still be in progress. Calcite engulfs both chlorite (Figures 5.2.3a and b) and siderite cement, indicating that calcite cementation succeeded chlorite and siderite cementation. In well 7131/4-1 quartz overgrowths are not present within strongly calcite-cemented samples, which points to calcite cementation having taken place before quartz cementation. However, there are often very few quartz overgrowths anyway because of chlorite coatings on the quartz grains. In well 7222/11-1 quartz overgrowths are mainly not present. However, in a few cases thin quartz overgrowths covered by later precipitated calcite cement are present. Therefore it is suspected that calcite cementation was mostly but not totally completed before quartz cementation started in this well.

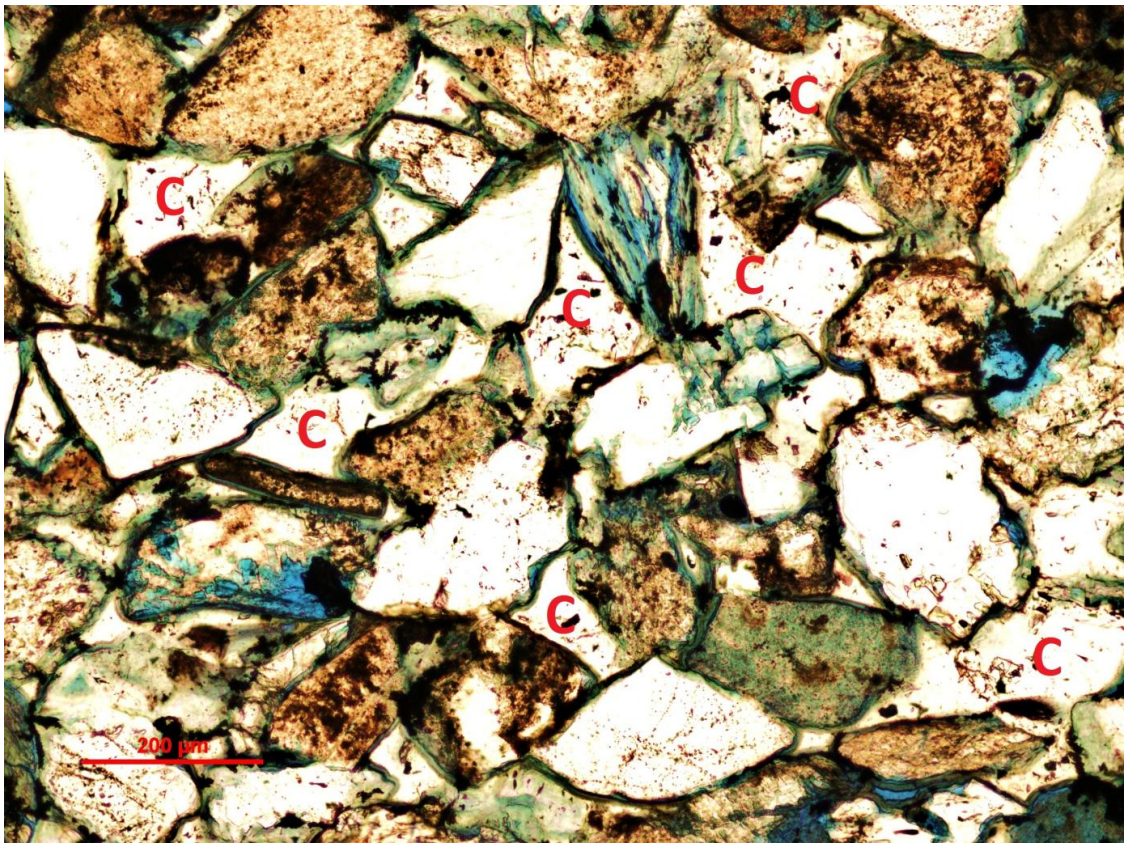

Figure 5.2.3a: Pore-filling calcite cement (C) engulfing chlorite coatings. Scale bar is 200µm. Snadd Formation, well 7131/4-1, 1112.15mRKB.

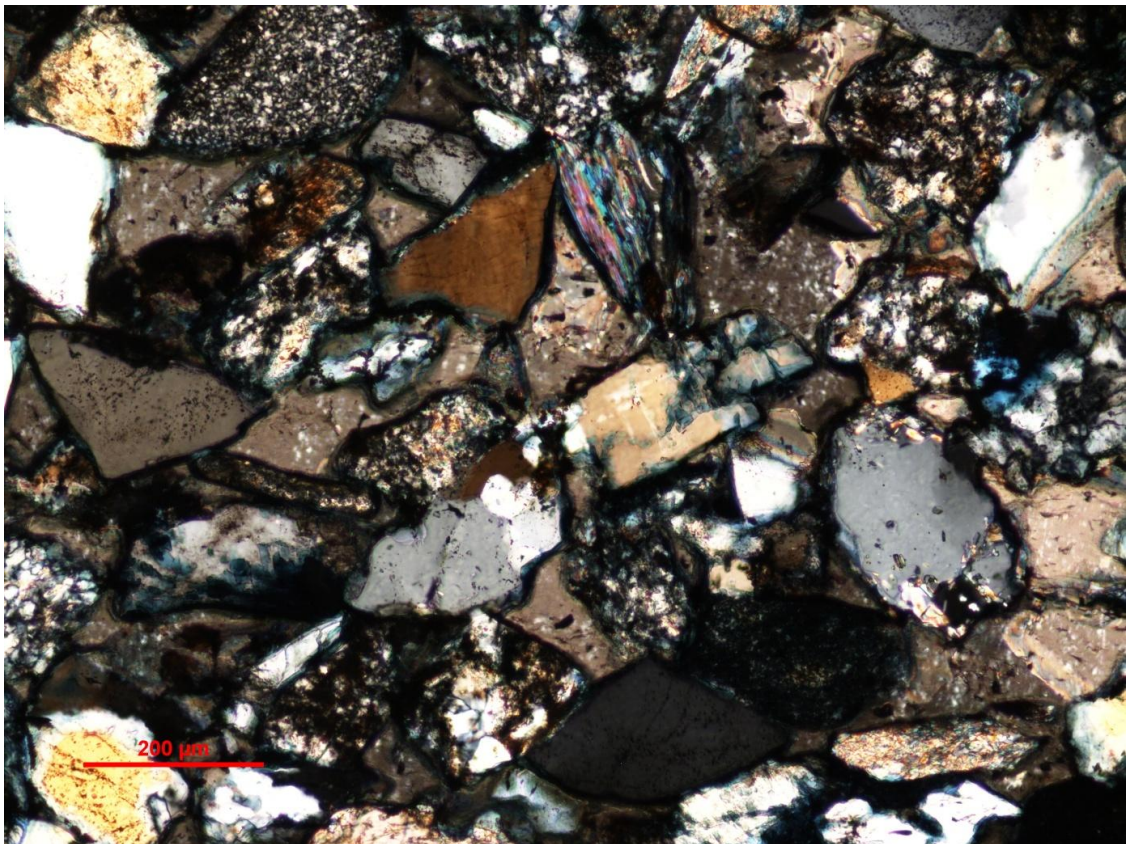

Figure 5.2.3b: Same field of view as shown in Figure 5.2.3a. Taken with crossed nichols. Scale bar is 200µm. Snadd Formation, well 7131/4-1, 1112.15mRKB.

The quartz cementation process is a late diagenetic process and was probably initiated when temperatures exceeded 70°C, as is normal for quartz cement on the Norwegian continental shelf and elsewhere (Bjørlykke et al., 1986; Ehrenberg, 1990; Giles et al., 1992; Walderhaug, 1994a). In the samples where almost all quartz grains are covered by chlorite, hardly any quartz overgrowths have formed, as quartz overgrowths only precipitate on clean quartz surfaces (Heald and Larese, 1974; Ehrenberg, 1993; Walderhaug, 1996). However, in samples from well 7222/11-1 where quartz cementation is not prevented by chlorite or other grain coatings, quartz cementation is seen to increase in abundance with depth. Quartz cementation probably continued while temperatures remained above 70°C, but will have stopped when uplift (see Section 5.4) caused temperature to fall. The main source for quartz cement is probably dissolution of quartz grains at the contacts between clay and quartz grains at stylolites or individual grain contacts (Bjørlykke et al., 1986; Ehrenberg, 1990; Walderhaug, 1994a; Bjørkum, 1996).

5.2.3 The Kobbe Formation

Trace volumes of pyrite present in the Kobbe Formation have a framboidal morphology suggesting that they probably formed very close to the sediment surface due to microbiological sulphate reduction (Berner, 1970; 1981). In addition, the pyrite framboids are engulfed within calcite cement which also indicates that pyrite cement is early diagenetic.

The small volumes of authigenic kaolin present may possibly point to meteoric water flushing, feldspar dissolution and precipitation of the dissolved minerals as kaolin (Bjørlykke et al., 1979). Alternatively, minor volumes of silica- and alumina-rich gels flocculated in the mixing zone between fluvial and marine water may have crystallized to kaolin during burial (Walderhaug, 2000). The non-continuous chlorite rims on some grains must predate quartz cementation because they have inhibited quartz overgrowth precipitation when they are present. Chlorite precursors may have been flocculated in the mixing zone between fresh and meteoric water in a similar manner to what may have been the case for kaolin precursors (Ehrenberg, 1993). The chlorite precursors may have formed well-crystallized chlorite during burial.

Siderite crystals often occur within quartz overgrowths and ferroan calcite cement. Siderite is therefore considered to be fairly early diagenetic.

The source of the ferroan calcite cement was probably biogenic carbonate that formed part of the Kobbe Formation at the time of deposition. Calcite is seen to often engulf pyrite and siderite cement, and is therefore considered to postdate these cements. In addition, quartz cement is not seen within pervasively calcite-cemented patches, indicating that calcite cement predates the quartz cementation process.

The quartz overgrowths probably formed when temperatures rose to above 70°C, as is normal for quartz cement on the Norwegian continental shelf (Bjørlykke et al., 1986; Ehrenberg, 1990; Giles et al., 1992; Walderhaug, 1994a). The quartz cementation process continues as long as temperature stays above this value (Bjørkum et al., 1998), but as temperature dropped due to uplift (see Section 5.4), the quartz cementation process is thought to have been strongly reduced. The probable source of quartz cement is dissolution of quartz grains at stylolites and at individual contacts between quartz grains and detrital clay or mica (Bjørlykke et al., 1986; Ehrenberg, 1990; Walderhaug, 1994a; Bjørkum, 1996, Figure 5.2.4).

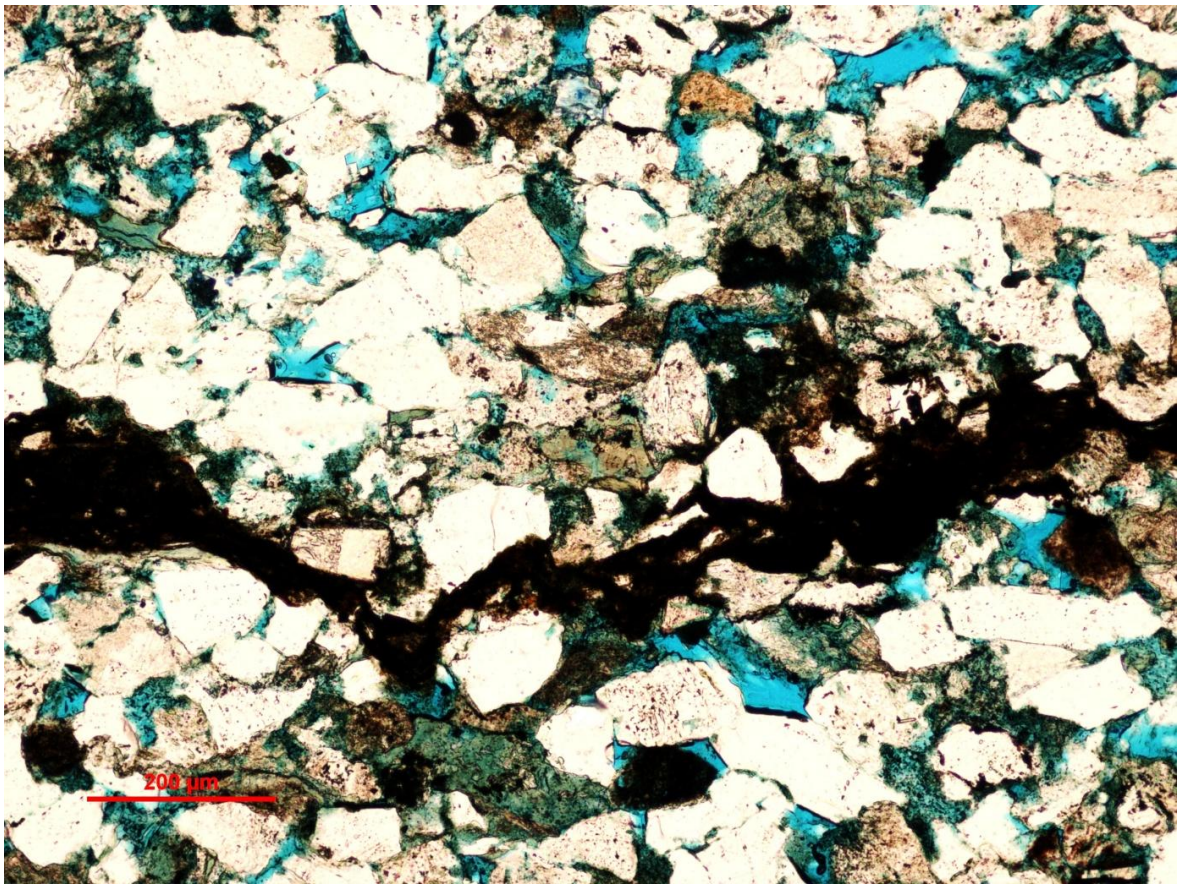

Figure 5.2.4: Stylolite evolved from clay-rich lamina. Scale bar is 200µm. Kobbe Formation, well 7222/11-1, 2237.00mRKB.

5.2.4 Diagenesis versus depositional environment

The type of depositional setting largely controls which early diagenetic reactions take place in a sandstone (Bloch and McGowan, 1994). For instance, development of phases that form due to evaporation of ground water (caliche, silcrete) is typical of arid continental environments (McBride, 1989; Morad, 1998) whereas formation of glauconite is typical of early marine diagenesis (McRae, 1972). The type of depositional facies may also have a large influence on later diagenetic reactions by controlling the presence of components such as carbonate fossils that dissolve during burial and form calcite cement (Bjørkum and Walderhaug, 1990).

In the present case, the common to abundant diagenetic chlorite in the Snadd Formation, and to a lesser degree in the Kobbe Formation, is probably a consequence of deposition in a largely marginal marine to estuarine environment where iron-rich chlorite precursors where flocculated when the fluvial waters mixed with marine waters (Ehrenberg, 1993).

The lower part of the cored Fruholmen Formation section in well 7131/4-1 may also have been deposited in tidal channels in an estuarine setting although it does not contain diagenetic chlorite. This may be due to the source area of the Fruholmen Formation not having supplied chlorite precursors, possibly due to a shift of source area and/or to a climate change (Bergan and Knarud, 1992; Mørk, 1999). The upper part of the Fruholmen Formation is probably too fluvial to contain chlorite coats.

Because chlorite coats prevent development of quartz overgrowths, the distribution of facies-controlled chlorite rim precipitation will also strongly influence the extent of late diagenetic quartz cementation. More quartz cement in the Fruholmen Formation than in the underlying Snadd Formation in well 7131/4-1 is an example of such an effect. Similarly, less complete chlorite coatings in the Kobbe Formation compared to in the Snadd Formation in well 7222/11-1 may partly explain why there is slightly more quartz cement in the Kobbe Formation than in the Snadd Formation in this well, although deeper burial of the Kobbe Formation is probably at least as important (see Section 5.4).

Siderite cement is not present in the Fruholmen Formation whereas it is present in volumes of up to 6% in the Snadd Formation in both wells and in trace amounts in the Kobbe Formation. In other words presence of diagenetic chlorite and siderite seems to be positively correlated. This could be due to both chlorite and siderite containing iron from colloids flocculated in the

fluvial-marine mixing zone. The abundance of siderite is therefore also probably related to depositional environment.

Calcite cement was found in the thin-sections from the Snadd Formation in both wells and in the Kobbe Formation. Calcite-cemented intervals are also shown on the core descriptions from the same intervals. Neither logs nor thin-sections show any calcite cement in the Fruholmen Formation. This distribution of calcite cement may be due to conditions having been more favourable for organisms with carbonate shells in the depositional environments characteristic of the Snadd and Kobbe formations compared to the depositional setting of the cored Fruholmen Formation interval. This is supported by a few bivalves still being present in thin-sections from the Kobbe Formation and on the core descriptions from the Snadd and Kobbe formations in well 7222/11-1.

Occurrence of a few pyrite framboids in parts of all three formations is probably due to deposition in marine to brackish settings where sulphate was available for sulphate-reducing bacteria (Berner, 1970; 1981).

Authigenic kaolin occurs in all three formations in similar amounts, and it is difficult to see any clear correlations with depositional facies.

Although albitic overgrowths on plagioclase occur only in the Kobbe Formation, this may be due to the high content of plagioclase in this formation rather than to the depositional environment.

5.3 Reservoir quality

5.3.1 The Fruholmen Formation

The high porosities and permeabilites of the Fruholmen Formation sandstones (Figure 5.3.1) are due to the dominance of chemically stable and strong quartz grains and the very low content of detrital clay. Even though some samples show presence of quartz cement, the quartz cement volumes are low and do not reduce porosity substantially. The low volumes of quartz cement are probably due to the sandstones not having spent a long time at high temperatures.

Poorer porosities and permeabilities in the interval 925-935mRKB are partly caused by the presence of siltstones with considerable detrital clay that enhances compaction, and tight grain packing. In clean siltstones quartz cementation is more extensive than in the sandstones due to the large quartz surface areas caused by the small grain size (Walderhaug, 1996; Bjørkum et al., 1998). Permeabilities are very much lower in the siltstones due to lower porosities and finer grain size as permeability is proportional to grain size squared (Kozeny, 1927).

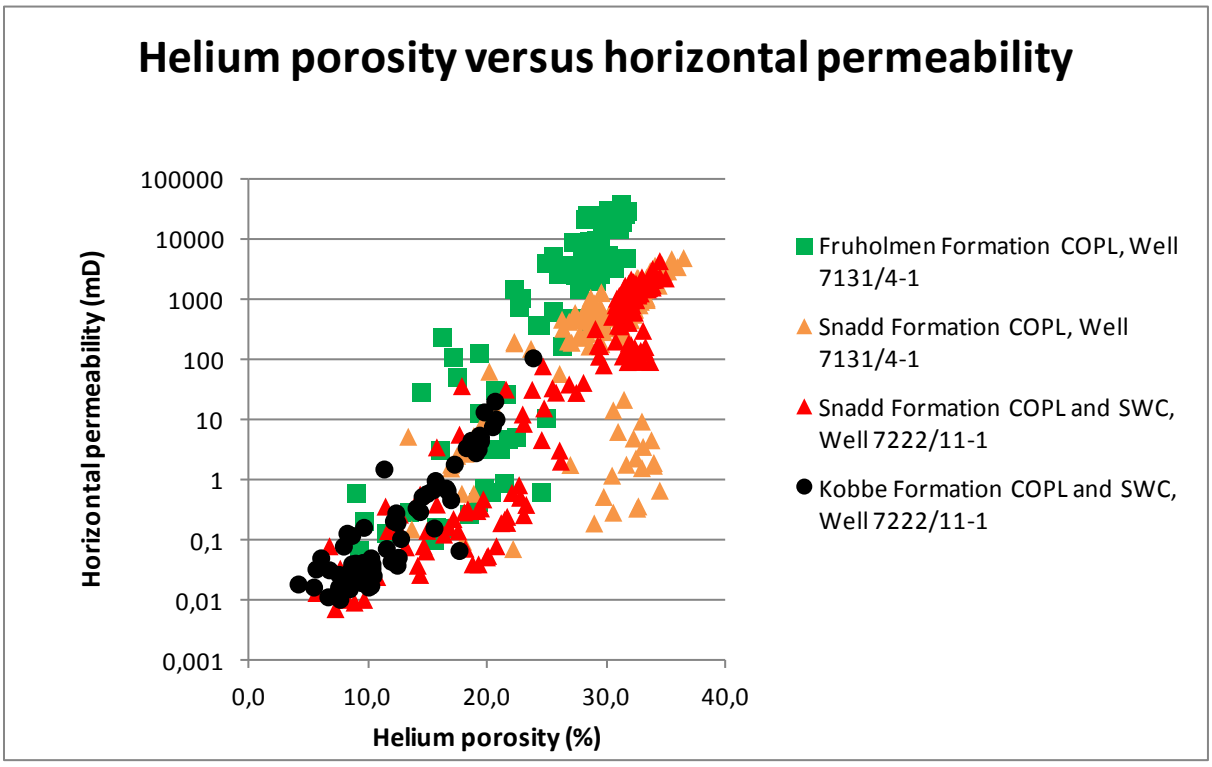

Figure 5.3.1: Helium porosity versus horizontal permeability for core plugs and side wall cores in all three formations. The Kobbe Formation shows the poorest reservoir quality with porosity and permeability values that do not exceed 25% and 100mD, respectively, whereas the Fruholmen Formation shows a cluster with very high permeability values, up to 38 000mD, and porosity values dominantly above 20%. The Snadd Formation shows varying reservoir quality, but the majority of the porosity values are above 30% and permeability values are largely 100-5 000mD. COPL: Core plug, SWC: Side wall core.

5.3.2 The Snadd Formation

The mostly good to very good porosities and permeabilities in the Snadd Formation sandstones (Figures 5.3.1) are due to the chemical stability of most sand grains, the very low detrital clay matrix contents, and the low volumes of diagenetic minerals. Low volumes of quartz overgrowths are mainly due to the presence of diagenetic chlorite coatings, and the abundance of non-quartz grains that do not develop quartz overgrowths.

The low permeabilities in the uppermost ten metres of the Snadd cores in well 7131/4-1, where helium porosities are very high (>30%), is a consequence of the very abundant pore-filling early-diagenetic chlorite being extremely microporous. In these samples the chlorite is so thick that it blocks pore throats and fills pores and thereby ruins permeability (Figure 5.3.2). However, deeper in the cores, reservoir quality improves, mostly due to the fact that the chlorite in the form of thin coatings covers almost all grains and therefore prevents quartz cementation (Figure 5.3.3). In the few samples from the Snadd Formation core (1102.00, 1112.15 and 1113.00mRKB) that contain large volumes of pore-filling calcite cement, this cement has seriously damaged reservoir quality by filling most pores, blocking pore throats and ruining the permeability. Compared to many samples in the Fruholmen Formation, permeabilites are quite low in the Snadd Formation. This is due to the fact that the best Fruholmen samples contain almost no ductile grains or detrital or diagenetic clay. The best Snadd Formation samples are also very low in detrital clay, but they contain some softer grains, in addition to the chlorite coatings. Therefore, grain packing is tighter and pore throats are smaller than in the quartz arenites of the Fruholmen Formation.

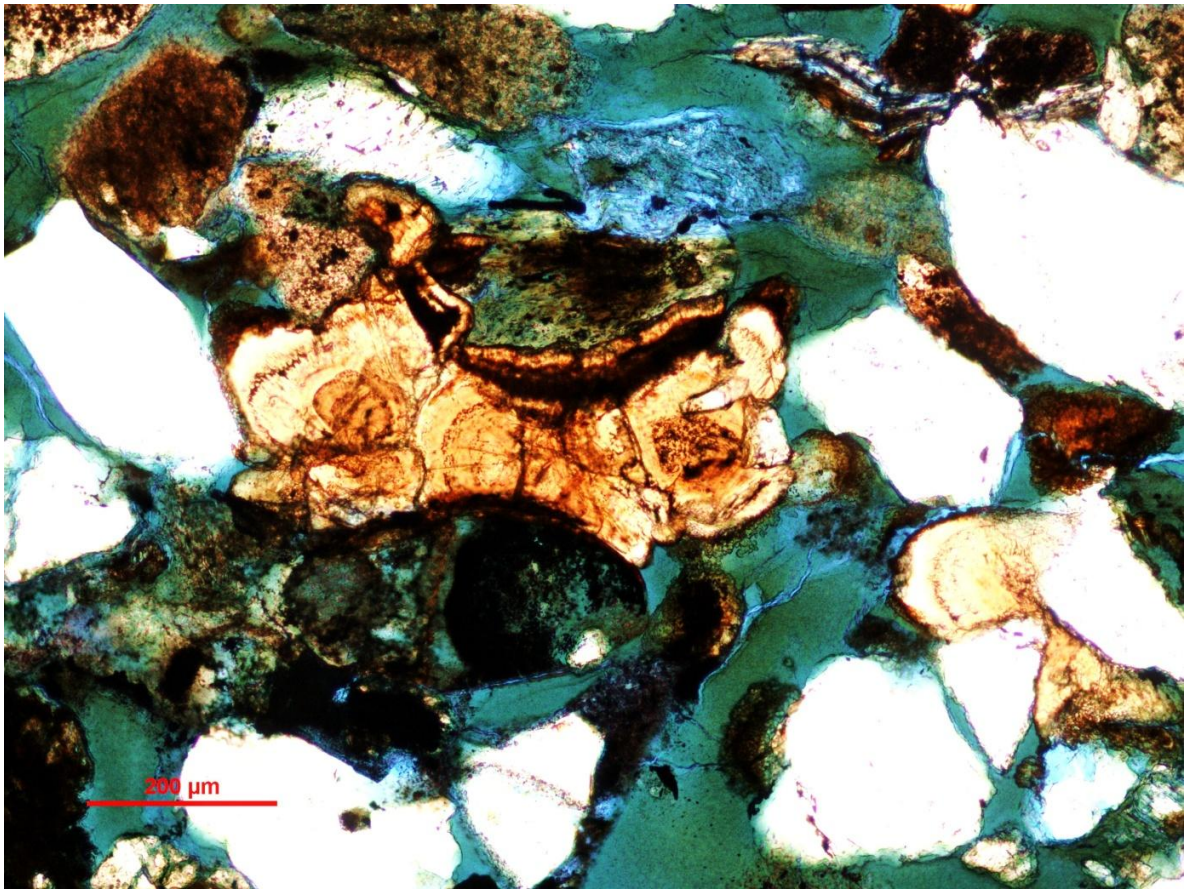

Figure 5.3.2: Thick dark green diagenetic chlorite filling pores and blocking pore throats. Reddish brown siderite cement is seen. Scale bar is 200µm. Snadd Formation, well 7131/4-1, 1077.00mRKB.

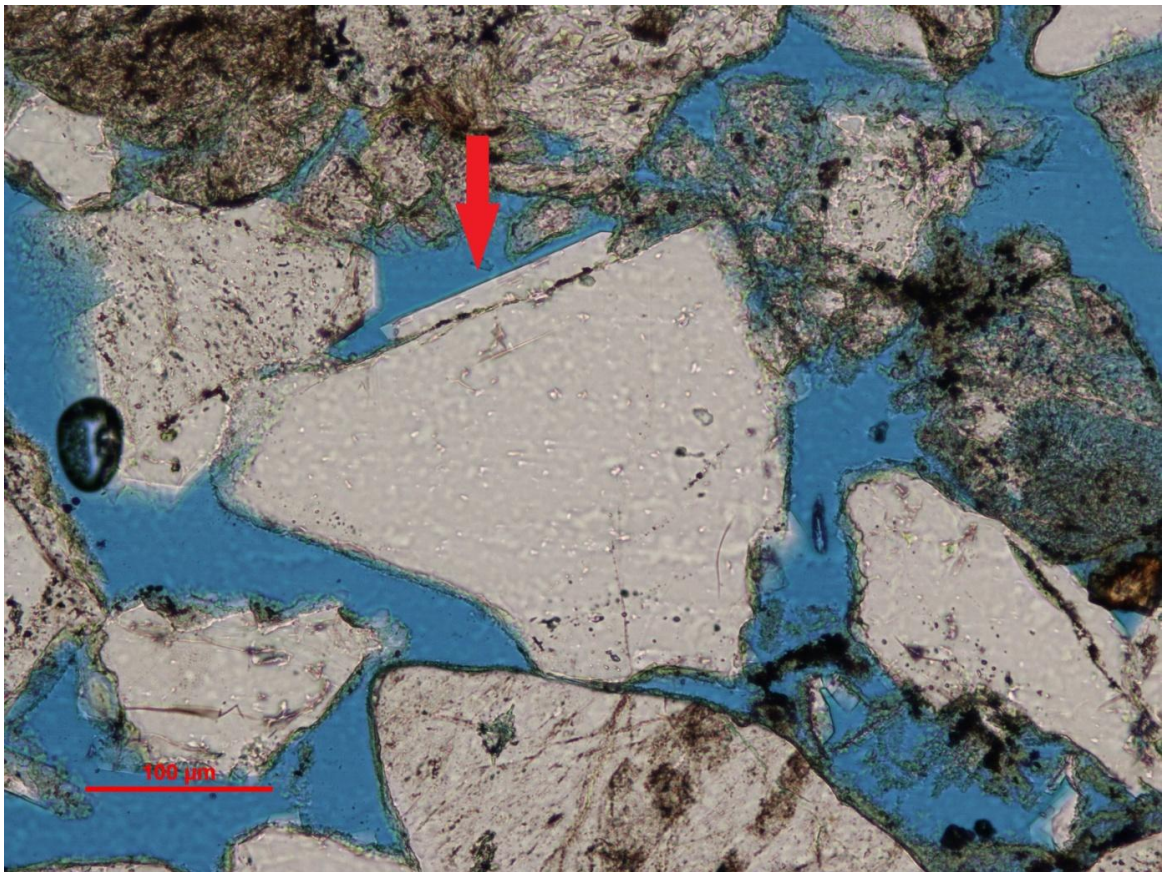

Figure 5.3.3: Thin rims of diagenetic chlorite cover almost all grains. Development of quartz overgrowths has started where chlorite coats are incomplete (indicated with red arrow). Scale bar is 100µm. Snadd Formation, well 7131/4-1, 1084.00mRKB.

Looking at well 7222/11-1, at present the Snadd Formation samples are situated at burial depths of only 0.25-1.4km, and even with 1-1.5km of uplift (see Section 5.4) maximum burial depth would be moderate (1.75-2.9km). Volumes of quartz cement are therefore low to moderate, but calcite cement is abundant in a few samples. The calcite cement is thought to have formed from carbonate fossils deposited as part of the sands, implying that calcite cement will be concentrated where biogenic carbonate was present.

Diagenetic chlorite coats have also contributed to reducing the volumes of precipitated quartz cement in well 7222/11-1, especially between 778mRKB and 1291mRKB where diagenetic chlorite covers almost all grains in most of the samples. Moreover, a considerable fraction of the grains are not quartz grains but feldspars and rock fragments. Quartz overgrowths do not precipitate on feldspar (Heald and Renton, 1966; Bjørlykke et al., 1986; Walderhaug, 1996), and only rarely on the rock fragments, including chert. The considerable volumes of feldspar and rock fragments will therefore also reduce quartz cementation.

The five deepest thin-sections from the Snadd Formation in well 7222/11-1 were taken from side wall cores. These side wall core samples (1495.40mRKB to 1800.60mRKB) lack chlorite coatings. More quartz cement is therefore present in these samples than in the shallower Snadd samples, and helium porositites are lower (6.8-23.8% in the side wall cores versus 31.4-33.9 in the core plugs).

Fine grain sizes enhance quartz cementation because quartz surface area available for precipitation of quartz overgrowths in a fixed volume of sandstone is inversely proportional to grain size (Walderhaug, 1996). As already mentioned, fine grain size also affects permeability negatively because permeability increases with the square of the grain size for a given porosity and rock texture (Kozeny, 1927). The two side wall cores of very fine detrital clay-poor sandstone and coarse siltstone from 641.70 and 680.70mRKB in well 7222/11-1 have permeabilites of only 213 and 93.2mD even though helium porosities are 34.3 and 32.2%. High contents of detrital clay in the intervals 800-807mRKB and 1292-1299.5mRKB in the Snadd Formation core from well 7222/11-1 have led to low permeability values in these samples. The high contents of detrital clay are due to the lower energy depositional environments for these intervals.

5.3.3 The Kobbe Formation

Reservoir quality in the Kobbe Formation is determined both by composition and texture at the time of deposition, and by diagenetic processes. The sandstones from the Kobbe Formation are very fine- and fine-grained with moderate to high clay contents. The considerable content of clay and mica-rich rock fragments has made the sandstones prone to mechanical compaction, and in addition micro-stylolitic grain contacts occur where clay is present between grains. Intergranular volumes and porosities are therefore quite low, even though the volumes of diagenetic minerals are not high. The Kobbe Formation contains a lot of rock fragments and plagioclase, which has slowed down the quartz cementation process since quartz cement does not precipitate on plagioclase and the parts of rock fragments that do not consist of quartz (Heald and Renton, 1966; Bjørlykke et al., 1986; Walderhaug, 1996). In addition, many of the monocrystalline quartz grains are coated by diagenetic clays which also prevents precipitation of quartz overgrowths.

Even though clay coats may be helpful in preventing quartz cementation and preserving pores, the quite thick clay coats in the Kobbe Formation tend to block pore throats and reduce

permeability. The severe compaction will also have closed and reduced many pore throats. The fine grain size is also a factor when considering permeability, as permeability is proportional to grain size squared (Kozeny, 1927). The combined effect of these three factors can probably explain permeabilites of only 2-20mD when porosity values are over 19% (Figure 5.3.1).

Finally, in subsequent sections it will be argued that the sandstones in the Kobbe Formation have been subjected to major uplift (Section 5.4), and were previously buried 1-1.5km deeper than at present. Quartz cementation and mechanical and chemical compaction are therefore more extensive than what is expected at present burial depth elsewhere on the Norwegian continental shelf (Ehrenberg, 1990; Walderhaug et al., 2000).

5.3.4 Reservoir quality versus depositional facies

Depositional environment largely controls factors such as grain size, sorting, clay matrix content, carbonate fossil content and presence of grain coatings, and therefore often has a major effect on sandstone reservoir quality (Bloch and McGowan, 1994).

The effects of depositional environment on reservoir quality are clearly present in the sandstones studied in this thesis. Firstly, it is apparent from the point-counting, the petrographic examination of the thin-sections and the plug measurements that samples with high contents of clay matrix and clay clasts tend to have much lower porosities and especially permeabilities than samples with little or no detrital clay. The clay lowers porosity by filling pores between the sand grains and also promotes compaction and causes the remaining porosity to largely consist of micropores that contribute far less to permeability than well-connected macropores. High detrital clay content is in turn related to low energy settings with little reworking and winnowing of clay, such as the lagoon or bay facies in the Fruholmen Formation (Figures 5.3.4a and b), the paleosols and swamps in the Snadd Formation in well 7131/4-1 (Figures 5.3.5a and b), the bay and offshore transition zone deposits in the Snadd Formation in well 7222/11-1 (Figures 5.3.6a and b and 5.3.7a and b), and the muddy shelf, distal mouth bar and muddy sandflat deposits in the Kobbe Formation (Figures 5.3.8a and b).

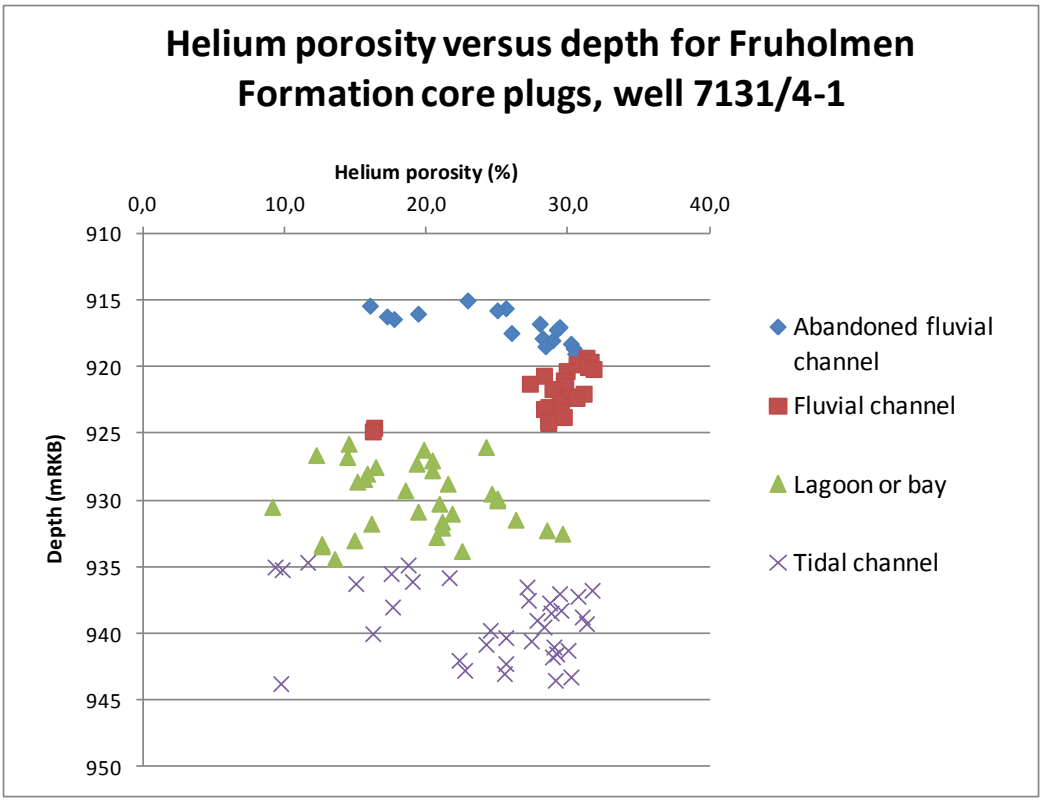

Figure 5.3.4a: Helium porosity versus depth for Fruholmen Formation core plugs, well 7131/4-1. The best porosities are found in the fluvial channel and parts of the tidal channel facies. Porosities are lowest in the lagoon or bay deposits, in parts of the abandoned fluvial channel, and in parts of the tidal channel.

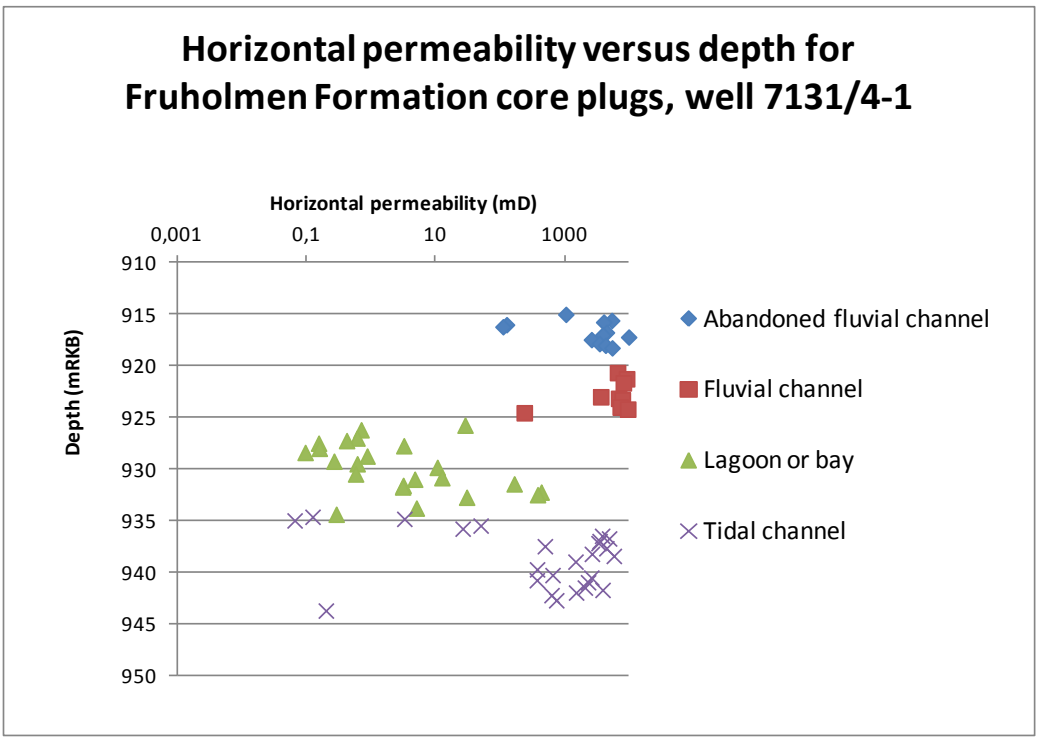

Figure 5.3.4b: Horizontal permeability versus depth for Fruholmen Formation core plugs, well 7131/4-1. The best permeabilities are found in the fluvial channel and parts of the tidal channel. Lagoon or bay deposits and the uppermost part of the tidal channel have the lowest permeabilities.

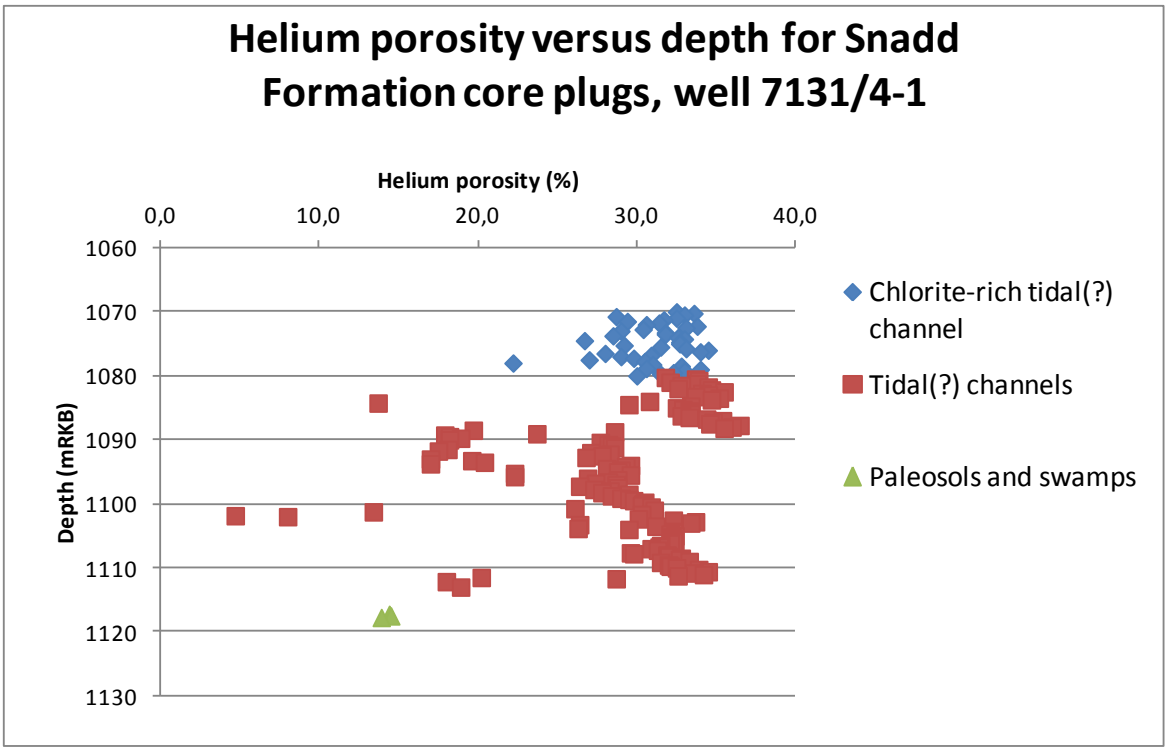

Figure 5.3.5a: Helium porosity versus depth for Snadd Formation core plugs, well 7131/4-1. Porosities are high to very high in most parts of the channel sandstones. The paleosols and swamp deposits have very low porosities. The channel facies samples with the lowest porosities are in some cases pervasively calcite-cemented, and in other cases contain large volumes of muddy intraclasts.

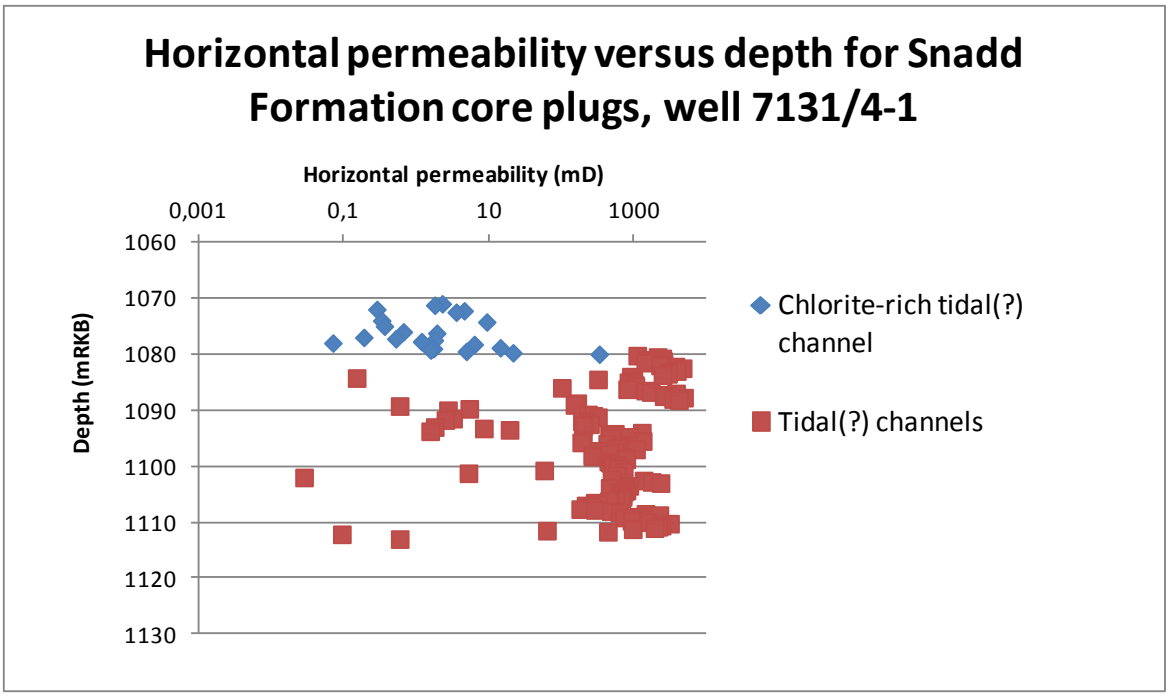

Figure 5.3.5b: Horizontal permeability versus depth for Snadd Formation core plugs, well 7131/4-1. The low permeabilities in the very porous upper tidal(?) channel (1070-1080mRKB) are caused by almost all pores being filled by very microporous diagenetic chlorite. Chlorite rims are thin in the deeper channel sandstones and permeability is therefore much higher. A few calcite-cemented samples and samples containing abundant muddy intraclasts have low permeabilities. Permeability measurements are not available for the paleosol and swamp deposits.

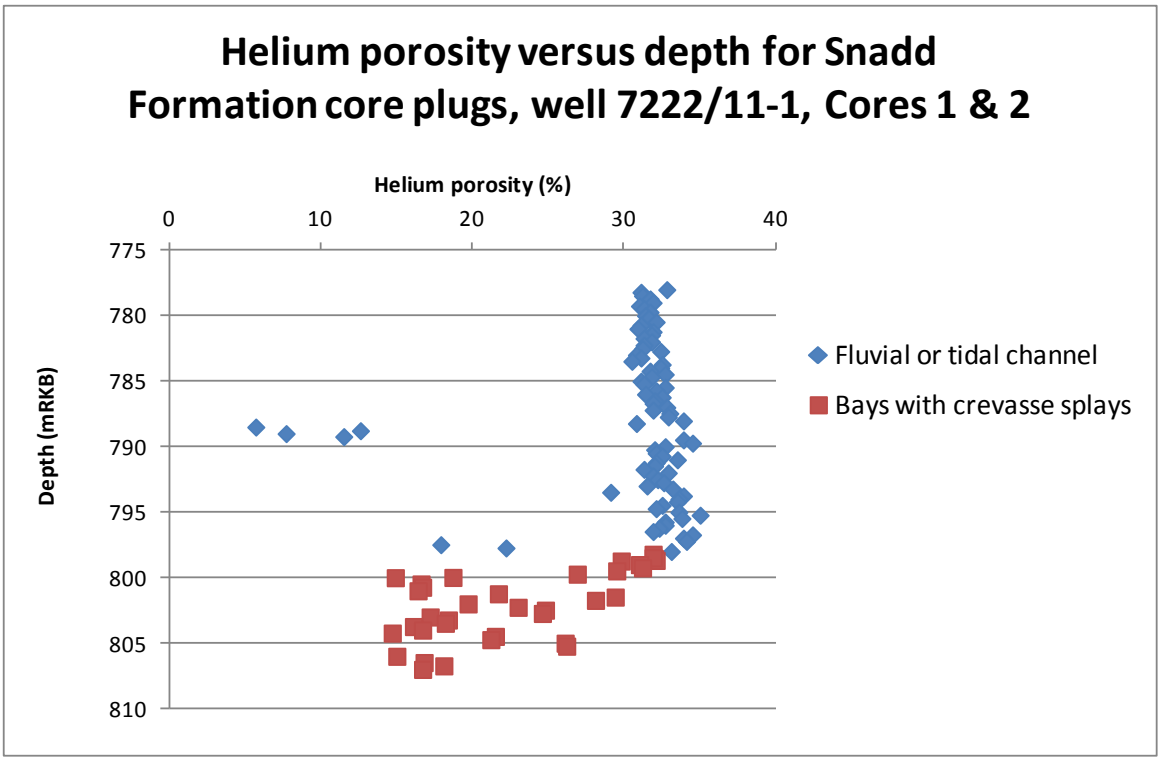

Figure 5.3.6a: Helium porosity versus depth for Snadd Formation core plugs from Cores 1 and 2 in well 7222/11-1. Porosities are dominantly 30-33% in the channel facies, but largely much lower in the bay and crevasse splay deposits. The four low porosity values in the channel sandstones around 789mRKB are due to abundant calcite cement in these samples. The two porosity values of approximately 18 and 22% in the base of the channel sandstones occur within the channel lag.

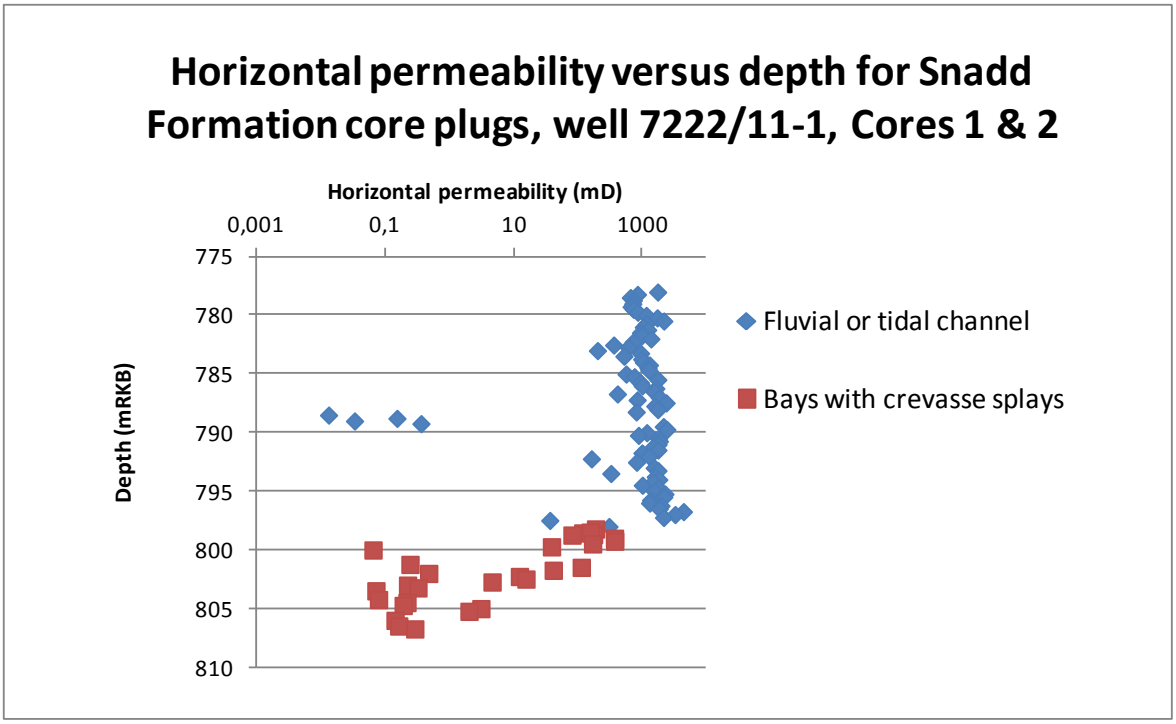

Figure 5.3.6b: Horizontal permeability versus depth for Snadd Formation core plugs from Cores 1 and 2 in well 7222/11-1. Permeability values show a very good positive correlation with the porosity values shown in the previous figure. Permeabilities are highest in the channel sandstones except for in the calcite-cemented interval around 789mRKB. Values are much lower and more variable in the bay and crevasse splay facies.

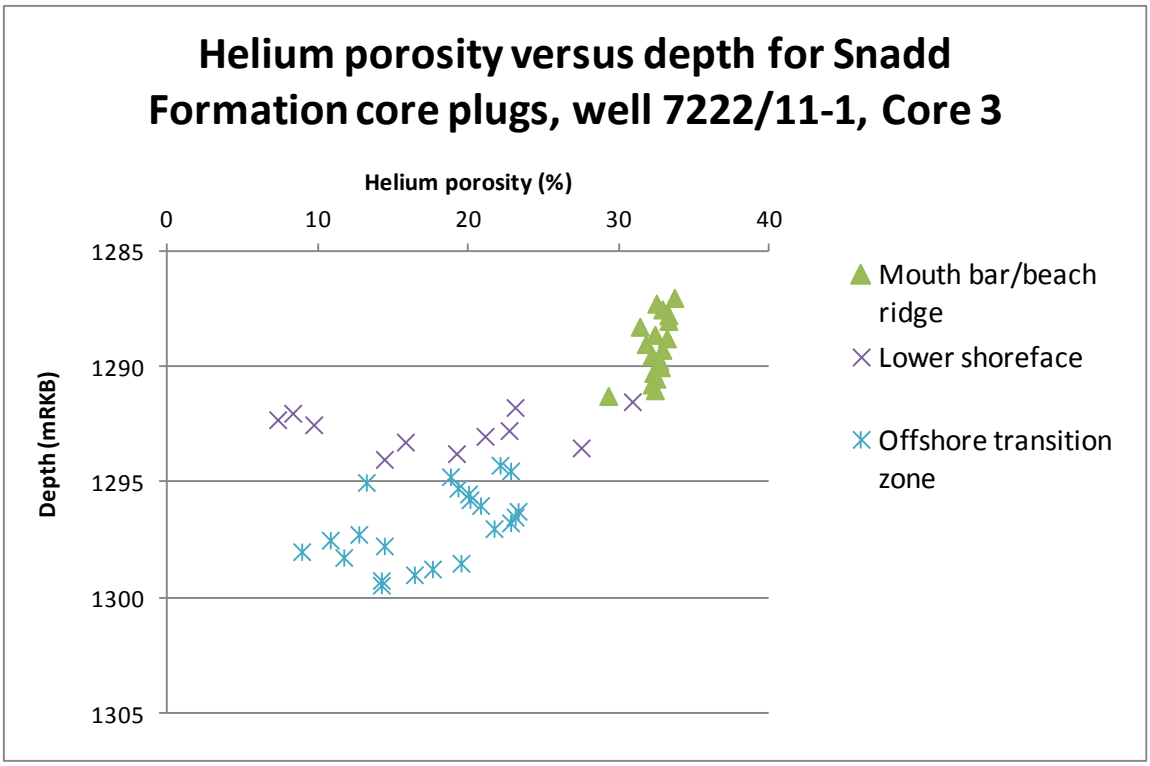

Figure 5.3.7a: Helium porosity versus depth for Snadd Formation core plugs from Core 3 in well 7222/11-1. Porosities in the mouth bar/beach ridge facies are markedly higher than in the muddier lower shoreface and the offshore transition zone deposits.

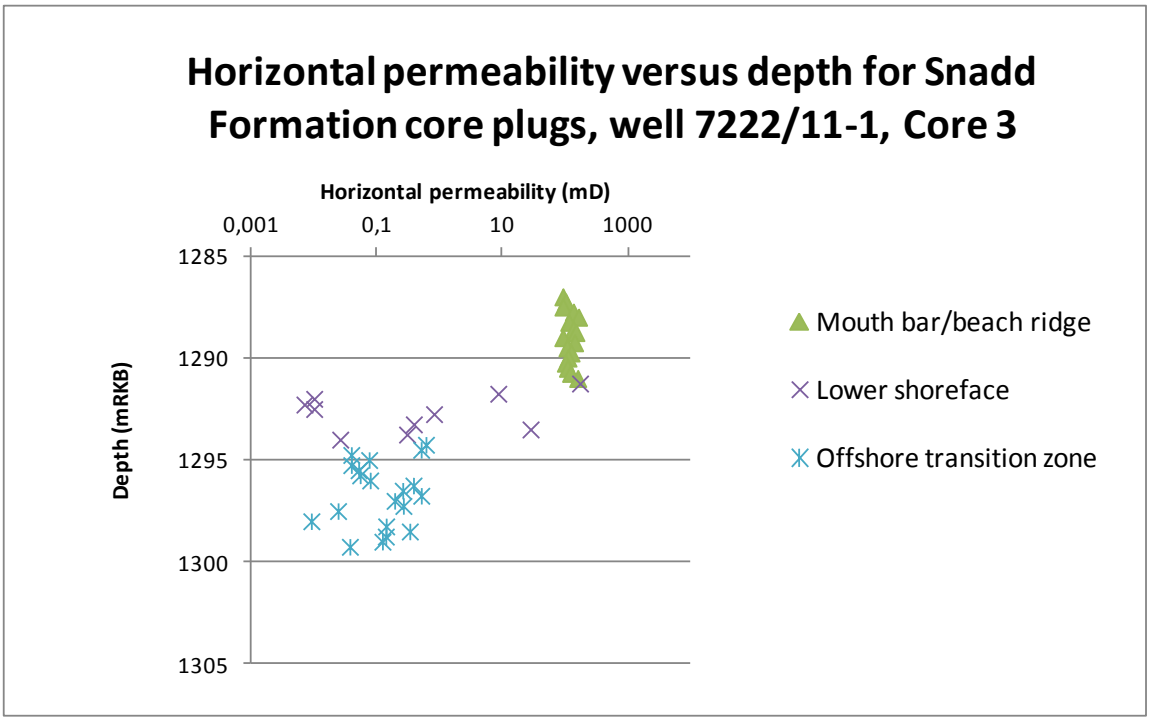

Figure 5.3.7b: Horizontal permeability versus depth for Snadd Formation core plugs from Core 3 in well 7222/11-1. Permeability values vary in the same manner as the porosity values (Figure 5.3.7a). The mouth bar/beach ridge has the best and most consistent permeabilities, approximately 90-160mD, whereas the lower shoreface and offshore transition zone deposits have permeabilities dominantly in the range 0.007-0.8mD.

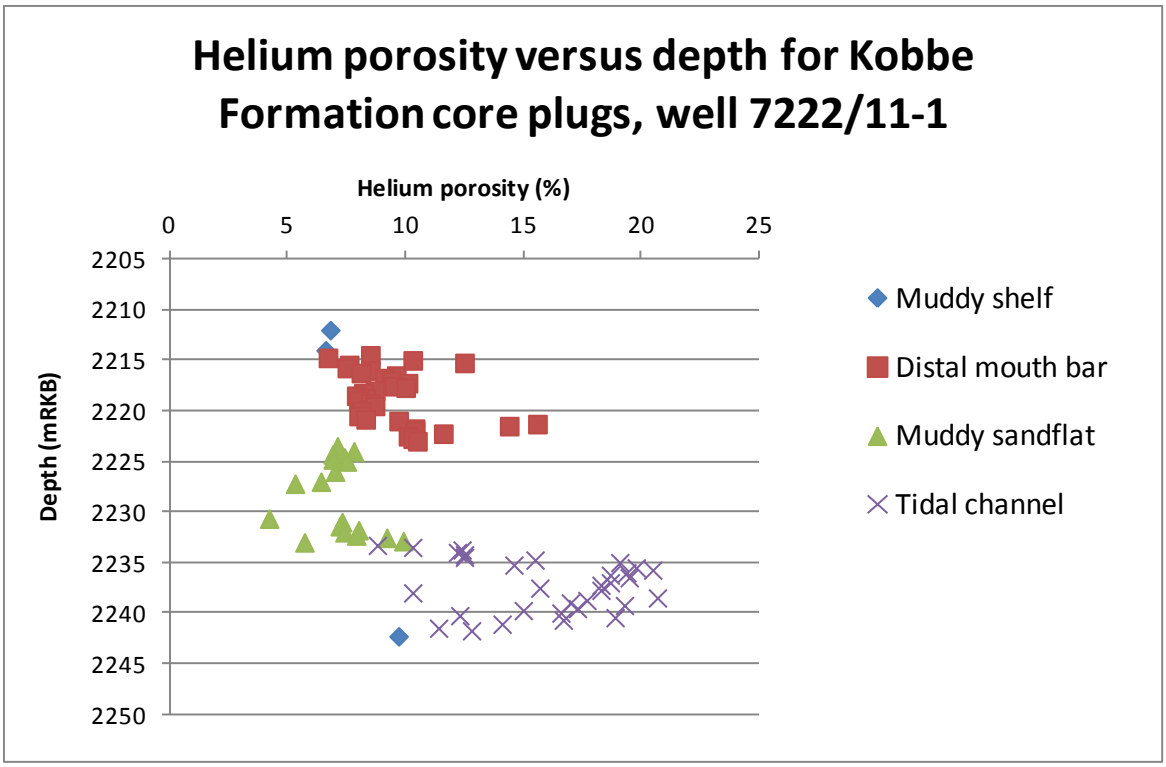

Figure 5.3.8a: Helium porosity versus depth for Kobbe Formation core plugs, well 7222/11-1. The largely muddy and very fine-grained facies (muddy shelf, distal mouth bar and muddy sandflat) dominantly have very low to low porosities (4-13%), whereas most of the tidal channel samples are less muddy and slightly coarser grained and have porosities of 15-20%.

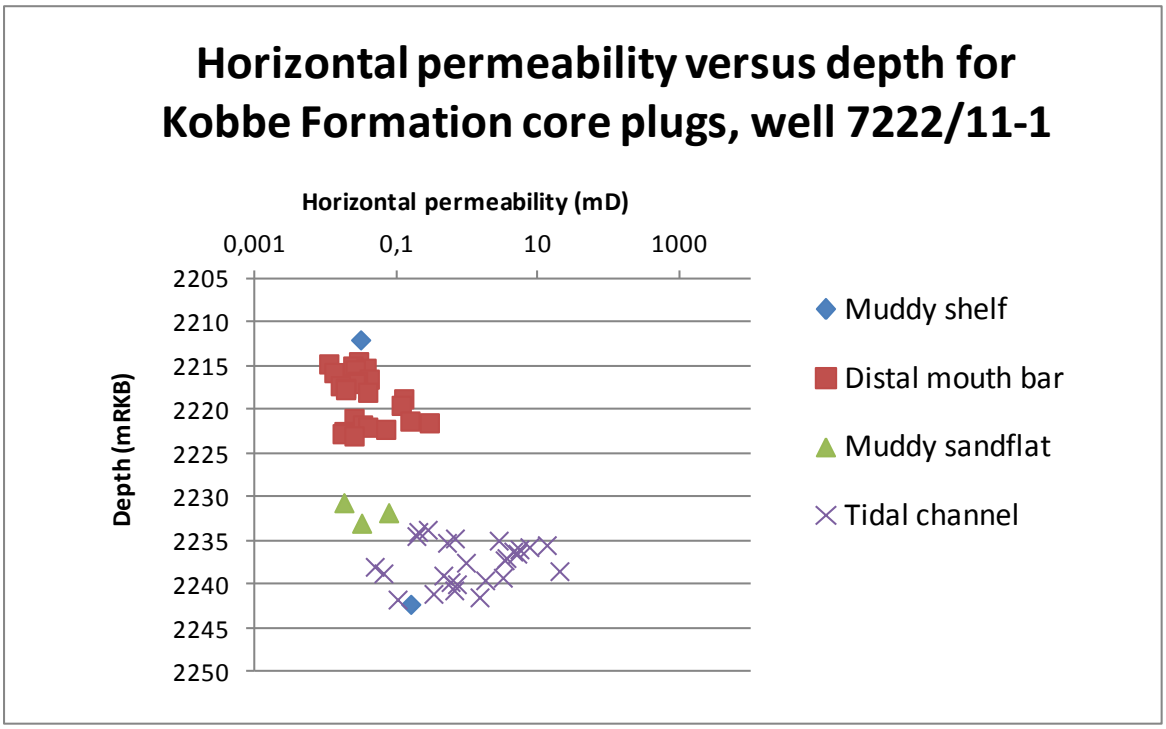

Figure 5.3.8b: Horizontal permeability versus depth for Kobbe Formation core plugs, well 7222/11-1. The muddy shelf, distal mouth bar and muddy sandflat all have very low permeabilites, 0.01-0.3mD, whereas most of the coarser grained and less muddy tidal channel sandstones have somewhat higher permeabilites, 1-20mD.

In the Fruholmen Formation samples from high energy active fluvial and possibly tidal channels are on the other hand practically clay-free with excellent porosities and permeabilites, largely 1000-38 000mD and above 25% porosity (Figures 5.3.4a and b).

In the Snadd Formation channel sandstones in well 7131/4-1 there are some sandstones with abundant clay-rich intraformational clasts that have porositites below 20% and permeabilities that rarely exceed 10mD, but the greatest negative effect of depositional environment on reservoir quality in the Snadd Formation channel sandstones in well 7131/4-1 is through the precipitation of very large amounts of diagenetic chlorite in the interval 1070-1080mRKB. Almost all pores are filled with microporous chlorite in this interval, and despite helium porosities of 29-35%, permeabilities are only 0.1-20mD. These samples form the distinct group of high porosity but low permeability Snadd Formation samples in the lower right hand corner of the porosity versus permeability plot (Figure 5.3.1). Exactly how the depositional environment controlled the formation of the exceptional volumes of chlorite is uncertain, but the occurrence within one specific channel sandstone strongly suggests that this is an effect of depositional setting. In the rest of the Snadd Formation channel sandstones in both wells, chlorite coats are thin and the effect of chlorite is largely positive by preventing quartz cementation. As discussed by Ehrenberg (1993) occurrence of this type of chlorite coating is clearly related to depositional settings where fluvial waters mix with marine waters and chlorite precursors are flocculated and deposited. Detrital clay matrix contents in these channel sandstones of the Snadd Formation are low, porosities are high (25-35%), the pore system mostly consists of well connected macropores, and permeabilites are therefore high (100-5 000mD).

Grain size is clearly also related to depositional environment in the studied sandstones, and because permeability is strongly dependent on grain size (Kozeny, 1927), and because quartz surface area and therefore volumes of quartz cement are also affected by grain size, the sedimentological control of grain size may have a large impact on reservoir quality.

The coarsest grained sandstones in the examined intervals from the three formations are the channel sandstones of the Fruholmen Formation (0.3-0.7mm). These are also the most permeable of the studied sandstones with most values in the 1000-38 000mD range (Figure 5.3.4b). Despite the even higher porosities in parts of the Snadd Formation, permeabilities are lower than in equally porous and less porous Fruholmen Formation sandstones, 100-5 000mD

in the most permeable Snadd Formation samples versus 1000-38 000mD in the Fruholmen Formation (Figures 5.3.4b and 5.3.5b). Grain sizes in the Snadd Formation do not exceed 0.33mm versus 0.3-0.7mm in the most permeable parts of the Fruholmen Formation. The high permeabilites in the Fruholmen Formation are, however, also due to less dertital and authigenic clay in the high energy channel sandstones of the Fruholmen Formation.

The Kobbe Formation has the poorest reservoir quality of the three studied formations, and porosity and permeability hardly ever rise above 20% and 10mD (Figures 5.3.8a and b). Grain size is part of the explanation, the coarsest Kobbe Formation samples have grain sizes of only 0.14-0.15mm, and contents of clay matrix plus clay clasts plus mica-dominated rock fragments are 10-18% even in the point-counted samples which are the samples with the least clay and mica. In summary, the dominance of low energy more or less muddy and fine-grained mudflat to sandflat and distal mouth bar deposits in the Kobbe Formation cores leads to fine grain sizes, high clay contents and therefore poor reservoir quality. However, it should also be noted that the Kobbe Formation has been more deeply buried than the other studied intervals (see Section 5.4). One effect of the deep burial of these clay- and mica-rich sandstones is low intergranular volumes, only 17-21% in the point-counted samples.

Lastly, the marine to estuarine depositional settings for the Snadd and Kobbe formations have led to the presence of carbonate fossils that dissolved and precipitated as calcite cement during burial. The occurrence of a few strongly calcite-cemented tight samples is therefore due to the depositional environment locally being favourable for the accumulation of biogenic carbonate. The low porosities and permeabilities encountered at approximately 789mRKB in the thick channel sandstone in the Snadd Formation in well 7222/11-1 (Figures 5.3.6a and b) are due to calcite cementation.

5.3 5 Reservoir quality versus depth

Reservoir quality is generally considered to decrease with depth (Byrnes, 1994). Whether or not this is the case for the studied formations has been investigated by plotting porosity and permeability against depth for each well. Because the studied sandstones probably have been uplifted, and the uplift probably is different in the two wells (see Section 5.4), data from each well has been plotted separately (Figures 5.3.9a and b and 5.3.10a and b).

In well 7131/4-1 the Fruholmen Formation samples are approximately 200m shallower than the Snadd Formation samples. However, the helium porosity of the Snadd Formation samples actually tends to be higher than for the Fruholmen Formation samples (Figure 5.3.9a). This lack of porosity reduction with depth is thought to be a result of the two formations containing different types of sandstones. The Fruholmen Formation quartz arenites contain almost only compact quartz grains without intragranular micropores, and intragranular dissolution porosity is almost zero. This is in turn related to the very low feldspar content. The sublitharenites and the lithic arenites of the Snadd Formation, on the other hand, contains more feldspar and the feldspar is typically partly dissolved. Point-counted dissolution porosity is 0.3-4.7% (Table 4.1.1). In addition, microporous clay clasts and rock fragments are common. It is therefore suggested that the reason for the highest helium porosities occurring in the Snadd Formation rather than in the more shallow Fruholmen Formation in well 7131/4-1 is the presence of partly dissolved feldspar grains and more intragranular microporosity in this formation.

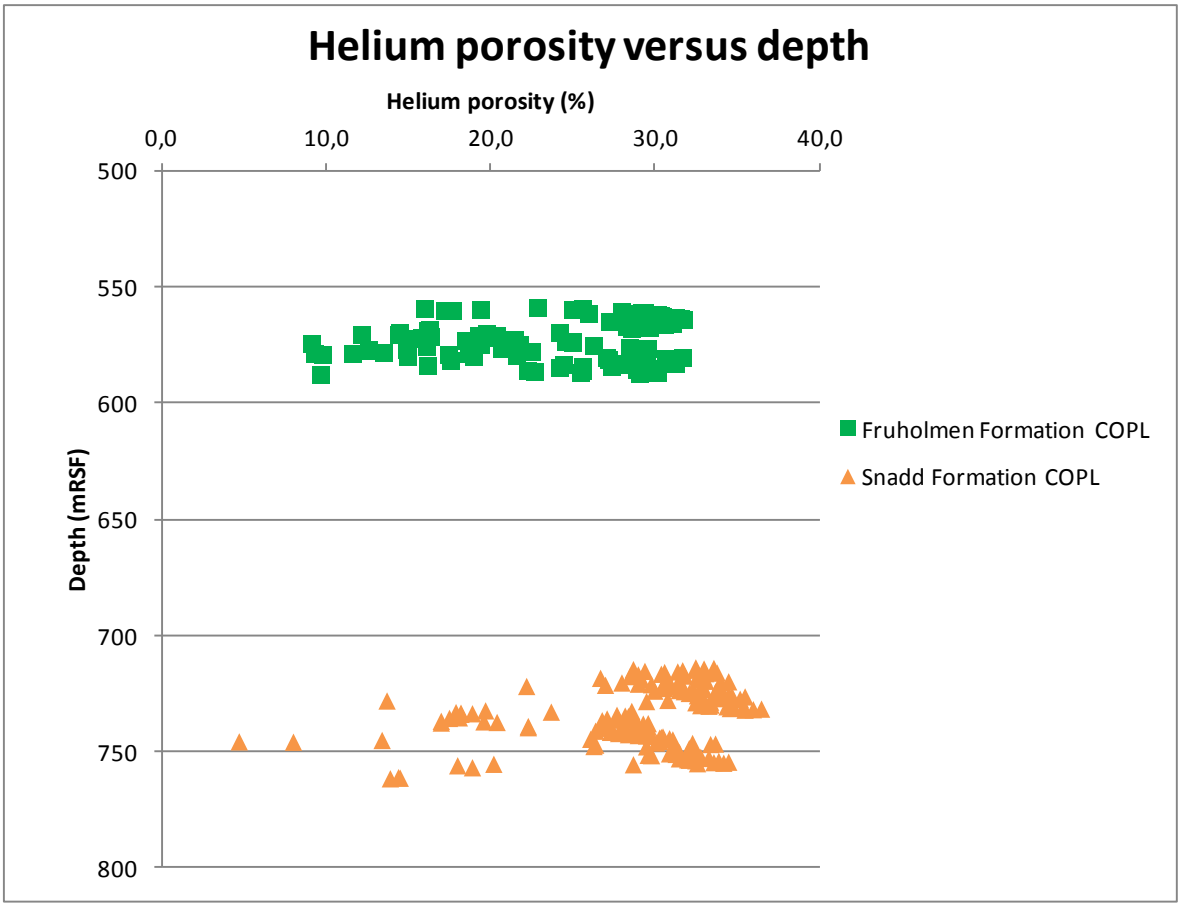

Figure 5.3.9a: Helium porosity versus depth for Fruholmen and Snadd Formation core plugs (COPL) from well 7131/4-1. Porosity does not systematically decrease with depth. On the contrary, the highest helium porosities are found in the Snadd Formation.

For permeability the situation is somewhat different, and the highest permeabilities are found in the Fruholmen Formation (Figure 5.3.9b). This is probably partly due to practically all the porosity in the Fruholmen Formation being well connected primary intergranular macroporosity, whereas, as discussed above, a substantial proportion of the pore system in the Snadd Formation consists of dissolution porosity within feldspar grains and microporosity within clay clasts and rock fragments. Intergranular macroporosity has previously been found to strongly influence permeability in reservoir sandstones on the Norwegian continental shelf, whereas microporosity contributes far less to permeabilities (Ehrenberg, 1990). The second factor that contributes to explaining the high permeabilities in the Fruholmen Formation is the slightly coarser grain size in the most permeable part (919-925mRKB) of this formation compared to the Snadd Formation in well 7131/4-1 (Kozeny, 1927).

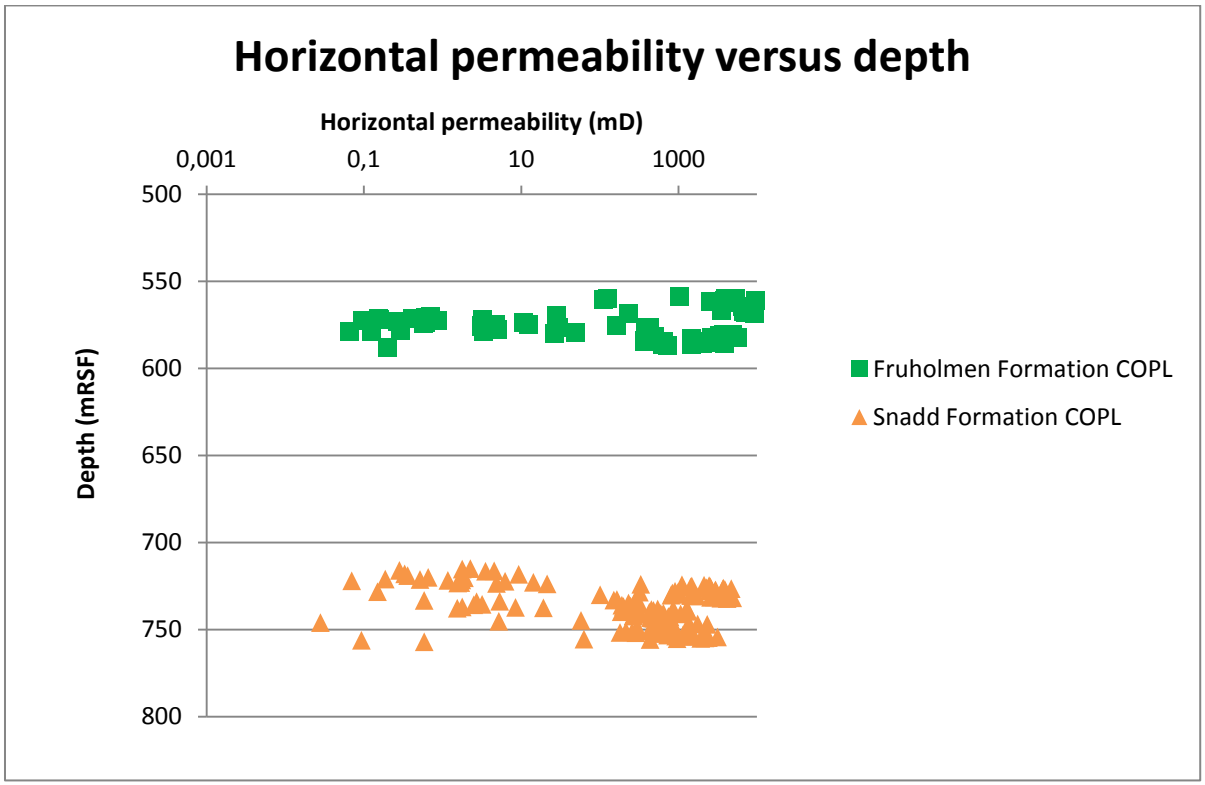

Figure 5.3.9b: Horizontal permeability versus depth for Fruholmen and Snadd Formation core plugs (COPL) from well 7131/4-1. Maximum permeabilities decrease with depth and are highest in parts of the Fruholmen Formation.

In well 7222/11-1 there is a relatively clear reduction of helium porosity with depth (Figure 5.3.10a). This may partly be due to the samples spanning a much larger depth range (approximately 1.7km) than in well 7131/4-1, where the depth range was only around 200m. In addition, the compositions of the Snadd and Kobbe formations in well 7222/11-1 are much

more similar than what is the case for the Fruholmen and Snadd formations in well 7131/4-1 (Tables 3.1.1 and 4.1.1, Figure 5.1.4). It is therefore likely that the Snadd and Kobbe formations in well 7222/11-1 will follow similar porosity versus depth trends during burial (Byrnes, 1994). The main reason for the porosity being much less in the Kobbe Formation compared to in the Snadd Formation in well 7222/11-1 is more extensive compaction in the Kobbe Formation. The volumes of quartz cement present in the Kobbe Formation are often only around 1% higher than in the Snadd Formation.

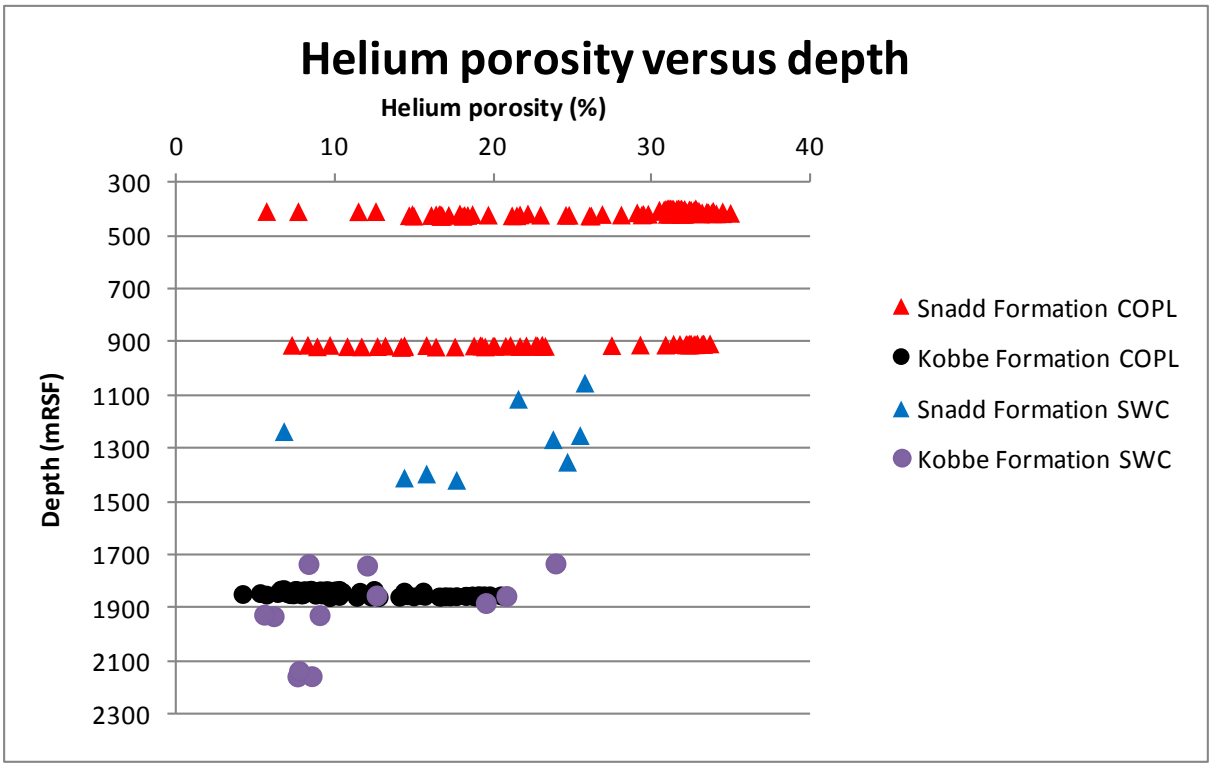

Figure 5.3.10a: Helium porosity versus depth for Snadd and Kobbe Formation core plugs (COPL) and side wall cores (SWC) from well 7222/11-1. Helium porosities decrease quite systematically with depth.

Permeability also shows a relatively systematic decrease with depth in well 7222/11-1 (Figure 5.3.10b). This is as expected because of the systematic reduction of porosity with depth (Figure 5.3.10a), and the rather well-defined positive correlation between porosity and permeability in well 7222/11-1 (Figure 5.3.1).

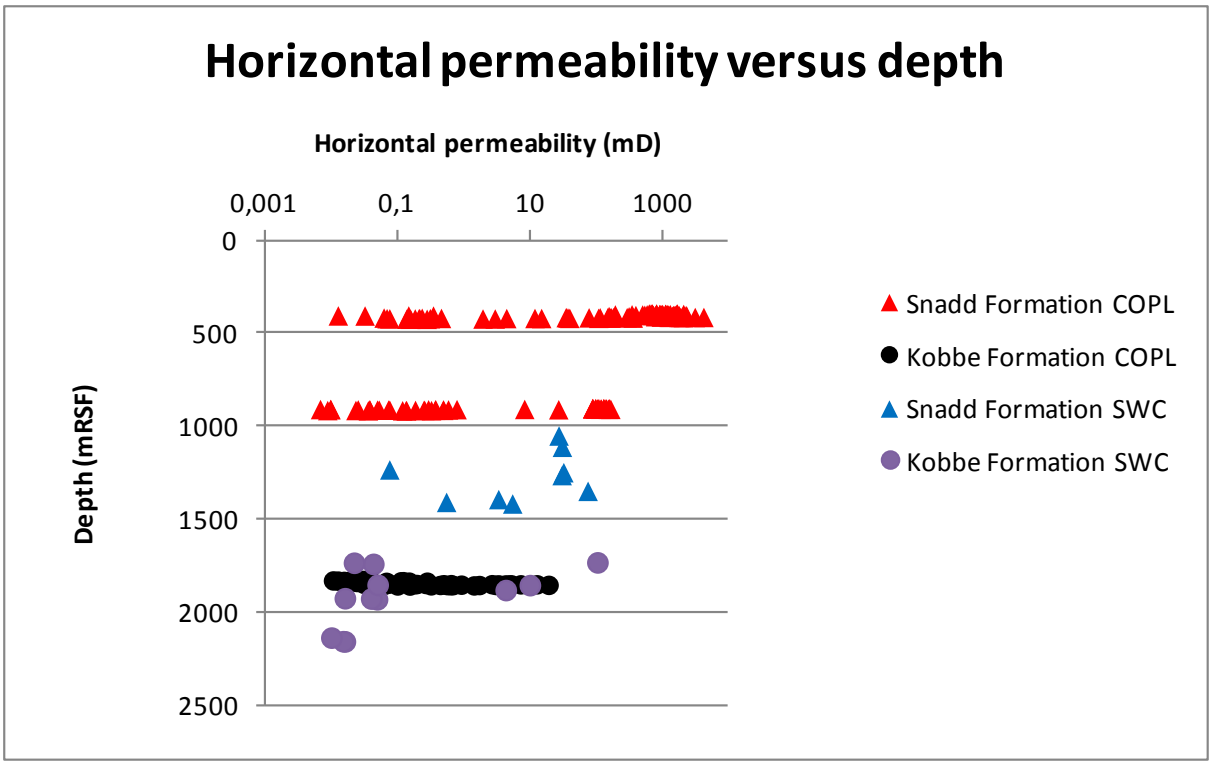

Figure 5.3.10b: Horizontal permeability versus depth for Snadd and Kobbe Formation core plugs (COPL) and side wall cores (SWC) from well 7222/11-1. Permeabilities decrease quite systematically with depth.

5.4 Previous deeper burial and uplift

The studied thin-sections have several indications of the studied sandstones previously being buried to much greater depths and temperatures than at present, and later being subjected to major uplift.

Firstly, even the shallowest cores are consolidated and of good quality, which is not expected for present burial depths of 559-762m in well 7131/4-1, and 399-428.2m in well 7222/11-1. Cores from such shallow depths would normally be very unconsolidated and consist of loose sand (Bjørlykke and Egeberg, 1993). It is therefore natural to explain the consolidated nature of these cores by the sandstones having previously been buried to much greater depths.

The occurrence of quartz overgrowths in both wells indicates temperatures above approximately 70-80°C since normal quartz cement precipitation is not initiated before these temperatures are reached (Bjørlykke et al., 1989; Ehrenberg, 1990; Walderhaug, 1994a). In addition, stylolites are considered as the main source of quartz cement (Bjørlykke et al., 1986; Ehrenberg, 1990; Bjørkum, 1996), and stylolites were registered in thin-sections from all three formations. The formation of stylolites also needs temperatures of around 70-80°C,

however, formation temperatures provided by Statoil are 27°C and 33°C in the shallowest Snadd Formation core in well 7222/-11-1 and in the Fruholmen Formation core in well 7131/4-1, respectively. It is therefore implied that the sandstones have been exposed to higher temperatures in the past, and as temperature is considered to increase with increasing depth, the presence of stylolites and quartz overgrowths is a strong indication of previous deeper burial and subsequent uplift.

At present shallow burial depths, presence of unstable heavy minerals such as amphibole, sphene, epidote, kyanite and staurolite could be expected (Walderhaug and Porten, 2007). However, except for trace amounts of staurolite in the Snadd Formation in well 7222/11-1, none of these minerals were observed in the study. This could also be an indication of previous deeper burial with subsequent uplift, although it must be taken into consideration that these minerals may not have been present at the time of deposition of the sands in these wells.

Some assumptions can be made concerning how much the temperature has decreased and how much the sandstones have been uplifted. Authigenic kaolin is present in many of the thin-sections from the two wells. No illite was observed, and the kaolin has not been illitized. In the Snadd Formation in well 7222/11-1 both K-feldspar and kaolin are present in the deepest Snadd Formation sample, 1420.60mRKB, but no illite is seen. The same applies to the Snadd Formation sample 1107.00mRKB in well 7131/4-1. The illitization process has been shown to initiate at temperatures of approximately 130°C in other parts of the Norwegian continental shelf without uplift (Bjørlykke et al., 1986; Ehrenberg and Nadeau, 1989), which suggests that temperatures before uplift did not exceed 130°C in the mentioned samples.

Because quartz cementation is a very slow process at 70-80°C (Walderhaug, 1994b; Walderhaug, 1996), it seems probable that the well developed quartz overgrowths present in the Kobbe Formation and the Snadd Formation in well 7222/11-1 and in the Snadd Formation in well 7131/4-1, even in the shallowest core (Figure 5.4.1), may have required temperatures of around 100°C to form, although lack of illitization 1450m deeper in well 7222/11-1 excludes significantly higher palaeotemperatures. Present temperatures for the shallowest point-counted Snadd Formation samples are 38°C in well 7131/4-1 and 27°C in well 7222/11-1 according to Statoil. Probable palaeotemperatures of 100°C at these depths therefore suggest 62 and 73°C of cooling in well 7131/4-1 and 7222/11-1, respectively. With a

palaeogeothermal gradient of approximately 40°C/km this would represent uplift of around 1.5km in well 7131/4-1 and 1.8km in well 7222/11-1. However, the geothermal gradient is often highest close to the surface where porosity is higher and thermal conductivity therefore is low (Fjeldskaar et al., 2009). It is therefore possible that geothermal gradients were as high as 45°C/km. This corresponds to uplift of 1.4km for the sandstones in well 7131/4-1, and 1.6km in well 7222/11-1.

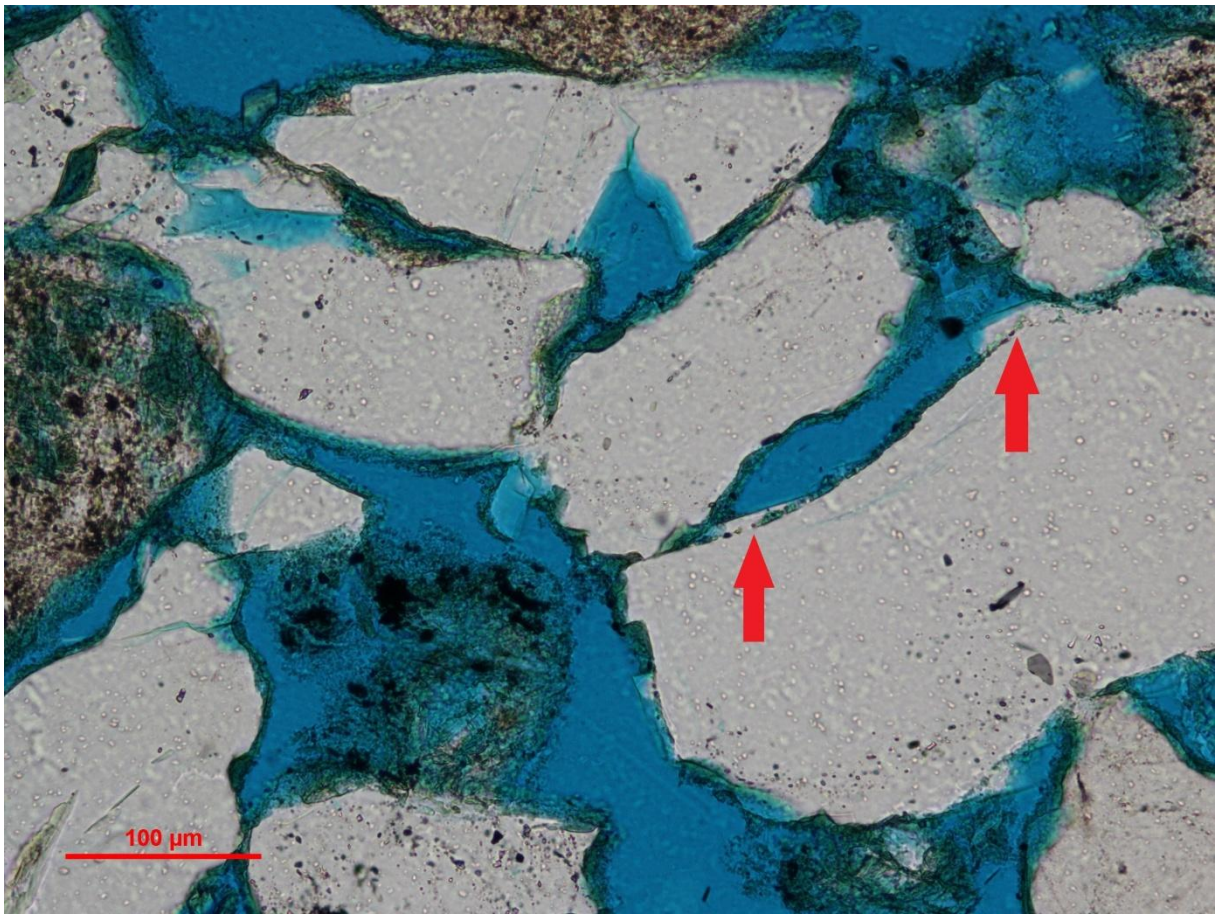

Figure 5.4.1: Thin rims of diagenetic chlorite cover almost all grains. Development of quartz overgrowths has started where chlorite rims are incomplete, indicated with red arrows. Scale bar is 100µm. Snadd Formation, well 7222/11-1, 796.02mRKB.

Estimates of uplift can also be made by comparing measured porosities of uplifted sandstones with porosity versus depth trends for the same type of sandstone in areas without uplift (Walderhaug, 1992). Ehrenberg (1990) has constructed a porosity versus depth trend for the Middle Jurassic Garn Formation in the Haltenbanken area. The Garn Formation is typically quartz-rich with low detrital clay content (Ehrenberg, 1990), i.e., the Garn Formation is very similar to the fluvial channel sandstone between 919 and 925mRKB in the Fruholmen Formation core in well 7131/4-1. The average helium porosity for this Fruholmen Formation

interval is 29.8%, which is the same as the average Garn Formation helium porosity at 2.0km below the sea floor (Ehrenberg, 1990). Present burial depth for the channel sandstone in the Fruholmen Formation is 563-569mRSF. The porosity of the Fruholmen Formation channel sandstone therefore suggests uplift of approximately 1.45km. This is the same value of uplift as estimated above on the basis of sandstone diagenesis. The Snadd and Kobbe Formations are compositionally different from the Garn Formation, and there is not available other porosity versus depth trends from the Norwegian continental shelf for sandstones of the same composition and texture as the Snadd and Kobbe formations. It is therefore not possible to estimate uplift with the same technique for the samples from these formations.

In addition, the stratigraphy in the two wells suggests that major erosion has taken place. In well 7131/4-1 the Cretaceous Kolmule Formation is located only 74m below the sea floor (NPD factpages) whereas in well 7222/11-1 the Triassic Kapp Toscana Group is encountered 72m below the sea floor (NPD factpages).

Major erosion and uplift in the Barents Sea area has previously been proposed by a number of workers (e.g., Nyland et al., 1992; Doré et al., 2002; Ohm et al., 2008), partly on the basis of the more extensive diagenetic cementation and lower porosities encountered in the Barents Sea area compared to in other parts of the Norwegian continental shelf (Berglund et al., 1986; Walderhaug, 1992). Ohm et al. (2008) present a map of probable uplift estimated from vitrinite reflectance values, here reproduced as Figure 5.4.2a and b. According to this map maximum uplift at the locations of wells 7131/4-1 and 7222/11-1 are considered to be less than 1000m and around 1500m, respectively, although little data is available in the vicinity of well 7131/4-1. These values are similar to what has been estimated here for uplift in well 7222/11-1, but the work performed in this thesis suggests that the uplift for 7131/4-1 is approximately 500m greater than what has been tentatively suggested by Ohm et al. (2008).

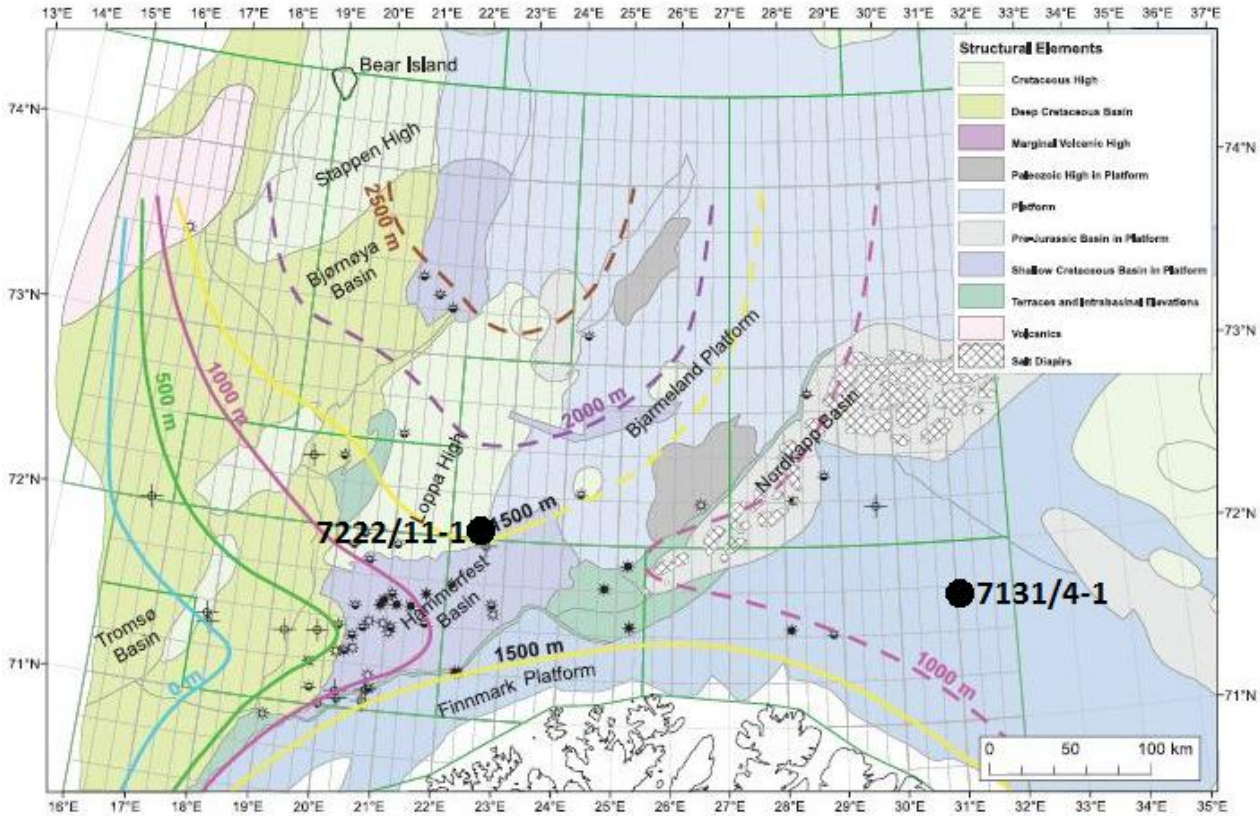

Figure 5.4.2a: Map showing the estimated magnitude of uplift in the Barents Sea. Modified from Ohm et al. (2008).

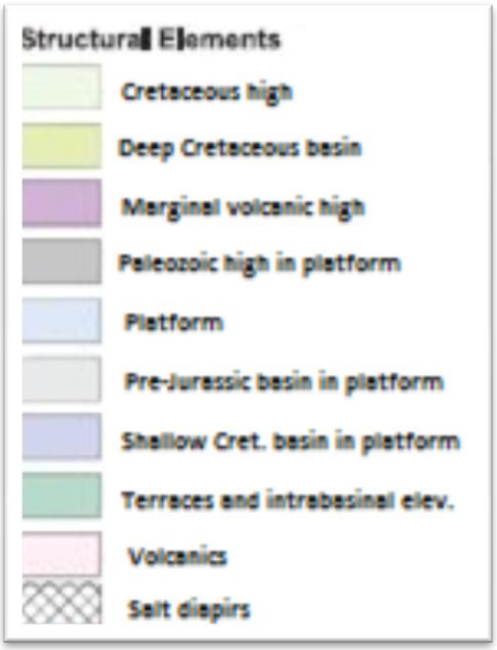

Figure 5.4.2b: Legend.

6 Conclusion

The sandstones of the Fruholmen Formation are dominantly quartz arenites, whereas the Snadd and Kobbe formation sandstones are sublitharenites and lithic arenites. However, the feldspar in the Snadd Formation is a mixture of both K-feldspar and plagioclase, whereas the Kobbe Formation contains plagioclase only. The marked difference in composition between the Fruholmen Formation and the other two formations may partly be due to the change to a more humid climate in the uppermost Triassic causing more intense weathering and dissolution of feldspar. However, since chemically stable chert is common in the Snadd and Kobbe formations and practically absent in the Fruholmen Formation, the compositional differences are probably also due to changes in provenance. Possibly, the lithic arenites and sublitharenites of the Snadd and Kobbe formations were largely derived from an eastern source area, whereas the quartz arenites of the Fruholmen formation may have a source on the Scandinavian land mass. The heavy minerals apatite, garnet, chloritoid, staurolite and spinel were found in the Snadd and Kobbe formations, but not in the Fruholmen Formation, which also indicates different source areas for the Fruholmen Formation versus the Snadd and Kobbe formations.

In addition to mechanical compaction, diagenetic processes in the Fruholmen Formation comprise precipitation of a few per cent quartz overgrowths, traces of authigenic kaolin, and traces of early diagenetic pyrite cement. In addition to these diagenetic minerals, the Snadd Formation also contains abundant chlorite grain coats, commonly up to around 6% siderite cement, and in a few cases pore-filling calcite cement. The Kobbe Formation contains the same diagenetic phases as the Snadd Formation, plus a few albitic overgrowths on some of the plagioclase grains. The diagenetic chlorite may have formed from iron-rich colloidal material supplied by rivers and flocculated in the fluvial-marine mixing zone, possibly in an estuarine setting. Some of the iron may also have been a source for the siderite cement. Quartz cementation probably started at 70-80°C, and the source of quartz cement is thought to be dissolution of quartz grains at the stylolites observed in all three formations. A few partly dissolved shells are present in the Snadd and Kobbe formations, and the rare calcite-cemented zones in these formations probably formed from dissolution of biogenic carbonate. Quartz overgrowths are usually absent within calcite-cemented intervals, suggesting that most calcite cementation took place before quart cementation started.

The excellent porosity and permeability in the Fruholmen Formation quartz arenites is due to near absence of detrital clay and mechanically weak grains, and very low volumes of diagenetic cements. Detrital clay contents and volumes of diagenetic cements are quite often low in the Snadd Formation as well, and reservoir quality is therefore good to very good in parts of this formation. However, some Snadd Formation intervals contain considerable detrital clay, and in some cases microporous diagenetic chlorite fills almost all pores. Even though helium porosities are above 30% in these intervals, the microporous chlorite reduces permeabilities to very low values. Where chlorite coatings are thin, they have a positive effect on reservoir quality by inhibiting quartz cementation. The Kobbe Formation has the poorest reservoir quality of the three formations. Contents of diagenetic minerals are low, but the sandstones are strongly compacted with low intergranular volumes. The strong compaction is mainly a result of a high content of mechanically weak components (detrital clay, authigenic clay and mica-rich rock fragments), although microstylolitic dissolution at grain contacts containing clay has also promoted compaction. In addition, the Kobbe Formation samples have been at the greatest burial depths of the sample set, around 3.5km. The fine grain-size of the Kobbe Formation sandstones has also had a negative effect on permeability.

The shallowest cores from both studied wells are well consolidated and contain some quartz overgrowths, despite present burial depths being only 0.4 and 0.56km. Quartz overgrowths are normally not found at temperatures of less than 70-80°C, whereas present formation temperatures in the shallowest cores are around 30°C. The lack of illitization of kaolin in the deepest Snadd Formation samples indicates that they have not been subjected to temperatures of more than 130°C. Together with the observed volumes of quartz cement in the deeper samples, this suggests that the sandstones have been uplifted around 1.5km in well 7131/4-1 and around 1.7km in well 7222/11-1. Comparison of present porosities in the Fruholmen Formation with porosity depth trends for the Garn Formation also suggests approximately 1.5km of uplift in well 7131/4-1.

7 References

Amieux, P., 1982: La cathodoluminescence: Méthode d'étude sédimentologique des carbonates. *Bulletin des Centres Recherches Exploration-Production Elf-Aquitaine 6,* 437-483.

Bergan, M., Knarud, R., 1992: Apparent changes in clastic mineralogy of the Triassic-Jurassic succession, Norwegian Barents Sea: possible implications for palaeodrainage and subsidence. In: T.O. Vorren, E. Bergsager, Ø.A. Dahl-Stamnes, E. Holter, B. Johansen, E. Lie and T.B. Lund (Editors), Arctic geology and petroleum potential, *NPF Special publication no. 2, Elsevier, Amsterdam,* 481-493.

Berglund, L.T., Augustson, J., Færseth, R., Gjelberg, J., Ramberg-Moe, H., 1986: The evolution of the Hammerfest Basin. In: A.T. Spencer, E. Holter, C.J. Campell, S.H. Hanslien, P.H.H. Nelson, E. Nysæther and E. Ormaasen (Editors), Habitat of hydrocarbons on the Norwegian continental shelf, *Graham and Trotman, London,* 319-338.

Berner, R. A., 1970: Sedimentary pyrite formation. *American Journal of Science 268,* 1-23.

Berner, R. A., 1981: A new geochemical classification of sedimentary environments. *Journal of Sedimentary Petrology 51,* 359-365.

Bjørkum, P.A., 1996: How important is pressure in causing dissolution of quartz in sandstones? *Journal of Sedimentary Research 66,* 147-154.

Bjørkum, P.A., Oelkers, E.H., Nadeau, P.H., Walderhaug, O., Murphy, W.M., 1998: Porosity prediction in quartzose sandstones as a function of time, temperature, depth, stylolite frequency, and hydrocarbon saturation. *AAPG Bulletin 82,* 637-648.

Bjørkum, P.A., Walderhaug, O., 1990: Geometrical arrangement of calcite cementation within shallow marine sandstones. *Earth-Science Reviews 29,* 145-161.

Bjørlykke, K., 1980: Clastic diagenesis and basin evolution. *Diputación Provincial, Universidad de Barcelona, Revista, Instituto de Investigaciones Geológicas 34,* 21-44.

Bjørlykke, K., 2010: Petroleum Geoscience: From sedimentary environments to rock physics. *Berlin, Springer,* 508 pages.

Bjørlykke, K., Aagaard, P., Dypvik, H., Hastings, D.S., Harper, A.S., 1986: Diagenesis and reservoir properties of Jurassic sandstones from the Haltenbanken area, offshore mid Norway. In: A.T. Spencer, E. Holter, C.J. Campell, S.H. Hanslien, P.H.H. Nelson, E. Nysæther and E. Ormaasen (Editors), Habitat of hydrocarbons on the Norwegian continental shelf, *Graham and Trotman, London,* 275-286.

Bjørlykke, K., Egeberg, P.K., 1993: Quartz cementation in sedimentary basins. *AAPG Bulletin 77,* 1538-1548.

Bjørlykke, K., Elverhøi, A., Malm, A.O., 1979: Diagenesis in Mesozoic sandstones from Spitsbergen and the North Sea – A comparison. *Geologische Rundschau 68,* 1152-1171.

Bjørlykke, K., Ramm, M., Saigal, G.C., 1989: Sandstone diagenesis and porosity modification during basin evolution. *Geologische Rundschau 78,* 243-268.

Bloch, S., McGowan, J.H., 1994: Influence of depositional environment on reservoir quality prediction. In: M.D. Wilson (Editor), Reservoir quality assessment and prediction in clastic rocks, *SEPM Short Course 30,* 41-57.

Brekke, H., Olaussen, S., 2007: Høyt hav og lave horisonter. In: I.B. Ramberg, I. Bryhni and A. Nøttvedt (Editors), Landet blir til, Norges geologi, *Norsk Geologisk Forening, Trondheim,* 382-415.

Bugge, T., Elvebakk, G., Fanavoll, S., Mangerud, G., Smelror, M., Weiss, H. M., Gjelberg, J., Kristensen, S. E., Nilsen, K., 2002: Shallow stratigraphic drilling applied in hydrocarbon exploration of the Nordkapp Basin, Barents Sea. *Marine and Petroleum Geology 19,* 13-37.

Bugge, T., Mørk, A., Sollid, K., 2007: Nordkappbassenget. In: I.B. Ramberg, I. Bryhni and A. Nøttvedt (Editors), Landet blir til, Norges geologi, *Norsk Geologisk Forening, Trondheim,* 349.

Byrnes, A.P., 1994: Empirical methods of reservoir quality prediction. In: M.D. Wilson (Editor), Reservoir quality assessment and prediction in clastic rocks, *SEPM Short Course 30,* 9-21.

Deer, W.A., Howie, R.A., Zussman, J., 1966: An introduction to the rock-forming minerals, *Longman Group Ltd, Harlow,* 528 pages.

Dickson, J.A.D., 1966: Carbonate identification and genesis as revealed by staining. *Journal of Sedimentary Petrology 36,* 491-505.

Doré, A.G., 1995: Barents Sea geology, petroleum resources and commercial potential. *Arctic 48,* 207-221.

Doré, A.G., Corcoran, D.V., Scotchman, I.C., 2002: Prediction of the hydrocarbon system in exhumed basins, and application to the NW European margin. In: A.G. Doré, J.A., Cartwright, M.S. Stoker, J.P. Turner and N.J White (Editors), Exhumation of the North Atlantic margin: Timing, mechanism and implications for petroleum exploration, *Geological Society of London Special Publications 196,* 401-429.

Ehrenberg, S.N., 1990: Relationship between diagenesis and reservoir quality in sandstones of the Garn Formation, Haltenbanken, Mid-Norwegian continental shelf. *AAPG Bulletin 74,* 1538-1558.

Ehrenberg, S.N., 1993: Preservation of anomalously high porosity in deeply buried sandstones by grain-coating chlorite: Examples from the Norwegian continental shelf. *AAPG Bulletin 77,* 1260-1286.

Ehrenberg, S.N., 2004: Factors controlling porosity in Upper Carboniferous – Lower Permian carbonate strata of the Barents Sea. *AAPG Bulletin 88,* 1653-1676.

Ehrenberg, S.N., Nadeau, P.H., 1989: Formation of diagenetic illite in sandstones of the Garn Formation, Haltenbanken, mid-Norwegian continental shelf. *Journal of Sedimentary Petrology 63,* 929-944.

Fjeldskaar, W., Christie, O.H.J., Midttømme, K., Virnovsky, G., Jensen, N.B., Lohne, A., Eide, G.I., Balling, N., 2009: On the determination of thermal conductivity of sedimentary rocks and the significance for basin temperature history. *Petroleum Geoscience 15,* 367-380.

Folk, R.L., 1974: Petrology of sedimentary rocks. *Hemphill Publishing Company, Austin,* 182 pages.

Folkestad, A., 2007: Snøhvitfeltet. In: I.B. Ramberg, I. Bryhni and A. Nøttvedt (Editors), Landet blir til, Norges geologi, *Norsk Geologisk Forening, Trondheim,* 378.

Gabrielsen, R.H., Faleide, J.I., Pascal, C., Torsvik, T.H., 2011: Plate tectonics and tectonic inversion in the Barents Sea. *AAPG Search and Discovery Article #90130©2011 3P, Arctic, The Polar Petroleum Potential Conference & Exhibition, Halifax, Nova Scotia, Canada, 30 August-2 September, 2011*.

Gabrielsen, R.H., Færseth, R.B., Jensen, L.N., Kalheim, J.E., Riis, F., 1990: Structural elements of the Norwegian continental shelf, Part I: The Barents Sea Region. *NPD Bulletin 6,* 33 pages.

Giles, M.R., Stevenson, S., Martin, S.V., Cannon, S.J.C., Hamilton, P.J., Marshall, J.D., Samways, G.M., 1992: The reservoir properties and diagenesis of the Brent Group: a regional perspective. In: A.C. Morton, R.S. Haszeldine, M.R. Giles and S. Brown (Editors), Geology of the Brent Group, *Geological Society of London Special Publication 61,* 289-327.

Heald, M.T., Larese, R.E., 1974: Influence of coatings on quartz cementation. *Journal of Sedimentary Petrology 44,* 1269-1274.

Heald, M.T., Renton, J.J., 1966: Experimental study of sandstone cementation. *Journal of Sedimentary Petrology 36,* 977-991.

Johannessen, E.P., Nøttvedt, A., 2007: Landet omkranses av deltaer. In: I.B. Ramberg, I. Bryhni and A. Nøttvedt (Editors), Landet blir til, Norges geologi, *Norsk geologisk forening, Trondheim,* 354-381.

Johnson, M.R., 1994: Thin section grain size analysis revisited. *Sedimentology 41*, 985-999.

Kozeny, J., 1927: Üeber kapillare Leitung des Wassers im Boden. *Sitzungsberichte der Akademie der Wissenschaften., Wien 136(2a)*, 271-306.

Larssen, G.B., Elvebakk, G., Henriksen, L.B., Kristensen, S.-E., Nilsson, I., Samuelsberg, T.J., Svånå, T.A., Stemmerik, L., Worsley, D., 2002: Upper Palaozoic lithostratigraphy of the Southern Norwegian Barents Sea, *NPD Bulletin 9*, 69 pages.

Marshall, J.D., 1988: Cathodoluminescence of geological materials. *Unwin Hyman Ltd, London*, 146 pages.

McBride, E., 1989: Quartz cement in sandstones: A review. *Earth-Science Reviews 26*, 69-112.

McRae, S.G., 1972: Glauconite. *Earth-Science Reviews 8*, 397-440.

Morad, S., 1998: Carbonate cementation in sandstones: distribution patterns and geochemical evolution. In: S. Morad (Editor), Carbonate cementation in sandstones, *International Association of Sedimentologists Special Publication 26*, 179-192.

Mørk, M. B. E., 1999: Compositional variations and provenance of Triassic sandstones from the Barents Shelf. *Journal of Sedimentary Research 69*, 690-710.

Norwegian Petroleum Directorate factpages: http://factpages.npd.no/factpages

Nyland, B., Jensen, L.N., Skagen, J., Skarpnes, O., Vorren, T., 1992: Tertiary uplift and erosion in the Barents Sea: Magnitude, timing and consequences. In: R.M. Larsen, H. Brekke, B.T. Larsen and E. Talleraas (Editors), Structural and tectonic modeling and its application to petroleum geology, *NPF Special Publication 1, Elsevier, Amsterdam*, 153-162.

Nystuen, J.P., Müller, R., Mørk, A., Nøttvedt, A., 2007: Fra ørken til elveslette – fra land til hav. In: I.B. Ramberg, I. Bryhni and A. Nøttvedt (Editors), Landet blir til, Norges geologi, *Norsk Geologisk Forening, Trondheim*, 328-353.

Nøttvedt, A., Johannessen, E.P., 2007: Grunnlaget for Norges oljerikdom. In: I.B. Ramberg, I. Bryhni and A. Nøttvedt (Editors), Landet blir til, Norges geologi, *Norsk Geologisk Forening, Trondheim,* 382-415.

Nøttvedt, A, Worsley, D., 2007: Vidstrakte sletter, kull og salt. In: I.B. Ramberg, I. Bryhni and A. Nøttvedt (Editors), Landet blir til, Norges geologi, *Norsk Geologisk Forening, Trondheim,* 258-283.

Ohm, S.E., Karlsen, D.A., Austin, T.J.F., 2008: Geochemically driven exploration models in uplifted areas: Examples from the Norwegian Barents Sea. *AAPG Bulletin 92,* 1191-1223.

Olaussen, S., Dalland, A., Gloppen, T.G., Johannessen, E., 1984: Depositional environment and diagenesis of Jurassic reservoir sandstones in the eastern part of Troms I area. In: A.M. Spencer, E. Holter, S.O. Johnsen, A. Mørk, E. Nysæther, P. Songstad and Å. Spinnangr (Editors), Petroleum geology of the north European margin, *Graham & Trotman, London,* 61-79.

Pettijohn, F.J., Potter, P.E., Siever, R., 1972: Sand and sandstone. *Springer-Verlag, Berlin,* 618 pages.

Ramberg, I.B., Bryhni, I., Nøttvedt, A., 2007: Landet blir til, Norges geologi. *Norsk Geologisk Forening, Trondheim,* 608 pages.

Rasmussen, B., Glover, J.E., Alexander, R., 1989: Hydrocarbon rims on monazite in Permian-Triassic arenites, northern Perth Basin, Western Australia: Pointers to the former presence of oil. *Geology 17,* 115-118.

Riis, F., Lundschien, B. A., Høy, T., Mørk, A., Mørk, M. B. E., 2008: Evolution of the Triassic shelf in the northern Barents Sea. *Polar Research 27,* 318-338.

Ryseth, A., Augustson, J.H., Charnock, M., Haugerud, O., Knutsen, S.-M., Midbøe, P.S., Opsal, J.G., Sundsbø, G., 2003: Cenozoic stratigraphy and evolution of the Sørvestnaget Basin, southwestern Barents Sea. *Norwegian Journal of Geology 83,* 107-130.

Scholle, P.S., 1979: A color illustrated guide to constituents, textures, cements and porosities of sandstones and associated rocks. *AAPG Memoir 28*, 185 pages.

Scotese, C.R., 1987: Phanerozoic plate tectonic reconstructions. Paleoceanographic mapping project. *Institute of Geophysics, University of Texas Technical Report 90,* Map portfolio.

Statoil ASA homepages: http://www.statoil.com

Vorren, T. O., Mangerud, J., 2007: Istider kommer og går. In: I.B. Ramberg, I. Bryhni and A. Nøttvedt (Editors), Landet blir til, Norges geologi, *Norsk Geologisk Forening, Trondheim,* 478-531.

Walderhaug, O., 1992: Magnitude of uplift of the Stø and Normela Formations in the Hammerfest Basin – a diagenetic approach. *Norsk Geologisk Tidsskrift 72,* 321-323.

Walderhaug, O., 1994a: Temperatures of quartz cementation in Jurassic sandstones from the Norwegian continental shelf – evidence from fluid inclusions. *Journal of Sedimentary Research A 64,* 311-323.

Walderhaug, O., 1994b: Precipitation rates for quartz cement in sandstones determined by fluid-inclusion microthermometry and temperature-history modeling. *Journal of Sedimentary Research A 64,* 324-333.

Walderhaug, O., 1996: Kinetic modeling of quartz cementation and porosity loss in deeply buried sandstone reservoirs. *AAPG Bulletin 80,* 731-745.

Walderhaug, O., 2000: Modeling quartz cementation and porosity in Middle Jurassic Brent Group sandstones of the Kvitebjørn Field, northern North Sea. *AAPG Bulletin 84,* 1325-1339.

Walderhaug, O., Bjørkum, P.A., 2003: The effect of stylolite spacing on quartz cementation in the lower Jurassic Stø Formation, southern Barents Sea. *Journal of Sedimentary Research 73,* 146-156.

Walderhaug, O., Lander, R.H., Bjørkum, P.A., Oelkers, E.H., Bjørlykke, K., Nadeau, P.H., 2000: Modelling quartz cementation and porosity in reservoir sandstones: examples from the Norwegian continental shelf. In: R.H. Worden and S. Morad (Editors), Quartz cementation in sandstones. *International Association of Sedimentologists Special Publication 29,* 39-49.

Walderhaug, O., Porten, K.W., 2007: Stability of detrital heavy minerals on the Norwegian continental shelf as a function of depth and temperature. *Journal of Sedimentary Research 77,* 992-1002.

Worsley, D., 2008: The post-Caledonian development of Svalbard and the western Barents Sea. *Polar Research 27,* 298-317.

Worsley, D., Johansen, R., Kristensen, S.E., 1988: The Mesozoic and Cenozoic succession of Tromsøflaket. In: A. Dalland, D. Worsley and K. Ofstad (Editors), A lithostratigraphic scheme for the Mesozoic and Cenozoic succession offshore mid- and northern Norway, *NPD Bulletin 4,* 42-61.